KINEMATICS, SPECIAL CONFIGURATIONS AND PERFORMANCE EVALUATION OF SERIAL MANIPULATORS

BY

RESIT SOYLU

A DISSERTATION PRESENTED TO THE GRADUATE SCHOOL
OF THE UNIVERSITY OF FLORIDA IN
PARTIAL FULFILLMENT OF THE REQUIREMENTS
FOR THE DEGREE OF DOCTOR OF PHILOSOPHY

UNIVERSITY OF FLORIDA

1988

ACKNOWLEDGMENTS

The author wishes to express his gratitude to his committee chairman, Professor Joseph Duffy, for his guidance, encouragement and support.

In addition, the author would like to thank Gilbert Lovell for the many fruitful discussions, Enis Ozgul, Lotfi Romdhane and Li Young for their support, Ugurhan Onsan for his valuable assistance in the final stages of this work and Ms. Cindy Zimmerman for the excellent typing.

Finally, the author extends his deepest appreciation to his parents who were literally thousands of miles away, yet so close.

The financial support of the Scientific and Technical Research Council of Turkey and of the National Science Foundation (Grant No. MEA83-04752) is also appreciated.

TABLE OF CONTENTS

Page

ACKNOWLEDGMENTS....................ii

ABSTRACT....................v

CHAPTERS

1 INTRODUCTION....................1

2 THEORY AND DEVELOPMENT OF THE HYPERSURFACES OF SPECIAL CONFIGURATIONS....................7

2.1 Plücker Line Coordinates in Different Coordinate Systems....................7
2.2 Optimal Coordinate Systems....................11
2.3 Hypersurfaces of Special Configurations....................25
  2.3.1 Minimal Coordinate Systems....................25
  2.3.2 Determining Equations....................28

3 CONCEPTS RELATED TO THE HYPERSURFACES OF SPECIAL CONFIGURATIONS....................34

3.1 Passive Joints and Dimensions....................34
3.2 Configurations and Component Manifolds....................41
3.3 Some Applications....................47
3.4 A Theorem for the Existence of Passive Joints.......50
3.5 Synthesis for Passive Joints....................54
3.6 Examples....................58
  3.6.1 Manipulators with 6 Degrees of Freedom.......58
  3.6.2 Manipulators with 5 Degrees of Freedom.......70

4 MEASURES FOR THE POSITION AND ORIENTATION SPACE OF THE END EFFECTOR....................71

4.1 Hand Freedom Numbers....................71
4.2 A Second Measure....................74
4.3 Lowest Upper Bounds of the Hand Freedom Numbers.....80
4.4 Example....................92

5 REVERSE VELOCITY ANALYSIS....................................99

5.1 Manipulators with 6 Degrees of Freedom..............99
5.1.1 Manipulators Without Any Special Geometry....99
5.1.2 Manipulators With Special Geometry..........104
5.2 Manipulators Containing a Planar Pair..............113
5.3 Manipulators Containing a Spherical Pair...........119
5.4 Singularities......................................120
5.4.1 Planar Wrist Manipulators...................121
5.4.2 Spherical Wrist Manipulators................127

6 CONFIGURATIONS OF 6 DEGREE-OF-FREEDOM MANIPULATORS......131

6.1 One-to-Oneness of the Configurations...............131
6.2 Planar Wrist Manipulators..........................142
6.2.1 Signed-Planes...............................142
6.2.2 Reverse Displacement Analysis...............145
6.2.3 Uncertainty and Stationary Configurations...154
6.2.4 Workspace of the Wrist Plane................158
6.3 Upper Bound of the Number of Configurations........162

7 SYMBOLIC MANIPULATION......................................173

8 CONCLUSIONS..175

APPENDICES

A DEFINITIONS OF THE P, Q, R, U, V, W, X, Y AND Z ELEMENTS...177

B A THEOREM AND TWO COROLLARIES ON THE NUMBER OF REGIONS FORMED BY AN ALGEBRAIC CURVE....................179

REFERENCES...190

BIOGRAPHICAL SKETCH..193

Abstract of Dissertation Presented to the Graduate School
of the University of Florida in Partial Fulfillment of the
Requirements for the Degree of Doctor of Philosophy

KINEMATICS, SPECIAL CONFIGURATIONS AND PERFORMANCE EVALUATION OF SERIAL MANIPULATORS

BY

RESIT SOYLU

April, 1988

Chairman: Dr. Joseph Duffy
Major Department: Mechanical Engineering

The first major topic covered in this dissertation is the special (or singular) configurations of N degree of freedom (DOF) serial manipulators. These configurations are classified according to the number of degrees of freedom lost. This classification yields hypersurfaces in the joint space, the union of which is designated by HSC. An efficient methodology is developed for the identification of each such hypersurface via Screw Theory and Linear Algebra. The efficiency of this methodology stems from a novel theorem and the utilization of the minimal reference frames which depend on the type and sequence of the joints. Various novel concepts associated with the HSC are also introduced and it is demonstrated that these concepts are useful in the kinematic design, analysis, motion planning and control of manipulators.

The second major topic discussed is the quantification of the freedom of the end effector for a 6 DOF manipulator. A computable measure, which includes joint limitations and scale, is introduced for this purpose. The computation of this measure is considerably simplified if the forward displacement mapping is one-to-one when restricted to a region which is, loosely speaking, bounded by the HSC. Sufficient conditions are derived for this useful property and simple expressions are obtained for the upper bound of the number of these regions.

The reverse velocity analysis of 6 DOF manipulators constitutes the third topic. Efficient and systematic methods, applicable to any type of manipulator with or without any special geometry, are developed. The relations between the dimensions of the manipulator and the complexity of the reverse velocity analysis are also investigated.

Further, the dissertation contains an in-depth analysis of the Planar Wrist manipulators including workspace and closed-form reverse displacement analyses.

CHAPTER 1
INTRODUCTION

The kinematics of a serial manipulator, which is essential for the control and motion planning algorithms, is built around the Forward Displacement Mapping (FDM) and the mappings induced from it. This highly nonlinear mapping is from the joint space into the Position and Orientation Space of the Hand (POH space) which is also referred to as the Cartesian space. The derivation of the reverse mapping, i.e., reverse displacement analysis, can be quite challenging especially if the manipulator does not have a simple geometry (see Duffy, 1980).

The Forward Velocity Mapping (FVM), on the other hand, is a linear transformation from the joint velocity space into the hand twist [(generalized) hand velocity] space. Any matrix which represents this transformation is called a Jacobian matrix, [J]. The transpose of the same matrix transforms the hand wrench [(generalized) hand force] into the (generalized) joint torques. Both of these transformations are vital for almost all control algorithms and thus various methods have been proposed for the determination of [J] (see Orin and Schrader (1984) for a comprehensive review).

During the motion of a robot, sometimes the joint freedoms become dependent and the robot loses one or more degrees of freedom. Such configurations are known as special (or singular) configurations of the manipulator. When the manipulator is in a special configuration the reverse velocity analysis breaks down. However this is not necessarily true for the reverse displacement analysis. The special configurations have been investigated using screw theory (see Sugimoto et al. (1982); Waldron et al. (1985)) and the FDM represented by 4×4 transformation matrices (Litvin and Castelli, 1985; Litvin et al., 1985; 1987). The question of "escape" from a special configuration has been discussed by Hunt (1986).

The workspace of a manipulator is also closely related to the FDM. After the inspiring paper by Roth (1976), Kumar and Waldron (1980, 1981) identified the two different types of workspaces which they called the reachable and dextrous workspaces. They defined the reachable workspace to be the collection of all points that can be reached by a reference point on the end effector. The portion of the reachable workspace that is reachable with any desired orientation of the hand was named as the dextrous workspace. Numerous other researchers have also contributed in this area (see the references contained in Vijaykumar et al. (1986)).

The contents of the chapters are described next.

The special configurations of an N DOF manipulator can be classified according to the instantaneous number of degrees of freedom lost. In Chapter 2 it is demonstrated that this natural classification yields hypersurfaces in the joint space (labelled as the hypersurfaces of special configurations) the union of which is designated in short by HSC. An efficient methodology (via screw theory and linear algebra) is developed for the identification of each such hypersurface. The efficiency of this methodology stems from Theorem 2.1 and the utilization of the minimal reference frames. These frames are obtained and tabulated for all possible types of 3, 4, 5 and 6 DOF manipulators. Furthermore the adaptability of a manipulator to a common control algorithm is quantified via an index. The numerical values of these indices are listed for all possible types of manipulators.

Chapter 3 is primarily concerned with the novel concepts related to the HSC. In Section 3.1 a passive joint is defined as a joint with the property that when actuated alone it cannot change the incidence relationship between the joint variable vector and the HSC. A joint which is not passive is said to be an active joint. The HSC is at most an (A-1)-manifold in the active joint space of the manipulator, the dimension of which is denoted by A. The lowest upper bounds of A for all possible types of 6 DOF manipulators are determined and tabulated in this section. The results indicate that these bounds lie between 1 and 4. It should be noted that when $A \leq 3$ the HSC is at most a 2-manifold and it is thus possible to visualize the hypersurface of special configurations.

In Section 3.2 the novel concepts of component/subcomponent manifolds of the HSC, configurations and subconfigurations are introduced. These concepts are useful in the kinematic design, control and motion planning of manipulators. Some applications are given in Section 3.3.

In Section 3.4 a theorem which predicts the existence of passive joints is presented. The hypothesis of the theorem is a sufficient but not necessary condition for the existence of such joints. Hence, an algorithm for the synthesis of passive joints is also developed. Using this algorithm it is possible to design manipulators with simple HSC's. In general, the reverse displacement and velocity analyses will be simple for such manipulators. Finally, in Section 3.6 some of the concepts introduced in Chapters 2 and 3 are illustrated by way of examples which include three existing industrial manipulators.

Chapter 4 focuses on the quantification of the freedom of the end effector (considered as a rigid body in R^3) for a 6 DOF manipulator. This is accomplished by introducing two different measures, HFN(D) and M(D), into the position and orientation space of the end effector where D denotes a region in the joint space. A theorem proved in Section 4.2 indicates that the two measures are equivalent for the spherical wrist (SW) manipulators.

The cumulative freedoms of the end effector with and without joint limitations ($CHFN_l$ and $CHFN_u$) can be determined via the $HFN(CO_i)$'s. The regions CO_i's ($i=1,2,\ldots,NC$) signify the different configurations of the manipulator discussed in Chapter 3 and, loosely speaking, are the regions bounded by the subsets of the HSC. The performance of a manipulator can be evaluated on the basis of $CHFN_l$, $CHFN_u$, $\|CHFN_l\|_k$ and $\|CHFN_u\|_k$. The latter two measures are the normalized versions (with respect to $\|\underline{l}\|_k$) of the former two where $\underline{l}$ denotes the vector of active linear dimensions of the manipulator. The lowest upper bounds of $\|HFN(CO_i)\|_1$ and $\|CHFN_u\|_1$ are obtained and tabulated in Section 4.3 for all types of SW manipulators. In the last section, the concepts introduced in this chapter are illustrated via a numerical example using the MBA robot.

Chapter 5 is devoted to the reverse velocity analysis of 6 DOF manipulators via screw theory. It has been demonstrated in Chapter 2 that the special Jacobian matrix $[J_B]$, which transforms the actuator velocity vector into the twist representing the instantaneous motion of the hand (formulated in the base coordinates), can be expressed as the product of two 6×6 matrices in several different ways. Here, the components of these matrices are explicitly given for any type of 6 DOF manipulator. The alternative formulations of $[J_B]$ lead to a classification of manipulators based on their geometrical designs. The inverse of $[J_B]$ for any manipulator belonging to either one of the seven broad classes thus identified can be determined by inverting a single 4×4 matrix. All possible types of manipulators which contain a kinematic chain equivalent to a planar or a spherical pair are also investigated. It is shown that for these manipulators the reverse velocity analysis reduces to the inversion of a 3×3 matrix for which there are several alternatives. These alternatives are exploited to further simplify the reverse velocity analysis. Finally, closed-form equations for the HSC's of all types of spherical wrist and planar wrist (PW) manipulators are obtained. A manipulator, the last three links of which are kinematically equivalent to a planar pair, is here labelled as a planar wrist manipulator.

In Section 6.1 an important class of manipulators (labelled as the echelon manipulators) which includes, for instance, the majority of the SW manipulators is identified. It is then proved that for an echelon manipulator the FDM is one-to-one when restricted to a region CO_i (i=1,2,...,NC).

Section 6.2 contains an in-depth analysis of the PW manipulators. Closed-form reverse displacement analyses of all possible types of PW manipulators are performed via signed-planes which are defined to be planes in R^3 with unique normals attached to them. Using these analyses it is demonstrated that the majority of the PW manipulators are echelon manipulators. Furthermore the totality of the uncertainty and stationary configurations of each type of PW manipulator is identified. In the same section, an efficient algorithm is developed to determine the "workspace" of a special signed-plane (labelled as the wrist plane) associated with a PW manipulator. This algorithm is then extended to the workspace (of the wrist point) of the SW manipulators.

In the last section, simple expressions are developed for the upper bound of the number of configurations (NC) of a manipulator. These expressions are based on the equations of the component manifolds and a novel theorem and two corollaries (on the number of regions formed by an algebraic curve) which are proved in Appendix B. The upper bound of the number of configurations for all types of PW and SW manipulators are obtained and tabulated using the aforementioned expressions.

CHAPTER 2
THEORY AND DEVELOPMENT OF THE HYPERSURFACES OF SPECIAL CONFIGURATIONS

In this chapter the capped and uncapped reference frames, optimal and minimal coordinate systems and the hypersurfaces of special configurations of different orders are discussed. Familiarity with the fundamentals of screw theory and linear algebra is assumed.

2.1 Plücker Line Coordinates in Different Coordinate Systems

Consider the open loop spatial structure shown in Fig. 2.1. The angle between two successive $\underline{S}$ ($\underline{a}$) vectors, say $\underline{S}_h$ ($\underline{a}_{gh}$) and $\underline{S}_i$ ($\underline{a}_{hi}$), is denoted by α_{hi} (θ_h) which is measured from $\underline{S}_h$ ($\underline{a}_{gh}$) to $\underline{S}_i$ ($\underline{a}_{hi}$) in a right-hand sense around $\underline{a}_{hi}$ ($\underline{S}_h$). Let B_β ($\hat{B}_\beta$) represent a right-handed coordinate system whose z and x axes are parallel to $\underline{S}_\beta$ ($\underline{S}_\beta$) and $\underline{a}_{\beta\gamma}$ ($\underline{a}_{\alpha\beta}$), respectively, the origin being located at O_β ($\hat{O}_\beta$) (see Fig. 2.1), where $\alpha\beta\gamma$ = efg, fgh, ..., ijk. Furthermore, the coordinates of a unit vector $\underline{S}_\beta$ (β = e, f, ..., k) with respect to the reference frames B_α and $\hat{B}_\alpha$ (α = e, f, ..., k) will be denoted by $\underline{S}_{\beta,\alpha}$ and $\underline{S}_{\beta,\hat{\alpha}}$.

The Plücker coordinates (in ray order) of a line g, on which the line bound vector $\underline{S}_g$ lies, in reference frame B_i ($\hat{B}_i$) are

$$\$_{g,i} = \begin{bmatrix} \underline{S}_{g,i} \\ \underline{S}_{og,i} \end{bmatrix} \qquad \left(\$_{g,\hat{i}} = \begin{bmatrix} \underline{S}_{g,\hat{i}} \\ \underline{S}_{og,\hat{i}} \end{bmatrix} \right) \tag{2.1}$$

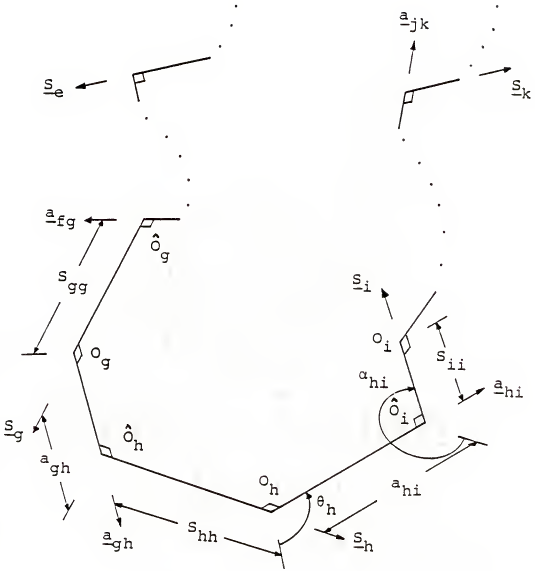

Fig. 2.1 Open Loop Spatial Structure

where

$$\underline{S}_{og,i} = \underline{r}_{g,i} \times \underline{S}_{g,i} \qquad (\underline{S}_{og,\hat{i}} = \underline{r}_{g,\hat{i}} \times \underline{S}_{g,\hat{i}}) \tag{2.2}$$

where $\underline{r}_{g,i}$ ($\underline{r}_{g,\hat{i}}$) is a vector, expressed in B_i ($\hat{B}_i$), from the origin 0_i ($\hat{0}_i$) to any point on the line g. For instance $\underline{r}_{g,i}$ can be conveniently taken as $\underline{r}_{g,i} = -(S_{ii}\,\underline{S}_{i,i} + a_{hi}\,\underline{a}_{hi,i} + S_{hh}\,\underline{S}_{h,i} + a_{gh}\,\underline{a}_{gh,i})$. The objective here is to obtain the Plücker coordinates of the lines e, f, ..., k in the reference frames B_h and $\hat{B}_h$.

The recursive notation, which is due to Lipkin and Duffy (1985), is summarized in Appendix A. A careful interpretation of this notation reveals that

$$\underline{S}_{h,h} = [0,0,1]^T \qquad \underline{S}_{i,h} = [0,\ -s_{hi},\ c_{hi}]^T$$
$$\underline{S}_{j,h} = [X_i,\ Y_i,\ Z_i]^T \qquad \underline{S}_{k,h} = [X_{ij},\ Y_{ij},\ Z_{ij}]^T \tag{2.3}$$

and

$$\underline{S}_{h,\hat{h}} = [0,0,1]^T \qquad \underline{S}_{g,\hat{h}} = [0,\ s_{gh},\ c_{gh}]^T$$
$$\underline{S}_{f,\hat{h}} = [\bar{X}_g,\ -\bar{Y}_g,\ \bar{Z}_g]^T \qquad \underline{S}_{e,\hat{h}} = [X_{gf},\ -Y_{gf},\ Z_{gf}]^T \tag{2.4}$$

where $s_{\beta\gamma} = \sin\alpha_{\beta\gamma}$ and $c_{\beta\gamma} = \cos\alpha_{\beta\gamma}$ ($\beta\gamma$ = ef, fg, ..., jk). The two coordinate frames B_h and $\hat{B}_h$ are related by the rotation matrix

$$[R_h] = \begin{bmatrix} c_h & -s_h & 0 \\ s_h & c_h & 0 \\ 0 & 0 & 1 \end{bmatrix} \tag{2.5}$$

where $c_h = \cos\theta_h$, $s_h = \sin\theta_h$. From equations (2.3), (2.4) and (2.5),

$$\underline{S}_{i,\hat{h}} = [R_h]\underline{S}_{i,h} = [s_{hi}\ s_h,\ -s_{hi}\ c_h,\ c_{hi}]^T$$

$$\underline{S}_{j,\hat{h}} = [R_h]\underline{S}_{j,h} = [X_{hi},\ X^*_{hi},\ Z_i]^T$$

$$\underline{S}_{k,\hat{h}} = [R_h]\underline{S}_{k,h} = [X_{hij},\ X^*_{hij},\ Z_{ij}]^T \tag{2.6}$$

and

$$\underline{S}_{g,h} = [R_h]^{-1}\ \underline{S}_{g,\hat{h}} = [s_{gh}\ s_h,\ s_{gh}\ c_h,\ c_{gh}]^T$$

$$\underline{S}_{f,h} = [R_h]^{-1}\ \underline{S}_{f,\hat{h}} = [X_{hg},\ -X^*_{hg},\ \bar{Z}_g]^T$$

$$\underline{S}_{e,h} = [R_h]^{-1}\ \underline{S}_{e,\hat{h}} = [X_{hgf},\ -X^*_{hgf},\ Z_{gf}]^T \tag{2.7}$$

where multiply subscripted X^* elements, with ascending or descending subscripts, are defined as

$$X^*_{fg\ldots jk} = s_f\ X_{g\ldots jk} + c_f\ Y_{g\ldots jk} \tag{2.8}$$

All the vectors $\underline{S}_{\gamma,h}$ and $\underline{S}_{\gamma,\hat{h}}$ (γ = e, f, ..., k) have thus been determined. The corresponding moment vectors $\underline{S}_{o\gamma,h}$ and $\underline{S}_{o\gamma,\hat{h}}$ are best found by taking the duals of the components of $\underline{S}_{\gamma,h}$ and $\underline{S}_{\gamma,\hat{h}}$. For example, $\underline{S}_{of,h} = [X_{ohg},\ -X^*_{ohg},\ Z_{og}]^T$ and $\underline{S}_{ok,\hat{h}} = [X_{ohij},\ X^*_{ohij},\ Z_{oij}]^T$. The dual (see Duffy, 1980) of $F_{\alpha\beta\ldots\gamma}$ (where F can be an X, Y, Z or X* term with or without bars, with single or multiple subscripts in an ascending or descending order) can be expressed in the form

$$F_{o\alpha\beta\ldots\gamma} = \sum_{IJ=ef}^{jk} a_{IJ}\ \frac{\partial F_{\alpha\beta\ldots\gamma}}{\partial\alpha_{IJ}} + \sum_{K=e}^{k} S_{KK}\ \frac{\partial F_{\alpha\beta\ldots\gamma}}{\partial\theta_K} \tag{2.9}$$

The Plücker coordinates for the lines e, ..., k in the capped and uncapped coordinate systems have been listed in Table 2.1 using equations (2.3), (2.4), (2.6) and (2.7).

2.2 Optimal Coordinate Systems

The Jacobian matrix, [J], of an N degree of freedom (DOF) serial manipulator (see Fig. 2.2) transforms the actuator velocities, $\underline{\dot{q}} = [\dot{q}_1, \dot{q}_2, \ldots, \dot{q}_N]^T$, into the twist $\underline{V} = [\underline{\omega}\ \underline{v}]^T$ representing the instantaneous motion of the hand and

$$\underline{V} = [J]\,\underline{\dot{q}} \tag{2.10}$$

Here $\underline{\omega}$ and $\underline{v}$ designate the angular velocity of the hand and the translational velocity of a reference point on the hand, respectively. The columns of the Jacobian are the coordinates of the screws representing the instantaneous joint motions 1, 2, ..., N in that order. These screw coordinates can be obtained using Table 2.1. For instance, for a fourth R (revolute) and fifth P (prismatic) joint they can be expressed by $\$_{4,2} = [X_3, Y_3, Z_3, X_{03}, Y_{03}, Z_{03}]^T$ and $\$_{5,2} = [0, 0, 0, X_{34}, Y_{34}, Z_{34}]^T$ in the frame B_2.

Utilizing Table 2.1, the screws constituting the columns of the Jacobian can be formulated in any of the bases B_1, B_2, ..., B_N or $\hat{B}_1$, $\hat{B}_2$, ..., $\hat{B}_N$, yielding the various forms of the Jacobian $[J_1]$, $[J_2]$, ..., $[J_N]$ or $[\hat{J}_1]$, $[\hat{J}_2]$, ..., $[\hat{J}_N]$. It is desirable to determine the "simplest" form in an algebraic sense, where the criterion for "simplicity" can be conveniently taken as the total number of terms in the components of the Jacobian when none of the dimensions of the robot is specified.

Table 2.1 Plücker Coordinates of the Lines in the Coordinate Systems B_h and $\hat{B}_h$.

Coordinate system B_h:

.
.
.

$$\$_{e,h} = [X_{hgf}, -X^*_{hgf}, Z_{gf}, X_{ohgf}, -X^*_{ohgf}, Z_{ogf}]^T$$

$$\$_{f,h} = [X_{hg}, -X^*_{hg}, \bar{Z}_g, X_{ohg}, -X^*_{ohg}, \bar{Z}_{og}]^T$$

$$\$_{g,h} = [s_{gh}s_h, s_{gh}c_h, c_{gh}, a_{gh}c_{gh}s_h + S_{hh}s_{gh}c_h, a_{gh}c_{gh}c_h \\ -S_{hh}s_{gh}s_h, -a_{gh}s_{gh}]^T$$

$$\$_{h,h} = [0, 0, 1, 0, 0, 0]^T$$

$$\$_{i,h} = [0, -s_{hi}, c_{hi}, 0, -a_{hi}c_{hi}, -a_{hi}s_{hi}]^T$$

$$\$_{j,h} = [X_i, Y_i, Z_i, X_{oi}, Y_{oi}, Z_{oi}]^T$$

$$\$_{k,h} = [X_{ij}, Y_{ij}, Z_{ij}, X_{oij}, Y_{oij}, Z_{oij}]^T$$

.
.
.

Coordinate system $\hat{B}_h$:

.
.
.

$$\$_{e,\hat{h}} = [X_{gf}, -Y_{gf}, Z_{gf}, X_{ogf}, -Y_{ogf}, Z_{ogf}]^T$$

$$\$_{f,\hat{h}} = [\bar{X}_g, -\bar{Y}_g, \bar{Z}_g, \bar{X}_{og}, -\bar{Y}_{og}, \bar{Z}_{og}]^T$$

$$\$_{g,\hat{h}} = [0, s_{gh}, c_{gh}, 0, a_{gh}c_{gh}, -a_{gh}s_{gh}]^T$$

$$\$_{h,\hat{h}} = [0, 0, 1, 0, 0, 0]^T$$

Table 2.1--continued.

$$\$_{i,\hat{h}} = [s_{hi}s_h,\ -s_{hi}c_h,\ c_{hi},\ a_{hi}c_{hi}s_h + S_{hh}s_{hi}c_h,\ -a_{hi}c_{hi}c_h + S_{hh}s_{hi}s_h,\ -a_{hi}s_{hi}]^T$$

$$\$_{j,\hat{h}} = [X_{hi},\ X^*_{hi},\ Z_i,\ X_{ohi},\ X^*_{ohi},\ Z_{oi}]^T$$

$$\$_{k,\hat{h}} = [X_{hij},\ X^*_{hij},\ Z_{ij},\ X_{ohij},\ X^*_{ohij},\ Z_{oij}]^T$$

.
.
.

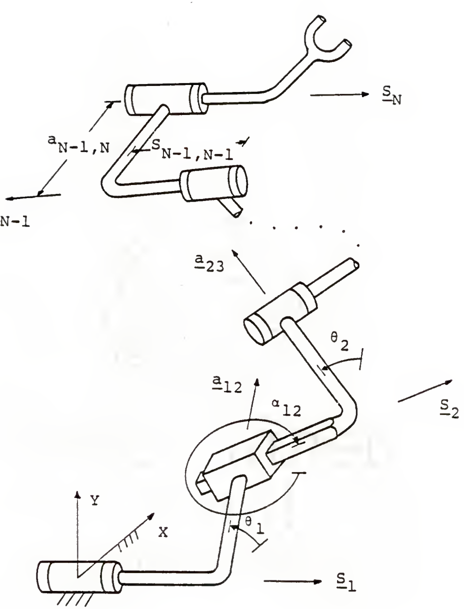

Fig. 2.2 A General Manipulator

The first step towards the solution is the calculation of the number of terms involved in the expansions of the recursive notations given in Appendix A. Let $X(i)$, $X^*(i)$, $Y(i)$ and $Z(i)$ designate the number of terms in the expansions of an X, X^*, Y and Z with i subscripts, where the subscripts can be in an ascending or descending order. Then, the recursive relations

$$X(i + 1) = X^*(i + 1) = X(i) + Y(i) \tag{2.11}$$

$$Y(i + 1) = Z(i + 1) = X(i) + Y(i) + Z(i) \tag{2.12}$$

can be used together with $X(1) = 1$ and $Y(1) = Z(1) = 2$ to obtain the results listed in Table 2.2(a). The table contains the number of terms in the P, P^*, Q, R, U, U^*, V and W terms also.

Table 2.2(b) lists the number of terms in the duals of P, P^*, Q, R, U, U^*, V, W, X, X^*, Y and Z, which are determined by the equation

$$F_o(i) = \sum_T \sum_{IJ} \sum_K \delta(s_{IJ}) + \delta(c_{IJ}) + \delta(s_K) + \delta(c_K) \tag{2.13}$$

where

F: Any one of P, P^*, Q, R, U, U^*, V, W, X, X^*, Y, Z.

K: Index running over all the possible subscripts of θ.

IJ: Index running over all the possible subscripts of α.

T: Term index running from 1 to $F(i)$.

and

$$\delta(s_{IJ}) = \begin{cases} 1 \text{ (if } s_{IJ} \text{ exists in the T'th term of F)} \\ 0 \text{ (otherwise)} \end{cases}$$

The variables $\delta(c_{IJ})$, $\delta(s_K)$ and $\delta(c_K)$ are similarly defined.

Table 2.2 Number of Terms in the Expansions of the Elements (and Their Duals) in Appendix A.

(a) Number of terms in the expansions of P, P^*, Q, R, U, U^*, V, W, X, X^*, Y, Z

	i					
	1	2	3	4	5	6
$P(i)$, $P^*(i)$, $U(i)$, $U^*(i)$	1	2	5	13	34	89
$Q(i)$, $R(i)$, $V(i)$, $W(i)$	1	3	8	21	55	144
$X(i)$, $X^*(i)$	1	3	8	21	55	144
$Y(i)$, $Z(i)$	2	5	13	34	89	233

(b) Number of terms in the expansions of the duals of P, P^*, Q, R, U, U^*, V, W, X, X^*, Y, Z

	i					
	1	2	3	4	5	6
$P_o(i)$, $P_o^*(i)$, $U_o(i)$, $U_o^*(i)$	1	5	20	71	235	744
$Q_o(i)$, $R_o(i)$, $V_o(i)$, $W_o(i)$	2	10	38	130	420	1308
$X_o(i)$, $X_o^*(i)$	2	10	38	130	420	1308
$Y_o(i)$, $Z_o(i)$	5	20	71	235	744	2285

Tables 2.1 and 2.2 can now be used to determine the optimal coordinate systems, B_{op}'s, for all types of 3, 4, 5 and 6 DOF serial manipulators consisting of R and P joints. Here the term "optimal" is used in the sense that the total number of terms in the Jacobian formulated in B_{op}, $[J_{op}]$, is a minimum. The results of this optimization are shown in the fourth and fifth columns of Table 2.3 where the manipulators are classified using the number of P joints. Groups 0 and 1... have, respectively, 0 and 1... prismatic joints.

The sixth column of the table provides the total number of terms (TNT) in $[\hat{J}_{N+1}]$, where N denotes the DOF of the manipulator. This number is an excellent indicator of the computational effort required to generate the Jacobian of a given type of manipulator with completely general dimensions. In order to facilitate the comparison of different types of manipulators, the normalized Hand Jacobian Performance Index, abbreviated by HJPI, is defined as

$$\text{HJPI} = \frac{\text{TNT in } [\hat{J}_{N+1}] \text{ for the given manipulator type}}{\text{TNT in } [\hat{J}_{N+1}] \text{ for the basis manipulator type}} \qquad (2.14)$$

where the basis manipulator types are PPP, PPPR, PPPRR and PPPRRR for 3, 4, 5 and 6 DOF robots, respectively. The type of the N DOF manipulator with the minimum TNT in $[\hat{J}_{N+1}]$ is here defined to be the basis manipulator type for the N DOF robots. Thus HJPI $\geq$ 1 and the numerical value for an HJPI indicates the difficulty, measured relative to the basis manipulator type, of generating $[\hat{J}_{N+1}]$.

During the design stage of a manipulator, the Hand Jacobian Performance Indices listed in Table 2.3 can be used for type synthesis

Table 2.3 Optimal and Minimal Coordinate Systems and Hand Jacobian Performances Indices for Serial Manipulators.

(a) 3 DOF Manipulators

Group	Type	B_{mi}	B_{op}	$TNT^{\dagger}$in $[J_{op}]$	$TNT^{\dagger}$in $[\hat{J}_4]$	HJPI
0	RRR	$B_2, \hat{B}_2$	$B_2, \hat{B}_2$	13	84	4.20
	PRR	B_2	B_2	8	34	1.70
1	RPR	$B_2, \hat{B}_2$	$B_2, \hat{B}_2$	13	72	3.60
	RRP	$\hat{B}_2$	$\hat{B}_2$	8	82	4.10
	PPR	B_2	$B_2, \hat{B}_3$	8	22	1.10
2	PRP	$B_2, \hat{B}_2$	$B_2, \hat{B}_2$	6	32	1.60
	RPP	$\hat{B}_2$	$B_1, \hat{B}_2$	8	70	3.50
3	PPP	$B_2, \hat{B}_2$	$B_2, \hat{B}_2$	6	20	1.00

Table 2.3--continued.

(b) 4 DOF Manipulators

Group	Type	B_{mi}	B_{op}	TNT†in $[J_{op}]$	TNT†in $[\hat{J}_5]$	HJPI
0	RRRR	$B_2, \hat{B}_3$	$B_2, \hat{B}_3$	30	298	5.32
1	PRRR	$\hat{B}_3$	$\hat{B}_3$	18	118	2.11
	RPRR	$\hat{B}_3$	$\hat{B}_3$	28	248	4.43
	RRPR	B_2	B_2	28	286	5.11
	RRRP	B_2	B_2	18	296	5.29
2	PPRR	$\hat{B}_3$	$B_3, \hat{B}_3$	16	68	1.21
	PRPR	B_2	$\hat{B}_3$	18	106	1.89
	PRRP	$B_2, \hat{B}_3$	$B_2, \hat{B}_3$	13	116	2.07
	RPPR	$B_2, \hat{B}_3$	$B_2, \hat{B}_3$	28	236	4.21
	RPRP	$\hat{B}_3$	B_2	18	246	4.39
	RRPP	B_2	$B_2, \hat{B}_2$	16	284	5.07
3	PPRP	$\hat{B}_3$	$\hat{B}_3$	11	66	1.18
	PPPR	B_3	$B_3, \hat{B}_3$	16	56	1.00
	RPPP	$\hat{B}_2$	$B_2, \hat{B}_2$	16	234	4.18
	PRPP	B_2	B_2	11	104	1.86

Table 2.3--continued.

(c) 5 DOF Manipulators

Group	Type	B_{mi}	B_{op}	TNT†in $[J_{op}]$	TNT†in $[\hat{J}_6]$	HJPI
0	RRRRR	B_3, $\hat{B}_3$	B_3, $\hat{B}_3$	63	987	6.29
	PRRRR	B_3	B_3	38	387	2.46
	RPRRR	B_3	B_3	58	807	5.14
1	RRPRR	B_3, $\hat{B}_3$	B_3, $\hat{B}_3$	63	937	5.97
	RRRPR	$\hat{B}_3$	$\hat{B}_3$	58	975	6.21
	RRRRP	$\hat{B}_3$	$\hat{B}_3$	38	985	6.27
	PPRRR	B_3	$\hat{B}_4$	31	207	1.32
	PRRPR	$\hat{B}_3$	B_3	36	375	2.39
	PRPRR	$\hat{B}_4$	B_3	38	337	2.15
	RPPRR	$\hat{B}_4$	B_3	58	757	4.82
2	PRRRP	B_3, $\hat{B}_3$	B_3, $\hat{B}_3$	26	385	2.45
	RPRPR	B_3, $\hat{B}_3$	B_3, $\hat{B}_3$	56	795	5.06
	RRPPR	B_2	$\hat{B}_3$	58	925	5.89
	RRPRP	B_2	$\hat{B}_3$	38	935	5.96
	RPRRP	B_3	$\hat{B}_3$	36	805	5.13
	RRRPP	$\hat{B}_3$	B_2	31	973	6.20
	PPRRP	B_3	B_3	21	205	1.31
	PPPRR	$\hat{B}_4$	$\hat{B}_4$	29	157	1.00
	PPRPR	B_3	B_3, $\hat{B}_4$	31	195	1.24
	PRPPR	$\hat{B}_3$	B_3	36	325	2.07
3	PRPRP	B_3, $\hat{B}_3$	B_3, $\hat{B}_3$	26	335	2.13
	RPPPR	B_3, $\hat{B}_3$	B_3, $\hat{B}_3$	56	745	4.75
	RPPRP	B_3	$\hat{B}_3$	36	755	4.81
	RPRPP	$\hat{B}_3$	B_2, $\hat{B}_3$	31	793	5.05
	RRPPP	B_2	B_2	29	923	5.88
	PRRPP	$\hat{B}_3$	$\hat{B}_3$	21	373	2.38

Table 2.3--continued.

(d) 6 DOF Manipulators

Group	Type	B_{mi}	B_{op}	TNT† in $[J_{op}]$	TNT† in $[\hat{J}_7]$	HJPI
0	RRRRRR	B_3, $\hat{B}_4$	B_3, $\hat{B}_4$	126	3128	7.11
1	PRRRRR	$\hat{B}_4$	$\hat{B}_4$	76	1220	2.77
	RPRRRR	$\hat{B}_4$	$\hat{B}_4$	114	2528	5.75
	RRPRRR	$\hat{B}_4$	$\hat{B}_4$	124	2948	6.70
	RRRPRR	B_3	B_3	124	3078	7.00
	RRRRPR	B_3	B_3	114	3116	7.08
	RRRRRP	B_3	B_3	76	3126	7.10
2	PPRRRR	B_3	B_4	59	620	1.41
	PRRRPR	$\hat{B}_4$	$\hat{B}_4$	71	1208	2.75
	PRPRRR	$\hat{B}_4$	$\hat{B}_4$	74	1040	2.36
	PRRPRR	B_3	$\hat{B}_4$	76	1170	2.66
	RPPRRR	$\hat{B}_4$	$\hat{B}_4$	112	2348	5.34
	RPRPRR	$\hat{B}_4$	$\hat{B}_4$	114	2478	5.63
	PRRRRP	B_3, $\hat{B}_4$	B_3, $\hat{B}_4$	51	1218	2.77
	RPRRPR	B_3, $\hat{B}_4$	B_3, $\hat{B}_4$	109	2516	5.72
	RRPPRR	B_3, $\hat{B}_4$	B_3, $\hat{B}_4$	124	2898	6.59
	RRPRPR	B_3	B_3	114	2936	6.67
	RRRPPR	B_3	B_3	112	3066	6.97
	RRPRRP	$\hat{B}_4$	B_3	76	2946	6.70
	RRRPRP	B_3	B_3	74	3076	6.99
	RPRRRP	B_3	B_3	71	2526	5.74
	RRRRPP	$\hat{B}_4$	$\hat{B}_3$	59	3114	7.08

Table 2.3--continued.

(d) 6 DOF Manipulators--continued

Group	Type	B_{mi}	B_{op}	TNT† in $[J_{op}]$	TNT† in $[\hat{J}_7]$	HJPI
3	PPRRRP	B_3	$\hat{B}_4$	39	618	1.40
	PRPRRP	$\hat{B}_4$	$\hat{B}_4$	49	1038	2.36
	PPPRRR	$\hat{B}_3$, B_4	B_4	54	440	1.00
	PPRRPR	B_3	B_4	57	608	1.38
	PPRPRR	B_3, $\hat{B}_4$	B_4	59	570	1.30
	PRPRPR	B_3, $\hat{B}_4$	$\hat{B}_4$	69	1028	2.34
	PRRPPR	B_3, $\hat{B}_4$	$\hat{B}_4$	71	1158	2.63
	PRPPRR	$\hat{B}_4$	$\hat{B}_4$	74	990	2.25
	RPPRPR	B_3	$\hat{B}_4$	107	2336	5.31
	RPPPRR	$\hat{B}_4$	$\hat{B}_4$	112	2298	5.22
	RRPPPR	B_3	B_3	112	2886	6.56
	RPRPPR	$\hat{B}_4$	B_3	107	2466	5.60
	RRPPRP	B_3	B_3	74	2896	6.58
	RPPRRP	B_3, $\hat{B}_4$	B_3	71	2346	5.33
	RPRPRP	B_3, $\hat{B}_4$	B_3	69	2476	5.63
	RRPRPP	B_3, $\hat{B}_4$	$\hat{B}_3$	59	2934	6.67
	RPRRPP	$\hat{B}_4$	$\hat{B}_3$	57	2514	5.71
	RRRPPP	$\hat{B}_3$, B_4	$\hat{B}_3$	54	3064	6.96
	PRRPRP	B_3	B_3	49	1168	2.65
	PRRRPP	$\hat{B}_4$	B_3	39	1206	2.74

---

†: Components of the Jacobian which are zero do not contribute to the total number of terms.

purposes, provided that the control algorithm to be implemented takes advantage of $[J_H]$. Since the indices provide a quantitative measure, it is also possible to make trade-offs between different types due to other design constraints. Here $[J_H]$ and $[J_B]$ designate the two Jacobians which yield $\underline{V} = [\underline{\omega}\ \underline{v}]^T$ in the hand and base coordinates, respectively, where $\underline{v}$ is the translational velocity of a fixed reference point on the end effector.

The Jacobian $[J_B]$ cannot be obtained directly by using one of the capped or uncapped coordinate systems. However, the screw transformation matrix (see Yuan and Freudenstein, 1971; Sugimoto and Matsumoto, 1984) can be conveniently used to transform either one of the natural Jacobians $[J_i]$ or $[\hat{J}_i]$ $(i = 1, 2, \ldots, N)$ into $[J_B]$.

An alternative derivation of the screw transformation matrix, $[{}^b\$_a]$, relating the coordinates of a screw $\$_e$ in the reference frames a and b via the equation

$$\$_{e,b} = [{}^b\$_a]\ \$_{e,a}$$

indicates that this matrix can be represented in the following two different, but equivalent, forms:

$$[{}^b\$_a] = \begin{bmatrix} [{}^bR_a] & [0] \\ [{}^bR_a]\,[E_a] & [{}^bR_a] \end{bmatrix} \qquad (2.15)$$

$$[{}^b\$_a] = \begin{bmatrix} [{}^bR_a] & [0] \\ [E_b]\,[{}^bR_a] & [{}^bR_a] \end{bmatrix} \qquad (2.16)$$

where the skew symmetric matrices $[E_a]$ and $[E_b]$ are given by

$$[E_a] = \begin{bmatrix} 0 & -m_a & l_a \\ m_a & 0 & -k_a \\ -l_a & k_a & 0 \end{bmatrix} \tag{2.17}$$

$$[E_b] = \begin{bmatrix} 0 & -m_b & l_b \\ m_b & 0 & -k_b \\ -l_b & k_b & 0 \end{bmatrix} \tag{2.18}$$

with $[k_a, l_a, m_a]^T$ and $[k_b, l_b, m_b]^T$ being the coordinates of the vector from 0_b to 0_a, $\underline{r}_{ba}$, in the a'th and b'th coordinate systems, respectively. Furthermore, $[{}^bR_a]$ denotes the 3 × 3 rotation matrix converting the coordinates of a vector in the a'th system to the coordinates in the b'th system. Either one of the forms of $[{}^b\$_a]$ can be used. This depends on the coordinate system used to express $\underline{r}_{ba}$. It should be noted that from equations (2.15) and (2.16)

$$[{}^a\$_b] = [{}^b\$_a]^{-1} = \begin{bmatrix} [{}^bR_a]^T & [0] \\ [E_a]^T\,[{}^bR_a]^T & [{}^bR_a]^T \end{bmatrix} \tag{2.19}$$

or

$$[{}^a\$_b] = [{}^b\$_a]^{-1} = \begin{bmatrix} [{}^bR_a]^T & [0] \\ [{}^bR_a]^T\,[E_b]^T & [{}^bR_a]^T \end{bmatrix} \tag{2.20}$$

Here, $[{}^bR_a]^T = [{}^bR_a]^{-1} = [{}^aR_b]$.

The Jacobian $[J_B]$ can now be determined from either of the equations

$$[J_B] = [{}^B\$_h]\ [J_h] \tag{2.21}$$

$$[J_B] = [{}^B\$_{\hat{h}}]\ [\hat{J}_h] \tag{2.22}$$

where h = 1, 2, ..., N (see Chapter 5).

2.3 Hypersurfaces of Special Configurations

2.3.1 Minimal Coordinate Systems

An N DOF manipulator is said to be in a special configuration, sometimes referred to as a singular configuration, whenever the screws constituting the columns of the Jacobian become dependent. This is equivalent to saying that instantaneously the order of the screw system (see Sugimoto and Duffy, 1982), which is defined as the number of screws in its base, is strictly less than N. Hence the robot loses at least one of its degrees of freedom.

For a set of N screws, $\$_e$, $\$_h$, ..., $\$_k$, $\$_m$, with $2 \le N \le 6$, let us define $G_\alpha(e, h, \ldots, k, m)$ by

$$G_\alpha(e, h, \ldots, k, m) = \left|[g_\alpha]^T\ [g_\alpha]\right| \tag{2.23}$$

where

$$[g_\alpha] = \begin{bmatrix} \$_{e,\alpha} & \$_{h,\alpha} & \cdots & \cdots & \$_{k,\alpha} & \$_{m,\alpha} \end{bmatrix} \tag{2.24}$$

Clearly, $G_\alpha(e, h, \ldots, k, m)$ is the Gramian of the screws $\$_e$, $\$_h$,

$\ldots, \$_k, \$_m$ computed in the coordinate system B_α. Hence, it follows immediately that these screws are dependent if and only if

$$G_\alpha(e, h, \ldots, k, m) = 0 \tag{2.25}$$

Since dependency, or independency, of a set of screws is invariant with respect to coordinate transformations,[1] any coordinate system can be used in equation (2.25). However, it is important to note that in general $G_\alpha(e, h, \ldots, k, m) \neq G_\beta(e, h, \ldots, k, m)$ unless the β'th coordinate system can be obtained from the α'th one by a pure rotation. Furthermore, for N=6 equation (2.23) yields $G_\alpha(1, 2, \ldots, 5, 6) = |J_\alpha|^2$, which is invariant with respect to all coordinate transformations. These results can be obtained by expanding the determinant

$$G_\beta(e, h, \ldots, k, m) = \left|[g_\alpha]^T \, [{}^\beta\$_\alpha]^T \, [{}^\beta\$_\alpha] \, [g_\alpha]\right| \tag{2.26}$$

utilizing the definition of $[{}^\beta\$_\alpha]$ from either of the equations (2.15) or (2.16).

Consider now the equation

$$\sum_{I=1}^{I={}_K C_N \;\leftarrow \binom{N}{K}} G_\alpha^2(\{D;K\}_I) = 0 \tag{2.27}$$

for an N DOF manipulator where $D = \{1, 2, \ldots, N\}$ and $\{D;K\}_I$ denotes the I'th combination of the elements of the set D taken K at a time.

---

[1] "Coordinate transformations" refer to translations and rotations only.

If this equation can be represented as $(G)^b = 0$ for an integer $b \geq 2$, it should be replaced by $G = 0$. Equation (2.27) defines a hypersurface in the joint space of the manipulator. This surface will be called the hypersurface of special configurations of order K which will be abbreviated by HSC-K. It follows from this definition that whenever the joint displacement vector, $\underline{q}$, satisfies equation (2.27) (i.e., $\underline{q}$ is on HSC-K) the order of the screw system defined by the joint screws of the manipulator becomes strictly less than K. Obviously, HSC-2 $\subset$ HSC-3 $\subset$ ... ... $\subset$ HSC-N. Further the manipulator has exactly K degrees of freedom whenever $\underline{q} \in$ [HSC-(K+1) \ HSC-K] where K = N, N-1, ... and \ denotes the "subtraction" operation of sets. For notational convenience HSC-N will simply be called the hypersurface of special configurations (HSC). It should be noted that here the terminology "hypersurface" is used loosely.

By using different coordinate systems, B_α's, for the different terms in equation (2.27), distinct closed-form equations are obtained for the HSC-K. These equations can be used to advantage in order to reduce the amount of work involved in the determination of HSC-K. This work may be considerable, especially for robots having general dimensions.

Let the I'th term of equation (2.27) be $G_\alpha^2(e, h, \ldots, k, m)$. The coordinate system which minimizes the number of terms (before any simplifications) in $G_\alpha(e, h, \ldots, k, m)$ will be said to be the minimal coordinate system, B_{mi}, for the I'th term. If all the terms are formulated in their respective B_{mi}'s, then the equation obtained will be called the minimal equation of the HSC-K. This is the most convenient equation for the HSC-K (K = 6, 5, ...). For instance, for a general 6R robot the number of terms (before any simplifications) in the equation for the HSC is 0.000013824×10^9, 0.16811736×10^9 and 4.9241043×10^9, respectively, when the coordinate systems B_3 (the minimal coordinate system), $\hat{B}_1$ and $\hat{B}_7$ are used in equation (2.27). It should be recalled that for the particular case of K = 6 all of the equations for the HSC-6 reduce to the same equation after regrouping of terms and introduction of trigonometric identities.

For a set of screws $\$_e, \$_h, \ldots, \$_k, \$_m$, where e, h, ..., k, m is a set of successive integers, the minimal coordinate system for $G_\alpha(e, h, \ldots, k, m)$ can be readily determined using Table 2.3 by appropriately incrementing the subscript of the minimal coordinate system shown there. For example, B_{mi} for $G_\alpha(3, 4, 5, 6)$, where the third, fourth and sixth joints are prismatic and the fifth one is revolute, is $\hat{B}_5$. This result is obtained simply by incrementing the subscript of $\hat{B}_3$, the minimal coordinate system for a PPRP manipulator, by 2. When e, h, ..., k, m fails to be a successive set, B_{mi} can be determined utilizing Tables 2.1 and 2.2.

2.3.2 Determining Equations

In this section it will be proved that when K < N there exists N equations which are equivalent to equation (2.27). This important result should be used to advantage since the simplest of these N equations formulated in their respective minimal coordinate systems provides the most convenient equation for the HSC-K. Each of these N equations, which is of the form of equation (2.28), has ${}_K C_{N-1}$ less $G_\alpha^2(\ldots)$ terms than (2.27).

Theorem 2.1: If $N \geq 3$ and $2 \leq K \leq N-1$, then the equation

$$\sum_{J=1}^{{}_{K-1}C_{N-1}} G_{\alpha}^{2}(E \cup \{D \setminus E;\ K-1\}_{J}) = 0, \tag{2.28}$$

where E designates any singleton subset of $D = \{1, 2, \ldots, N\}$, is equivalent to (2.27) which is repeated below for convenience.

$$\sum_{I=1}^{{}_{K}C_{N}} G_{\alpha}^{2}(\{D;K\}_{I}) = 0 \tag{2.27}$$

Proof: It is clear that equation (2.28) is true whenever equation (2.27) is true. However, in order to prove that (2.28) implies (2.27) it is necessary to show that

$$\sum_{H=1}^{{}_{K}C_{N-1}} G^{2}(\{D \setminus E;\ K\}_{H}) = 0 \tag{2.29}$$

provided that equation (2.28) is satisfied. Here (and throughout the rest of the proof) the subscript α is dropped for convenience, because the proof does not depend on the bases used to formulate the Gramians defined in equation (2.23). The proof is divided into 2 cases. In the first case $K = N-1$ and in the second one $2 \leq K \leq N-2$.

Case 1: $K = N-1$

Without loss of generality let $E = \{1\}$. Now, equation (2.28) implies that all possible combinations of the screws $\$_1, \$_2, \ldots, \$_N$ (which include $\$_1$) are dependent; i.e., there exists $a_{ij} \in R$ such that

$$
\begin{array}{l}
a_{11}\$_1 \qquad\qquad + a_{13}\$_3 + a_{14}\$_4 + \dots + a_{1N}\$_N = \$_o \\
a_{21}\$_1 + a_{22}\$_2 \qquad\qquad + a_{24}\$_4 + \dots + a_{2N}\$_N = \$_o \\
a_{31}\$_1 + a_{32}\$_2 + a_{33}\$_3 \qquad\qquad + \dots + a_{3N}\$_N = \$_o \\
\vdots \qquad\qquad\qquad\qquad\qquad \vdots \\
a_{(N-1)1}\$_1 + a_{(N-1)2}\$_2 + \dots + a_{(N-1)(N-1)}\$_{N-1} = \$_o
\end{array}
\tag{2.30}
$$

where $\$_o$ is the zero screw (i.e., $\$_o = [0, 0, 0, 0, 0, 0]^T$) and at least 2 of the a_{ik}'s for each $i = 1, 2, \dots, N-1$ are nonzero. This last assertion is a consequence of the fact that none of the screws $\$_1, \$_2, \dots, \$_N$ is the zero screw. Equation (2.29), on the other hand, implies that the screws $\$_2, \$_3, \dots, \$_{N-1}, \$_N$ are dependent, which is the claim that has to be proved. Let NZ denote the number of zeros in the set $\{a_{11}, a_{21}, \dots, a_{(N-1)1}\}$ and note that NZ stays invariant when each equation in the set (2.30) is multiplied by a nonzero real number. Now consider the 3 cases $NZ \geq 2$, $NZ = 1$ and $NZ = 0$.

(a) $NZ \geq 2$: Without loss of generality, let $a_{11} = a_{21} = 0$. Then, from the first and second equations of the set (2.30) we get

$$a_{13}\$_3 + a_{14}\$_4 + \dots \quad \dots + a_{1N}\$_N = \$_o \tag{2.31}$$

$$a_{22}\$_2 \qquad + a_{24}\$_4 + \dots \quad \dots + a_{2N}\$_N = \$_o \tag{2.32}$$

which yield $a_{22}\$_2 + a_{13}\$_3 + (a_{14} + a_{24})\$_4 + (a_{15} + a_{25})\$_5 + \dots + (a_{1N} + a_{2N})\$_N = \$_o$ when added together. If $a_{22} \neq 0$ or $a_{13} \neq 0$ or at least one of the sums $(a_{1j} + a_{2j})$ for $j = 4, 5, \dots, N$ is nonzero, then the screws $\$_2, \$_3, \dots, \$_N$ are dependent. Hence, the only remaining possibility for these screws to be independent is when $a_{22} = a_{13} = 0$ and $(a_{1j} + a_{2j}) = 0$ for $j = 4, 5, \dots, N$. But $a_{1j} + a_{2j} = 0$ implies either $a_{1j} = a_{2j} = 0$ or $a_{1j} = -a_{2j}$. Since all of $a_{13}, a_{14}, \dots, a_{1N}$ cannot be zero simultaneously, there is at least one case such that $a_{1j} = -a_{2j} \neq 0$. Let this be the case, for instance, for $(a_{14} + a_{24})$; i.e., $a_{14} + a_{24} = 0$; $a_{14} \neq 0$; $a_{24} \neq 0$. Multiplying equation (2.31) by any $\lambda \neq 0$ and adding to (2.32) we obtain $0\$_2 + 0\$_3 + (\lambda a_{14} + a_{24})\$_4 + 0\$_5 + \dots + 0\$_N = \$_o$. Clearly $\lambda a_{14} + a_{24} \neq 0$, and hence the screws $\$_2, \$_3, \dots, \$_N$ have to be dependent.

(b) NZ = 1: Without loss of generality, let $a_{11} = 0$. Then, from the first equation of the set (2.30), it follows that $\$_3, \$_4, \dots, \$_N$ (and hence $\$_2, \$_3, \dots, \$_N$) are dependent.

(c) NZ = 0:[1] Choose any two of the equations, say the first two, in the set (2.30). Solving for $\$_1$ in each of the equations we obtain

---

[1] For N = 3 only, the proof for NZ = 0 is modified as follows. Equations (2.33) and (2.34) will simplify to

$$\$_1 = \lambda_1\$_2 \tag{2.35}$$

and

$$\$_1 = \lambda_2\$_3 \tag{2.36}$$

for some $\lambda_1 \neq 0$, $\lambda_2 \neq 0$. Subtracting (2.36) from (2.35) we get

$$\$_o = \lambda_1\$_2 - \lambda_2\$_3$$

which implies that $\$_2$ and $\$_3$ are dependent.

$$\$_1 = \qquad b_3\$_3 + b_4\$_4 + \dots + b_N\$_N \tag{2.33}$$

$$\$_1 = d_2\$_2 \qquad + d_4\$_4 + \dots + d_N\$_N \tag{2.34}$$

where $b_3, \dots, b_N$ and $d_2, \dots, d_N$ are unique. Here, at least one of the b_i's and one of the d_i's must be nonzero. Subtracting equation (2.34) from equation (2.33) we get

$$-d_2\$_2 + b_3\$_3 + (b_4 - d_4)\$_4 + \dots + (b_N - d_N)\$_N = \$_o$$

If $d_2 \neq 0$ or $b_3 \neq 0$ or at least one of the differences $(b_i - d_i)$ for $i = 4, 5, \dots, N$ is nonzero, then the screws $\$_2, \$_3, \dots, \$_N$ are dependent. Hence, the only remaining possibility for these screws to be independent is when $d_2 = b_3 = 0$ and $b_i - d_i = 0$ for $i = 4, 5, \dots, N$. Now, suppose $b_4 \neq 0$ in equation (2.33). Then substituting $b_3 = 0$ into (2.33) and substituting the result into the third equation of the set (2.30) (i.e., the equation which does not contain $\$_4$) we obtain

$$(a_{32})\$_2 + (a_{33})\$_3 + (a_{31}b_4)\$_4 + (a_{31}b_5\$_5 + a_{35})\$_5$$

$$+ (a_{31}b_6 + a_{36})\$_6 + \dots + (a_{31}b_N + a_{3N})\$_N = \$_o.$$

Here, the coefficient of $\$_4$ is nonzero. Hence, the screws $\$_2, \$_3, \dots, \$_N$ must be dependent.

Case 2: $2 \leq K \leq N-2$

Consider any term in equation (2.29), say the H'th term $G^2(\{D \setminus E;\ K\}_H)$. Define $D' = E \cup \{D \setminus E;\ K\}_H$ and let $N' = K + 1$. Then it can be concluded that

$$\sum_{J=1}^{{}_{K-1}C_{N'-1}} G^2(E \cup \{D' \setminus E;\ K-1\}_J) = 0$$

because all of the $(N' - 1)$ terms in the above summation always exist in the left-hand side of equation (2.28) and hence have to be individually equal to zero. Therefore, from the result of case 1, it follows that $G^2(\{D \setminus E;\ K\}_H) = 0$. Each term in equation (2.29) can be shown to be equal to zero using this procedure and thus the proof is completed.

■

CHAPTER 3
CONCEPTS RELATED TO THE HYPERSURFACES OF SPECIAL CONFIGURATIONS

In this chapter the novel concepts of passive/active joints, component/subcomponent manifolds of the HSC, configurations/subconfigurations and their applications are presented. The chapter also contains a theorem which predicts the existence of passive joints, a synthesis procedure for passive joints and illustrative examples.

3.1 Passive Joints and Dimensions

It follows from equation (2.27) that the HSC is determined by $|J| = 0$. Although $|J|$ is invariant with respect to all coordinate transformations, it is useful to find expressions for it in the ten bases $B_1, \ldots, B_5$ and $\hat{B}_2, \ldots, \hat{B}_6$. Expressions for $|J_6|$ and $|\hat{J}_1|$ are omitted because they are excessively complicated. Before proceeding it is useful to introduce a number of definitions.

A naturally passive joint is defined here to be a joint such that when actuated alone, it cannot change the order of the screw system determined by the columns of the Jacobian. Equivalently, actuation of a naturally passive joint alone does not change the incidence relationship between $\underline{q}$ and the HSC of any order. Clearly, the first and last joints of a serial manipulator are always naturally passive. A passive joint of order K is defined as a joint with the property that when actuated alone it cannot change the incidence relationship between q and HSC-K. A joint which is not passive of order K will be said to be an active joint[1] of order K. For the sake of conciseness these two types of joints will simply be called passive and active when K = N. Finally, it should be noted that a passive joint of order K is not necessarily passive of order F unless K = F.

If all the HSC-K's (K = 6, 5, ...) of a manipulator are invariant with respect to changes in a dimension of the robot, then that dimension will be called a naturally passive dimension. For example, S_{11} and S_{NN} (θ_1 and θ_N) are naturally passive dimensions for all manipulators with R (P) joints as the first and last joints. Clearly, regardless of the type of the manipulator $a_{(N)(N+1)}$ is naturally passive as well. On the other hand, a passive dimension of order K is defined to be a dimension with respect to which HSC-K is invariant. As in the case of passive joints, this kind of dimension will simply be called a passive one whenever K = N.

Finally, the degrees of the HSC in the joint variables and dimensions of the manipulator are defined in the following manner. If P_j denotes the summation of the powers of s_i and c_i in the j'th term (the power of S_{ii} in the j'th term) of the equation for the HSC, and if the maximum of P_j over all the terms is equal to p, then the HSC will be said to be of degree p in the angular joint variable θ_i (linear, i.e., prismatic, joint variable S_{ii}). The definitions of the degrees of the HSC in the angular and linear dimensions of the manipulator can be obtained by replacing "joint variable" with "dimension" in the preceding statement. It should be noted that if the degree of the HSC in a joint variable or dimension is zero, then that joint or dimension is passive. However, the converse is not necessarily true.

---

[1] The active/passive joints defined in this dissertation are geometric concepts, and they do not imply the presence/absence of a motor or other primary drive.

Each of the Jacobian matrices formulated in the bases $B_1, B_2, \ldots, B_5$ contains a pair of columns of the form $[0\ 0\ 1\ 0\ 0\ 0]^T$ and $[0\ *\ *\ 0\ *\ *]^T$ (see Table 2.1). Thus, $|J_\alpha|$ ($\alpha = 1, 2, \ldots, 5$) can be expressed as the summation of three 4 × 4 determinants.

$$|J_\alpha| = j_{6\beta}\ |1,2,4,5;p,q,r,s| - j_{2\beta}\ |1,4,5,6;p,q,r,s| - j_{5\beta}|1,2,4,6;p,q,r,s| \tag{3.1}$$

where

$$[J_\alpha] = \begin{bmatrix} j_{11} & j_{12} & \cdots & j_{16} \\ \cdot & & & \cdot \\ \cdot & & & \cdot \\ \cdot & & & \cdot \\ j_{61} & j_{62} & \cdots & j_{66} \end{bmatrix}, \quad \beta = \alpha + 1,$$

p, q, r and s are the integers from 1 to 6, excluding α and β, in an ascending order; and $|r_1, r_2, \ldots, r_n; p_1, p_2, \ldots, p_n|$ is the shorthand notation for the determinant of the n × n submatrix formed from the rows $r_1, r_2, \ldots, r_n$ and columns $p_1, p_2, \ldots, p_n$ (in the given order) of $[J_\alpha]$. Using the Laplace expansion of determinants (see, for example, Hadley, 1977), equation (3.1) can be decomposed into the following 20 distinct 2 × 2 determinants.

$$
\begin{aligned}
|J_\alpha| = {} & |1,4;p,q| \; (-j_{2\beta}|5,6;r,s| + j_{5\beta} \; |2,6;r,s| \\
& -j_{6\beta} \; |2,5;r,s|) + |1,4;r,s| \; (-j_{2\beta} \; |5,6;p,q| \\
& +j_{5\beta} \; |2,6;p,q| - j_{6\beta} \; |2,5;p,q|) \\
& + |1,5;p,q| \; (j_{2\beta} \; |4,6;r,s| - j_{6\beta} \; |4,2;r,s|) \\
& + |1,6;p,q| \; (-j_{2\beta} \; |4,5;r,s| + j_{5\beta} \; |4,2;r,s|) \\
& + |4,5;p,q| \; (-j_{2\beta} \; |1,6;r,s| + j_{6\beta} \; |1,2;r,s|) \\
& + |4,6;p,q| \; (j_{2\beta} \; |2,5;r,s| - j_{5\beta} \; |1,2;r,s|) \\
& + |4,2;p,q| \; (j_{5\beta} \; |1,6;r,s| - j_{6\beta} \; |1,5;r,s|) \\
& + |1,2;p,q| \; (-j_{5\beta} \; |4,6;r,s| + j_{6\beta} \; |4,5;r,s|) \qquad (3.2)
\end{aligned}
$$

If the α'th joint of the manipulator is a P joint, the integers 4, 5 and 6 in (3.1) and (3.2) should be replaced by 3, 4 and 5, respectively.

The right-hand sides of equations (3.1) and (3.2) can be used to obtain $|\hat{J}_\alpha|$ (α = 2, 3, 4, 5, 6). Here, $\beta = \alpha - 1$ and j_{de} denotes the component of $[\hat{J}_\alpha]$ in the d'th row and e'th column.

The equation of the HSC for any type of 6 DOF manipulator is best determined using equation (3.2) together with Tables 2.1 and 2.3. It should be noted that all industrial robots have many angular dimensions which are multiples of π or $\pi/2$ and many linear dimensions are zero. This results in further simplifications and the expansions can be performed manually.

The degree of the HSC in any joint variable or in any dimension could be determined by fully expanding the equation of the HSC. This is a tedious and time consuming process for a robot with general dimensions. However, the apparent degree of the HSC in any parameter (joint variable or dimension) can be determined without expanding the 2 × 2 determinants of equation (3.2). The X, Y, Z and X^* terms are all linear in the sines and cosines of the joint variables and dimensions that they contain. Using equation (3.2) in conjunction with Table 2.1, the apparent degree of the HSC in any parameter can be determined in each of the 10 bases and the minimum degree thus obtained is selected. The results for all possible types of 6 DOF manipulators are listed in Table 3.1. It is interesting to note that reversing the order of the joints, viz PRRRRR and RRRRRP, reverses the degrees of the HSC in the various parameters. For instance the degrees of a_{12}, a_{23}, a_{34}, a_{45} and a_{56} for the PRRRRR robot are 0, 1, 2, 2 and 1 which are equal to the degrees of the HSC in a_{56}, a_{45}, a_{34}, a_{23} and a_{12} for the RRRRRP robot. The degrees of the HSC in $(S_{22}, S_{33}, S_{44}, S_{55})$, $(\alpha_{12}, \alpha_{23}, \alpha_{34}, \alpha_{45}, \alpha_{56})$, and $(\theta_2, \theta_3, \theta_4, \theta_5)$ exhibit this same property.

It is important to note that the degrees shown in Table 3.1 are lowest upper bounds which may be achieved when the robot has completely general, arbitrary dimensions. The same comment is valid for A, the dimension of the active joint space, shown in the last column of the table. However, when the upper bound of the degree of a joint variable or dimension is equal to zero, then that joint or dimension is always passive regardless of the other dimensions. For example all of the linear dimensions and prismatic joint variables of

Table 3.1 Degrees of the HSC in the Joint Variables and Dimensions.

		Degree* of the HSC in																	
Group	Type	a_{12}	a_{23}	a_{34}	a_{45}	a_{56}	S_{22}	S_{33}	S_{44}	S_{55}	α_{12}	α_{23}	α_{34}	α_{45}	α_{56}	θ_2	θ_3	θ_4	θ_5	A
0	RRRRRR	1	2	2	2	1	1	2	2	1	1	2	3	2	1	(1)	(2)	(2)	(1)	4
	PRRRRR	0	1	2	2	1	0	1	2	1	1	2	3	2	1	(1)	(2)	(2)	(1)	4
	RPRRRR	1	1	2	2	1	(1)	1	2	1	1	2	3	2	1	1	(2)	(2)	(1)	4
1	RRPRRR	1	1	1	2	1	1	(2)	2	1	1	2	3	2	1	(1)	2	(2)	(1)	4
	RRRPRR	1	2	1	1	1	1	2	(2)	1	1	2	3	2	1	(1)	(2)	2	(1)	4
	RRRRPR	1	2	2	1	1	1	2	1	(1)	1	2	3	2	1	(1)	(2)	(2)	1	4
	RRRRRP	1	2	2	1	0	1	2	1	0	1	2	3	2	1	(1)	(2)	(2)	(1)	4
	PPRRRR	0	0	1	1	1	(0)	0	1	1	1	2	2	2	1	1	(2)	(2)	(1)	3
	PRRRPR	0	1	1	1	1	0	1	1	(1)	1	2	3	2	1	(1)	(2)	(2)	1	4
	PRPRRR	0	1	1	1	1	0	(1)	1	1	1	2	3	2	1	(1)	2	(2)	(1)	4
	PRRPRR	0	1	1	1	1	0	1	(1)	1	1	2	3	2	1	(1)	(2)	2	(1)	4
	RPPRRR	1	0	1	1	1	(1)	(1)	1	1	1	2	3	2	1	1	2	(2)	(1)	4
	RPRPRR	1	1	1	1	1	(1)	1	(1)	1	1	2	3	2	1	1	(2)	2	(1)	4
	PRRRRP	0	1	1	1	0	0	1	1	0	1	2	3	2	1	(1)	(2)	(2)	(1)	4
2	RPRRPR	1	1	1	1	1	(1)	1	1	(1)	1	2	3	2	1	1	(2)	(2)	1	4
	RRPPRR	1	1	0	1	1	1	(1)	(1)	1	1	2	3	2	1	(1)	2	2	(1)	4
	RRPRPR	1	1	1	1	1	1	(1)	1	(1)	1	2	3	2	1	(1)	2	(2)	1	4
	RRRPPR	1	1	1	0	1	1	1	(1)	(1)	1	2	3	2	1	(1)	(2)	2	1	4
	RRPRRP	1	1	1	1	0	1	(1)	1	0	1	2	3	2	1	(1)	2	(2)	(1)	4
	RRRPRP	1	1	1	1	0	1	1	(1)	0	1	2	3	2	1	(1)	(2)	2	(1)	4
	RPRRRP	1	1	1	1	0	(1)	1	1	0	1	2	3	2	1	1	(2)	(2)	(1)	4
	RRRRPP	1	1	1	0	0	1	1	0	(0)	1	2	2	2	1	(1)	(2)	(2)	1	3

Table 3.1--continued.

Group	Type	Degree* of the HSC in a_{12}	a_{23}	a_{34}	a_{45}	a_{56}	S_{22}	S_{33}	S_{44}	S_{55}	α_{12}	α_{23}	α_{34}	α_{45}	α_{56}	θ_2	θ_3	θ_4	θ_5	A
3	PPRRRP	0	0	0	0	0	(0)	0	0	0	1	2	2	2	1	1	(2)	(2)	(1)	3
	PRPRRP	0	0	0	0	0	0	(0)	0	0	1	2	3	2	1	(1)	2	(2)	(1)	3
	PPPRRR	0	0	0	0	0	(0)	(0)	0	0	1	1	2	1	1	1	2	(2)	(1)	2
	PPRRPR	0	0	0	0	0	(0)	0	0	(0)	1	2	2	2	1	1	(2)	(2)	1	2
	PPRPRR	0	0	0	0	0	(0)	0	(0)	0	1	2	2	2	1	1	(2)	2	(1)	2
	PRPRPR	0	0	0	0	0	0	(0)	0	(0)	1	2	3	2	1	(1)	2	(2)	1	2
	PRRPPR	0	0	0	0	0	0	0	(0)	(0)	1	2	3	2	1	(1)	(2)	2	1	2
	PRPPRR	0	0	0	0	0	0	(0)	(0)	0	1	2	2	2	1	(1)	2	2	(1)	2
	RPPRPR	0	0	0	0	0	(0)	(0)	0	(0)	1	2	3	2	1	1	2	(2)	1	1
	RPPPRR	0	0	0	0	0	(0)	(0)	(0)	0	1	2	2	2	1	1	2	2	(1)	1
	RRPPPR	0	0	0	0	0	0	(0)	(0)	(0)	1	2	2	2	1	(1)	2	2	1	1
	RPRPPR	0	0	0	0	0	(0)	0	(0)	(0)	1	2	3	2	1	1	(2)	2	1	1
	RRPPRP	0	0	0	0	0	0	(0)	(0)	0	1	2	2	2	1	(1)	2	2	(1)	2
	RPPRRP	0	0	0	0	0	(0)	(0)	0	0	1	2	3	2	1	1	2	(2)	(1)	2
	RPRPRP	0	0	0	0	0	(0)	0	(0)	0	1	2	3	2	1	1	(2)	2	(1)	2
	RRPRPP	0	0	0	0	0	0	(0)	0	(0)	1	2	2	2	1	(1)	2	(2)	1	2
	RPRRPP	0	0	0	0	0	(0)	0	0	(0)	1	2	2	2	1	1	(2)	(2)	1	2
	RRRPPP	0	0	0	0	0	0	0	(0)	(0)	1	1	2	1	1	(1)	(2)	2	1	2
	PRRPRP	0	0	0	0	0	0	0	(0)	0	1	2	3	2	1	(1)	(2)	2	(1)	3
	PRRRPP	0	0	0	0	0	0	0	0	(0)	1	2	2	2	1	(1)	(2)	(2)	1	3

* Degrees of the joint variables are shown in parentheses.

group 3 manipulators are passive. This fact can easily be deduced by using the Laplace method to expand $|J|$ with respect to the columns which represent the screw coordinates of the P joints. Furthermore, it follows that for any group 3 manipulator the $|J|$ is dimensionless. It can be shown that the dimension of $|J|$ for any group 2, group 1 and group 0 manipulator is (length), (length)^2 and (length)^3, respectively.

3.2 Configurations and Component Manifolds

A single equation, $F(x_1, x_2, \ldots, x_n) = 0$, in the n variables $x_1, x_2, \ldots, x_n$ with $\frac{\partial F}{\partial x_i} \in C^\infty$ for $i = 1, 2, \ldots, n$ will be said to define an (n-1)-manifold, consisting of the points satisfying $F(x_1, x_2, \ldots, x_n) = 0$, in R^n. This manifold will be linear if $F(x_1, x_2, \ldots, x_n)$ is linear in all of the n variables. Here the term "manifold" is used loosely and can refer to arbitrary point sets as well. The (n-1)-dimensional $x_1, x_2, \ldots, x_{i-1}, x_{i+1}, \ldots, x_n$ slice at $x_i = c$ will denote the points of the (n-2)-manifold defined by $F(x_1, x_2, \ldots, x_n) = 0$ and $x_i - c = 0$. If all possible $x_1, x_2, \ldots, x_{i-1}, x_{i+1}, \ldots, x_n$ slices yield (n-2)-manifolds that can be obtained from each other by a translation of the origin along the x_i axis, then the (n-1)-manifold defined by $F(x_1, x_2, \ldots, x_n) = 0$ will be said to be parallel to the x_i axis.

The HSC of an N DOF manipulator, defined by equation (2.27), is an (N-1)-manifold in the joint space of the robot. However, this (N-1)-manifold is parallel to the naturally passive and passive joint axes. Therefore, it is sufficient to analyze it as an (A-1)-manifold in R^A consisting of the A active joints. Because there exists 2 naturally passive joints, the first and the last ones, for every manipulator, the lowest upper bounds of A for 6, 5, 4 and 3 DOF manipulators will be 4, 3, 2 and 1, respectively. This yields subsets of hypersurfaces, surfaces, curves and points (3, 2, 1 and 0-manifolds) as their HSC's. These upper bounds are not always achieved either due to the type of the manipulator or to special dimensions. For instance Table 3.1 shows that the upper bounds of A for different types of 6 DOF manipulators can lie between 1 and 4.

Consider an A-dimensional rectangular hyperprism with 2^A hyperfaces, each being a subset of a linear (A-1)-manifold, parallel to the active joint axes in the Euclidean space R^A. These hyperfaces will be end points, sides, faces and hyperfaces for A = 1, 2, 3, 4, respectively. The set of points inside a hyperprism, denoted by H, can be defined as the cartesian product of A sets.

$$H = \left(\prod_{i=1}^{I} \bar{\theta}_i \right) \times \left(\prod_{j=1}^{J} \bar{S}_j \right) \tag{3.3}$$

where $\bar{\theta}_i$ and $\bar{S}_j$ are 1-dimensional point sets given by

$$\bar{\theta}_i = \{\theta_i : \theta_{io} \leq \theta_i \leq \theta_{io} + 2\pi\} \qquad i = 1, 2, \ldots, I \tag{3.4}$$

$$\bar{S}_j = \{S_{jj} : -\infty < S_{jj} < \infty\} \qquad j = 1, 2, \ldots, J \tag{3.5}$$

and I and J are the number of active revolute and prismatic joints, respectively. The end points of each $\overline{\theta}_i$ is considered to be the same point. Hence, each such interval is topologically a circle. Figure 3.1 illustrates such a hyperprism, which is a rectangle, in the active joint space of a hypothetical manipulator with active joints S_{22} and θ_3. The subset of the HSC inside the hyperprism is also illustrated.

Let S be the set consisting of the points of the HSC inside the hyperprism of a 6 DOF manipulator. The region H\S can be covered by mutually disjoint regions (T_i's) in many different ways; i.e.,

$$H \setminus S = \bigcup_{i=1}^{i=NR} T_i \qquad \text{with } T_i \cap T_j = \emptyset \qquad \text{for } i \neq j$$

where NR is the number of regions. However, there is only one way of covering H\S while minimizing NR. In this case, every distinct region T_i will be said to correspond to a different configuration of the manipulator and the number of T_i's will be called the number of configurations (NC) of the manipulator. Hence, instantaneously the robot will be said to be in configuration i iff $\underline{q}_a = [q_{a1}, q_{a2}, \ldots, q_{aA}]$, where $q_{a1}, q_{a2}, \ldots, q_{aA}$ are active joint variables, is in T_i. Clearly the naturally passive and passive joint variables cannot affect the configuration that the manipulator is in. The regions which are convex (those for which any two points within the region can be joined with a line segment lying entirely in the region) will be said to correspond to the convex configurations of the manipulator.

The configuration of a manipulator at any instant can be determined by examining the HSC in more detail. The equation of the

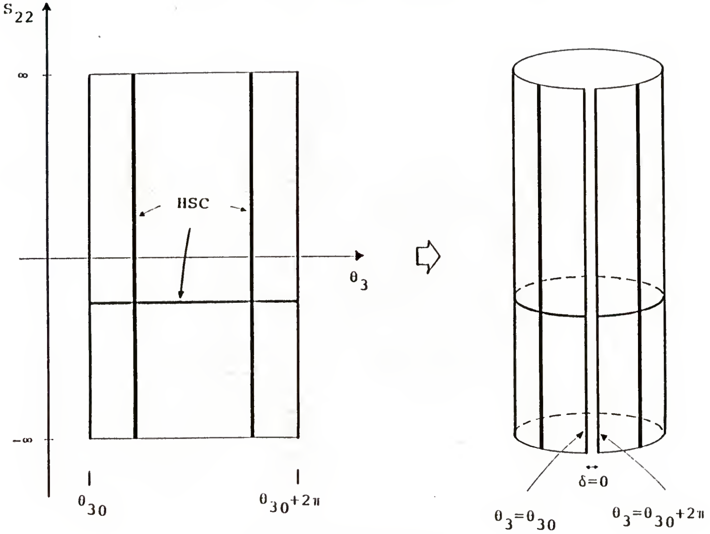

Fig. 3.1 A Hyperprism

HSC is a polynomial in the variables s_i, c_i (i = 1, 2, ..., I) and S_{jj} (j = 1, 2, ..., J) where I and J are the number of active revolute and prismatic joints, respectively. Here s_i and c_i are considered to be independent variables. The HSC will be said to be reducible if this polynomial is reducible over the field of real numbers. Otherwise it will be said to be irreducible. Clearly the factorization is unique, up to a real constant, for reducible HSC's. Suppose now that the equation of the HSC is reducible and can be expressed as the product of m factors (f_i's) raised to positive integer powers (r_i's) such that

$$c\ (f_1)^{r_1}\ (f_2)^{r_2} \ldots (f_m)^{r_m} = 0 \tag{3.6}$$

where an f_i is not a scalar multiple of an f_j and c is a real number. Clearly the same HSC will be determined by the simpler equation

$$c\ f_1\ f_2 \ldots f_m = 0 \tag{3.7}$$

The points satisfying $f_i = 0$ (i = 1, 2, ..., m) will be said to lie on the i'th subcomponent manifold (HSC_i) of the HSC. It should be noted that if HSC_i separates a hyperprism into two disjoint regions, then these regions can be identified by sgn (f_i). Here sgn denotes the sign function which yields +1 (-1) for a positive (negative) argument.

Equation (3.7) can always be rearranged into the form

$$c\ F_1\ F_2 \ldots F_k = 0 \tag{3.8}$$

where the factors F_i's $(i = 1, 2, \ldots, k)$ are groupings of the f_j's $(j = 1, 2, \ldots, m)$ in the product form $F_i = \pi_t f_t$, such that the number of factors, k, is a maximum with the constraint that any joint variable is contained in a single factor F_i only. For instance if $f_1 = s_2$, $f_2 = c_3$, $f_3 = s_4$ and $f_4 = c_4$ in equation (3.7), then $F_1 \equiv f_1 = s_2$, $F_2 \equiv f_2 = c_3$ and $F_3 \equiv f_3 f_4 = s_4 c_4$. The points satisfying an $F_i = 0$ in the active joint space will be said to lie on the i'th component manifold (HSC_{ii}) of the HSC. If F_i does not contain the variables θ_j, θ_k, ... and S_{dd}, S_{ee}, ... then HSC_{ii} will be parallel to the axes θ_j, θ_k, ... and S_{dd}, S_{ee}, ... in the joint space. However, the converse of this statement is not necessarily true.

It is sufficient to analyze each HSC_{ii} inside a hyperprism in the space of the joint variables that F_i contains. Consider that such an analysis for each HSC_{ii} reveals that the number of regions, defined by the hyperfaces which are orthogonal to the prismatic joint variables and the subset of the HSC_{ii} inside the hyperprism, is N_i. It can then be concluded that the number of configurations of the manipulator is given by

$$NC = \pi_{i=1}^{k} N_i \tag{3.9}$$

It should be noted that if HSC_{ii} is the empty set, i.e., HSC_{ii} is imaginary, then $N_i = 1$.

The first step in the investigation of an HSC is the determination of the component manifolds. This will facilitate the computation of NC and the identification of the configurations. Then each component manifold which contains at most 3 joint variables can be plotted independently. All types of 6 DOF manipulators with $A \leq 3$ have HSC's that are visualizable in 3D space even if the HSC consists of a single component. It should be recalled that $A \leq 3$ for

(i) Manipulators with $N \leq 5$.

(ii) All 6 DOF group 3 manipulators (see Table 3.1).

(iii) PPRRRR and RRRRPP manipulators (see Table 3.1) regardless of their dimensions.

For the remaining manipulators which do not fall into these 3 categories the visualization of the HSC is extensively enhanced if (i) the lowest upper bound of A, i.e., 4, is not achieved; (ii) the HSC consists of at least 2 components due to the dimensions of the robot. Almost all industrial manipulators satisfy at least one of these conditions.

Clearly the most difficult case occurs when $A = 4$ and the HSC consists of a single component. Here it is necessary to investigate the $q_{a1}\ q_{a2}\ q_{a3}$-slices at a sequence of values of q_{a4} within a hyperprism where q_{a4} can be any one of the active joint variables.

3.3 Some Applications

Before presenting applications of the new concepts, some definitions will be introduced.

The degree of a manipulator, DEG (DEG_1), will be defined as the maximum number of real solution sets obtained from the reverse displacement analysis without (with) joint limitations. Further the region CO_i (in the joint space) corresponding to the i'th configuration of the manipulator is defined to be the cartesian product of the point sets Q_1, Q_2, ..., Q_p and T_i where p is the number of naturally passive and passive joints and

$$Q_i = \begin{cases} \{q_i: \ -\infty < q_i < \infty\} \text{ if } q_i \text{ is a P joint} \\ \{q_i: \ q_{io} \leq q_i \leq (q_{io} + 2\pi)\} \text{ if } q_i \text{ is an R joint} \end{cases}$$

Due to the joint limitations, however, only certain subregions of the CO_i's will be reachable. Each such subregion will be called a subconfiguration and will be denoted by CO_{ij}. Here, the subscript i indicates that $CO_{ij} \subset CO_i$ and j = 1, 2, ..., m_i where m_i is the number of disjoint subregions of CO_i under the joint limitations. The number of these subregions will be designated by NC_l. Hence,

$$NC_l = \sum_{i=1}^{NC} m_i$$

For most 6 DOF manipulators each CO_i, i = 1, 2, ..., NC, maps onto some region in the position and orientation space of the end effector in a one-to-one manner (see Section 6.1). In this case NC constitutes a least upper bound (l.u.b.) for the degree of the manipulator and distinct, real solutions obtained from the reverse displacement analysis always belong to different configurations. Similarly, NC_l acts as an l.u.b. for DEG_l. In general, these two l.u.b.'s will be achieved if all of the CO_i's (or CO_{ij}'s) share a common k-manifold, with $k \leq N-1$, as part of their boundaries. Hence, it follows that the concepts of HSC, configurations and subconfigurations can be conveniently used for the synthesis of DEG and DEG_1 during the kinematic design stage. This is illustrated in Section 3.7.1 using the MBA robot.

A second application is in trajectory planning which is an important stage in controlling a robot. In this stage, the desired cartesian space motion of the manipulator is usually converted into a curve in the joint space which is the most convenient space to control the manipulator. A well known algorithm implementing this idea is due to Taylor (1979). In this algorithm the knot points in the cartesian space are converted into knot points in the joint space which are then connected by line segments. The method performs well as long as special configurations are avoided. It is clear that depending on the prescribed motion and the geometry of the manipulator it may or may not be possible to execute the motion without going through any special configurations. This can be easily verified using the concept of configurations presented in Section 3.2.

It is clear that during a specified motion the robot does not pass through any special configuration if and only if it stays within the same configuration. If the joint space curve consists of connected line segments, as in Taylor's algorithm for instance, and the manipulator is in a convex configuration, then it is sufficient to ensure that the knot points belong to the same configuration. The nonconvex regions in the active joint space corresponding to the nonconvex configurations can always be partitioned into the union of a finite number of convex regions. This partitioning is not unique and it can be performed in such a way that it yields the simplest criteria for a point to lie in one of these regions.

In general, the reverse displacement mapping is a multi-valued function. Therefore, there will exist a number of joint space curves corresponding to the same prescribed motion. The number of intersections of each of these curves with the HSC will yield the corresponding number of special configurations. The motion is best executed using the curve with the minimum number of special configurations.

3.4 A Theorem for the Existence of Passive Joints

Consider the screw systems $V_1 = \{\$_1, \$_2, \ldots, \$_{h-1}\}$ and $V_2 = \{\$_h, \$_{h+1}, \ldots, \$_N\}$ for an N DOF serial manipulator. Here $\$_i$ $(i = 1, 2, \ldots, N)$ denote the screws representing the relative instantaneous motions of the links. Further, let V_2 be an invariant screw system with respect to finite displacements of the joints h, h+1, ..., N (see Hunt, 1978, for a comprehensive list of invariant screw systems). Practical examples of such a system are the screws representing the relative motions of a number of successive links that are kinematically equivalent to a spherical, planar or cylindrical pair. The screws of V_1 can be expressed (in the coordinate system $\hat{B}_h$) in terms of the joint variables q_i by $\$_{1,\hat{h}} = f_1(q_2, q_3, \ldots, q_{h-1})$, $\$_{2,\hat{h}} = f_2(q_3, q_4, \ldots, q_{h-1})$, ..., and $\$_{h-1,\hat{h}}$ = constant. On the other hand, V_2 is an invariant screw system by hypothesis. Hence, in $\hat{B}_h$ there exists a basis (independent of the joint displacements q_h, q_{h+1}, ..., q_N) for V_2. This basis will be denoted by $\{\$'_h, \$'_{h+1}, ..., \$'_N\}$. The base $\{\$_{h,\hat{h}}, \$_{h+1,\hat{h}}, ..., \$_{N,\hat{h}}\}$ can be replaced by the base $\{\$'_h, \$'_{h+1}, ..., \$'_N\}$ in $\hat{G}_h(1, 2, ..., N)$ which is the Gramian of the screws 1, 2, ..., N in the reference frame $\hat{B}_h$. Thus it can be deduced that $\hat{G}_h(1, 2, ..., N)$ will be of the form $g_{12}(q_2, q_3, ..., q_{h-1})$ which, when equated to zero, gives a subset of the HSC. The Gramians $G_\gamma(h, h+1, ..., N)$ or $\hat{G}_\gamma(h, h+1, ..., N)$ (γ = h+1, h+2, ..., N-1) on the other hand, will be of the form $g_{22}(q_{h+1}, q_{h+2}, ..., q_{N-1})$ (see Table 2.1). Hence an equation of the HSC will be of the form

$$[g_{12}(q_2, q_3, ..., q_{h-1})][g_{22}(q_{h+1}, q_{h+2}, ..., q_{N-1})] = 0 \qquad (3.10)$$

Analogously it can be proved that if the screw system V_1 is invariant with respect to finite displacements of the joints 1, 2, ..., h, then there will exist an equation of the HSC which is of the form

$$[g_{11}(q_2, q_3, ..., q_{h-1})][g_{21}(q_{h+1}, q_{h+2}, ..., q_{N-1})] = 0 \qquad (3.11)$$

Therefore, the following theorem can be stated.

Theorem 3.1: If the screw system $V_1 = \{\$_1, \$_2, ..., \$_h\}$ ($V_2 = \{\$_h, \$_{h+1}, ..., \$_N\}$ of an N DOF manipulator is invariant with respect to finite displacements of the joints 1, 2, ..., h (h, h+1, ..., N), then the h'th joint of the manipulator is passive. Furthermore the HSC consists of two component manifolds, HSC_{11} and

HSC_{22}, for which there exists equations of the form $g_1(q_2, q_3, \ldots, q_{h-1}) = 0$ and $g_2(q_{h+1}, q_{h+2}, \ldots, q_{N-1}) = 0$. Further if the screws of V_1 (V_2) never become dependent, then the component manifold HSC_{11} (HSC_{22}) will be imaginary and hence the joints 2, 3, ..., h-1 (h+1, h+2, ..., N-1) will also be passive.

■

It should be noted, however, that if an h'th joint is passive it does not necessarily follow that either V_1 or V_2 is invariant. This can be demonstrated by considering the manipulator shown in Fig. 3.2. The dimensions of this robot are $S_{22} = S_{33} = S_{55} = 0$, $S_{44} \neq 0$, $a_{12} = a_{23} = a_{45} = 0$, $a_{34} \neq 0$ and $a_{56} \neq 0$. Further all the twist angles, α_{ij}'s, are equal to $\pi/2$. The equation of the HSC is given by

$$|J| = -a_{34}^2\, a_{56}\, [s_2]\, [(s_4)(c_4)] = 0 \qquad (3.12)$$

The first 3 joints, which are kinematically equivalent to a spherical joint, constitute an invariant screw system. Therefore, Theorem 3.1 predicts joint 3 to be passive, which is in agreement with equation (3.12). Furthermore as the theorem predicts the HSC consists of the 2 component manifolds given by $s_2 = 0$ and $s_4c_4 = 0$. Joint 5 is also passive. However, neither of the screw systems $V_1 = \{\$_1, \$_2, \ldots, \$_5\}$ or $V_2 = \{\$_5, \$_6\}$ are invariant.

The hypothesis of Theorem 3.1 is satisfied by many industrial manipulators indicating that $A \leq 3$ and their HSC's consist of component manifolds. Hence their HSC's are simple to analyze and visualize, facilitating the determination of NC and the identification of these configurations. For instance, many industrial robots have

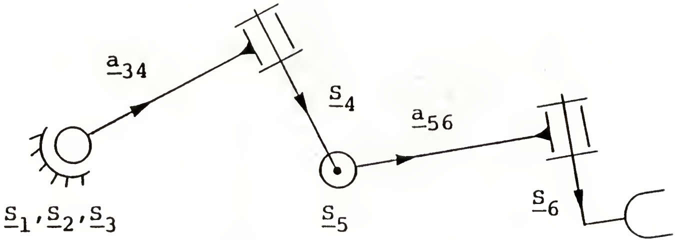

Fig. 3.2 Manipulator Used as a Counter Example

so-called "spherical wrists," where the last 3 revolute joint axes cointersect constituting an invariant screw system. Consequently the fourth joint is always passive for this class of manipulators. Another popular design is to have 3 successively perpendicular prismatic joints as the 3 initial joints, i.e., the so-called Cartesian Manipulators. In this case, the screws $\$_1$, $\$_2$ and $\$_3$ constitute an invariant system and they cannot become dependent. Thus the second and third joints are passive yielding a very simple HSC.

3.5 Synthesis for Passive Joints

The hypothesis of Theorem 3.1 is a sufficient but not necessary condition for the existence of passive joints in a manipulator. In this section a synthesis procedure for passive joints is presented.

Let $\underline{p}$ and $\underline{d}$ designate the vectors of specified and unspecified dimensions of an N DOF manipulator. The following algorithm can be used to determine $\underline{d}$ such that joint j is passive.

(i) Find an equation of the HSC using equation (2.27).

(ii) Transform all terms of the form $(\sin\theta)^m$ or $(\cos\theta)^m$ into the powers of sines and cosines in terms of multiple angles using standard trigonometrical identities. Here $m \geq 2$ and θ denotes an angular joint variable. This process ensures that no feasible solutions for $\underline{d}$ are omitted.

(iii) Express the resulting equation in the form

$$\sum_i D_i(\underline{d}) \cdot Q_i(\underline{q}) = 0$$

where $Q_i(\underline{q}) \neq Q_h(\underline{q})$ for $i \neq h$.

(iv) Equate the coefficient of each $Q_i(\underline{q})$ that contains q_j to zero.

(v) Solve the resulting system of equations for $\underline{d}$. Reject trivial solutions, i.e., solutions which satisfy the equation of the HSC identically.

The synthesis procedure is now illustrated using a 6R manipulator with $\underline{p} \equiv [a_{23}\ S_{33}\ S_{44}\ \alpha_{23}\ \alpha_{34}\ \alpha_{45}\ \alpha_{56}]^T = [0\ 0\ 0\ 90^1\ 90\ 90\ 90]^T$. The design variables are given by the vector $\underline{d} \equiv [a_{12}\ a_{34}\ a_{45}\ a_{56}\ S_{22}\ S_{55}\ \alpha_{12}]^T$. The details of steps (i) - (iv) are omitted because of space limitations and the solutions of $\underline{d}$ for the second joint to be passive can be expressed in the form

$\underline{d}_1 = [x\ 0\ x\ x\ 0\ x\ \pm 90]^T$ $\qquad$ $\underline{d}_2 = [x\ x\ 0\ 0\ 0\ 0\ \pm 90]^T$

$\underline{d}_3 = [x\ 0\ 0\ x\ x\ x\ x]^T$ $\qquad$ $\underline{d}_4 = [0\ 0\ x\ x\ 0\ x\ x]^T$

$\underline{d}_5 = [0\ x\ x\ x\ x\ x\ (0 \vee 180)]^T$ $\qquad$ $\underline{d}_6 = [0\ x\ 0\ 0\ 0\ 0\ x]^T$

where the design variables denoted by x are unconstrained. The nontrivial solutions are $\underline{d}_1$ (see Fig. 3.3) and $\underline{d}_2$[2] yielding

$$a_{12}\ a_{45}\ [s_3^2]\ [a_{56}\ c_4 + a_{45}\ c_4\ c_5 + S_{55}\ s_4\ c_5] = 0$$

and

$$a_{12}\ a_{34}^2\ [(s_3)(c_3)]\ [s_5] = 0$$

---

[1] In Sections 3.5 and 3.6 all angles are measured in degrees unless otherwise specified.

[2] The solutions $\underline{d}_3$ - $\underline{d}_6$ are trivial and satisfy the equation of the HSC identically.

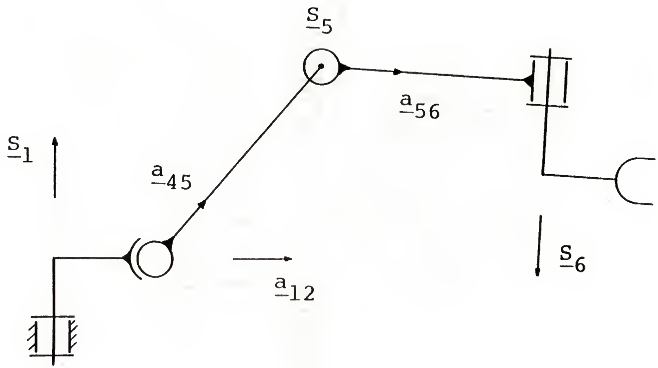

Fig. 3.3 A Manipulator with a Passive Second Joint

as the equations of their respective HSC's. The synthesis procedure for the third, fourth and fifth joints yields the nontrival solutions

$$\underline{d}_7 = [0\ x\ x\ x\ 0\ x\ x]^T \qquad \underline{d}_8 = [x\ x\ 0\ 0\ x\ 0\ x]^T$$

$$\underline{d}_9 = [0\ x\ 0\ x\ 0\ 0\ x]^T$$

respectively, which in turn yield the HSC equations

$$\begin{aligned} a_{34}\, s_{12}\, [s_2]\, [&-a_{34}\, a_{45}\, s_4\, c_4\, c_5 - a_{34}\, a_{56}\, s_4\, c_4 + a_{34}\, S_{55}\, c_4^2\, c_5 \\ &- a_{45}^2\, s_4\, c_5 - a_{45}\, a_{56}\, s_4 + a_{45}\, S_{55}\, c_4\, c_5] = 0 \end{aligned}$$

$$a_{34}^2\, [(c_3)(a_{12}\, s_{12}\, s_3 - a_{12}\, c_{12}\, s_2\, c_3 - S_{22}\, s_{12}\, c_2\, c_3)]\, [s_5] = 0$$

and

$$a_{34}^2\, a_{56}\, s_{12}\, [s_2]\, [(s_4)(c_4)] = 0$$

In these equations the component and subcomponent manifolds are indicated with brackets and parentheses, respectively. The example presented here and other examples indicate that when a manipulator is synthesized for a passive joint there will be more than one component and/or subcomponent manifold. This facilitates the analysis of the HSC.

In the selection of the prespecified dimensions, it is useful to refer to Table 3.1. If the vector $\underline{p}$ is selected such that the degrees of the HSC in the remaining variables are low, the solution of the system of equations obtained at the fourth step of the algorithm can be considerably simplified. Assignment of special dimensions to the components of $\underline{p}$ (such as 0, ±90, 180 for the angular ones and 0 for the linear ones) will simplify the system of equations even further.

3.6 Examples

3.6.1 Manipulators with 6 Degrees of Freedom

The first industrial robot to be examined is the MBA, which is illustrated in Fig. 3.4. The dimensions of this robot are

$S_{22} = 0$ $S_{33} = 0$ $S_{44} = 25''$ $S_{55} = 0$

$a_{12} = 5''$ $a_{23} = 22''$ $a_{34} = 0$ $a_{45} = 0$ $a_{56} = 0$

$\alpha_{12} = 90$ $\alpha_{23} = 0$ $\alpha_{34} = 90$ $\alpha_{45} = -90$ $\alpha_{56} = 90$

The Jacobian $[J_{op}] = [J_3]$ can be expressed in the form

$$[J_3] = \begin{bmatrix} (s_{2+3}) & (0) & (0) & (0) & (-s_4) & (c_4c_5) \\ (c_{2+3}) & (0) & (0) & (-1) & (0) & (-c_5) \\ (0) & (1) & (1) & (0) & (c_4) & (s_4s_5) \\ (0) & (a_{23}s_3) & (0) & (0) & (-S_{44}c_4) & (-S_{44}s_4s_5) \\ (0) & (a_{23}c_3) & (0) & (0) & (0) & (0) \\ (-a_{12}-a_{23}c_2) & (0) & (0) & (0) & (-S_{44}s_4) & (S_{44}c_4s_5) \end{bmatrix}$$

which yields the equation of the HSC,

$$|J| = a_{23}\, S_{44}\, [(c_3)(a_{12} + a_{23}c_2 + S_{44}s_{2+3})]\, [s_5]$$

$$= 550\, [(c_3)\, (5 + 22c_2 + 25s_{2+3})]\, [s_5]$$

$$\equiv 550\, [(f_1)\, (f_2)]\, [f_3] \equiv 550\, [F_1]\, [F_2] = 0 \qquad (3.13)$$

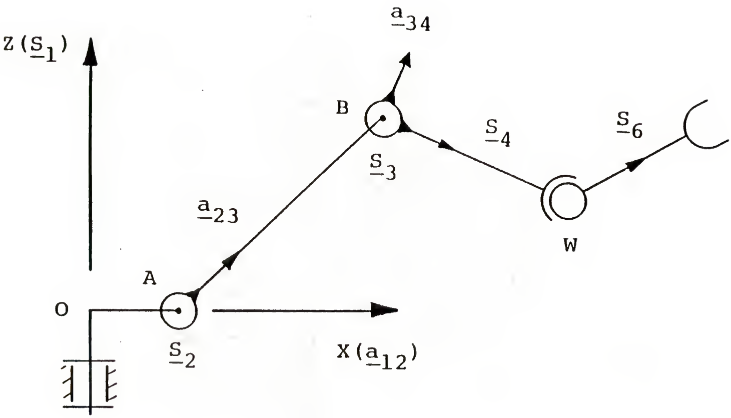

Fig. 3.4 The MB Associates (MBA) Robot

where $s_{2+3} = \sin(\theta_2 + \theta_3)$ and $c_{2+3} = \cos(\theta_2 + \theta_3)$. Since the screw system $V_2 = \{\$_4, \$_5, \$_6\}$ is an invariant one, joint 4 is passive as predicted by Theorem 3.1. Hence the HSC, which consists of 3 subcomponent manifolds and 2 component manifolds, becomes a 2-manifold in the active joint space $\theta_2\theta_3\theta_5$. The $\theta_2\theta_5$ slices of this surface are shown in Fig. 3.5. Essentially it consists of 4 planes and cylindrical type surface parallel to the θ_5 axis. The planes $\theta_3 = 90$ and $\theta_3 = 270$ belong to HSC_1, for which the points A, B and W in Fig. 3.4 will lie on a straight line. The remaining two planes $\theta_5 = 0$ and $\theta_5 = 180$, which indicate that joints 4 and 6 are aligned, belong to HSC_3. Finally the cylindrical type surface is obtained by equating f_2 to zero and represents the condition for the spherical wrist, W, to lie on the first joint axis. Clearly the number of regions defined by HSC_{11} and HSC_{22} inside the hyperprisms $\{(\theta_2, \theta_3)$: $\theta_{2o} \leq \theta_2 \leq \theta_{2o} + 360, \theta_{3o} \leq \theta_3 \leq \theta_{3o} + 360\}$ and $\{\theta_5$: $\theta_{5o} \leq \theta_5 \leq \theta_{5o} + 360\}$ are 4 and 2, respectively. Therefore, the number of configurations of the MBA robot is NC = (4) × (2) = 8. Furthermore, these configurations can be identified by 3-dimensional row vectors of the form [sgn f_1, sgn f_2, sgn f_3] where f_1, f_2 and f_3 are defined in equation (3.13). It should be noted that 4 of the 8 configurations namely, [-1, -1, -1], [-1, -1, +1], [1, -1, -1] and [1, -1, +1] are convex.

The actual dimensions of the MBA robot yield DEG = NC = 8. Suppose now that it is required to reduce the degree of the manipulator by modifying the linear dimensions. From equation (3.13) it is

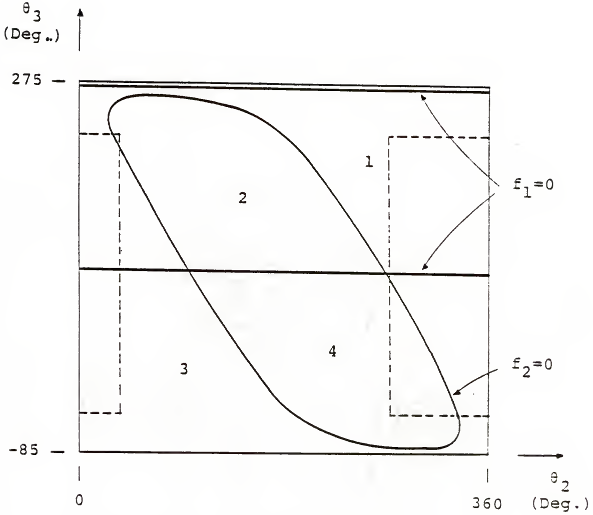

1:[-1,1,-1] 2:[-1,-1,-1]

3:[1,1,-1] 4:[1,-1,-1]

a) $\theta_2\theta_3$ Slice at θ_5 = -150°

Fig. 3.5 The HSC of the MBA Robot

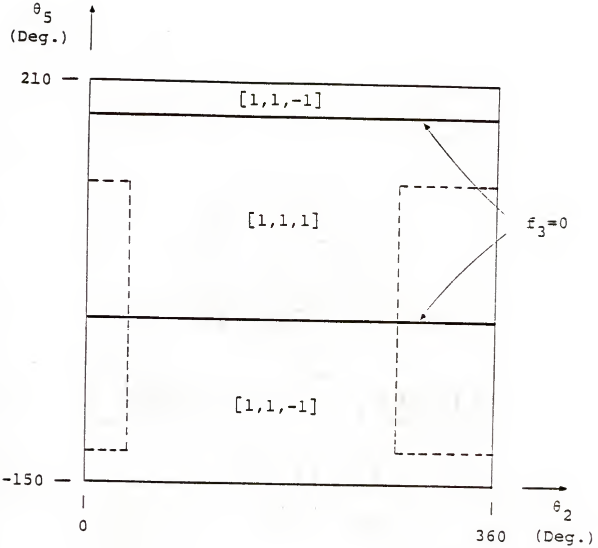

(b) $\theta_2\theta_5$ Slice at $\theta_3 = -85°$

Fig. 3.5--continued.

clear that HSC_1 and HSC_3 cannot be made imaginary. However, the subcomponent manifold HSC_2 becomes imaginary iff $|a_{12}| > |a_{23}| + |S_{44}|$. Satisfying this condition reduces both the NC and the DEG to 4. It is possible to modify the angular dimensions also. However, it would then be necessary to leave them as variables in the expression for $|J|$.

The minimal equation of HSC-5 for the MBA robot is given by

$$G_3^2(1,2,3,4,5) + G_3^2(1,2,3,4,6) + G_3^2(1,2,3,5,6)$$
$$+ \hat{G}_4^2(1,2,4,5,6) + \hat{G}_4^2(1,3,4,5,6) + \hat{G}_4^2(2,3,4,5,6) = 0 \qquad (3.14)$$

which, using Theorem 2.1 with E = {3}, is equivalent to

$$G_3^2(1,2,3,4,5) + G_3^2(1,2,3,4,6) + G_3^2(1,2,3,5,6)$$
$$+ \hat{G}_4^2(1,3,4,5,6) + \hat{G}_4^2(2,3,4,5,6) = 0 \qquad (3.15)$$

The determination of the HSC-5 is substantially simplified by recalling that HSC-5 $\subset$ HSC-6 and HSC-6 = $HSC_1 \cup HSC_2 \cup HSC_3$. Therefore, (3.15) reduces to the equivalent equations

$$[(1109 + 1100s_3)\, c_2^2 + (220 + 250s_3)\, c_2 + 25]^2$$
$$\times [s_4^4 + c_4^4\, s_5^4 + s_4^4\, c_5^4 + s_5^4] = 0 \qquad (3.16)$$

and

$$c_3^2\, c_4^2\, s_{2+3}^2 + s_4^2\, (-550s_{2+3} - 484c_2 - 110)^2$$
$$+ (c_3\, c_4)^2\, (-12100c_2 - 2750)^2 = 0 \qquad (3.17)$$

on HSC_1 (given by $f_1 = 0$) and HSC_3 (given by $f_3 = 0$), respectively.[1] The solutions of equations (3.16) and (3.17) are

$$\underline{t}_1 = [(96.1 \vee 263.9)\ 90\ x\ x]^T \tag{3.18}$$

$$\underline{t}_2 = [x\ (90 \vee 270)\ (0 \vee 180)\ (0 \vee 180)]^T \tag{3.19}$$

and

$$\underline{t}_3 = [103.1\ (76.9 \vee 256.9)\ x\ (0 \vee 180)]^T \tag{3.20}$$

$$\underline{t}_4 = [256.9\ (103.1 \vee 283.1)\ x\ (0 \vee 180)]^T \tag{3.21}$$

$$\underline{t}_5 = [y_2\ y_3\ (90 \vee 270)\ (0 \vee 180)]^T \tag{3.22}$$

where (y_2, y_3) denote the (θ_2, θ_3) coordinates of any point of HSC_2 and $\underline{t}_i = [\theta_2, \theta_3, \theta_4, \theta_5]^T$. Hence all points on HSC-5 are determined by $\underline{t}_1, \underline{t}_2, \ldots, \underline{t}_5$. At the outset it might have been expected that joint 4 should be passive of order 5 also and that the HSC-5 consists solely of all the geometrically singular points of HSC-6, i.e., points where the surface intersects itself. However, this example clearly shows that this is not the case. It should also be noted that when $\underline{q} \in HSC \setminus HSC\text{-}5$ the manipulator has exactly 5 degrees of freedom.

Consider now the T3-776 industrial manipulator which has the dimensions

---

[1] The solution of (3.15) on HSC_2 does not introduce any new solution sets.

$S_{22} = 0$ $S_{33} = 0$ $S_{44} = 55''$ $S_{55} = 0$

$a_{12} = 0$ $a_{23} = 44''$ $a_{34} = 0$ $a_{45} = 0$ $a_{56} = 0$

$\alpha_{12} = 90$ $\alpha_{23} = 0$ $\alpha_{34} = 90$ $\alpha_{45} = 61$ $\alpha_{56} = 61$

and is illustrated schematically in Fig. 3.6. The equation of the HSC is

$$\begin{aligned} |J| &= -0.765\, a_{23}\, S_{44}\, [(c_3)\,(a_{23}\, c_2 + S_{44}\, s_{2+3})]\,[s_5] \\ &= -1851.3\, [(c_3)\,(44c_2 + 55s_{2+3})]\,[s_5] \\ &= -1851.3\, [(f_1)\,(f_2)]\,[f_3] = [F_1]\,[F_2] = 0 \end{aligned} \tag{3.23}$$

which consists of 4 planes and a surface, $f_2 = 0$, which is parallel to the θ_5-axis (see Fig. 3.7). The manipulator has 8 nonconvex configurations which can be identified by row vectors of the form $[\mathrm{sgn}\ f_1,\ \mathrm{sgn}\ f_2,\ \mathrm{sgn}\ f_3]$.

The third manipulator to be investigated is the Stanford manipulator which is of the type RRPRRR (see Fig. 3.8). The specified dimensions of the robot are

$S_{44} = 0$ $S_{55} = 0$

$a_{12} = a_{23} = a_{34} = a_{45} = a_{56} = 0$

$\alpha_{12} = 270$ $\alpha_{23} = 90$ $\alpha_{34} = 0$ $\alpha_{45} = 270$ $\alpha_{56} = 90$

yielding

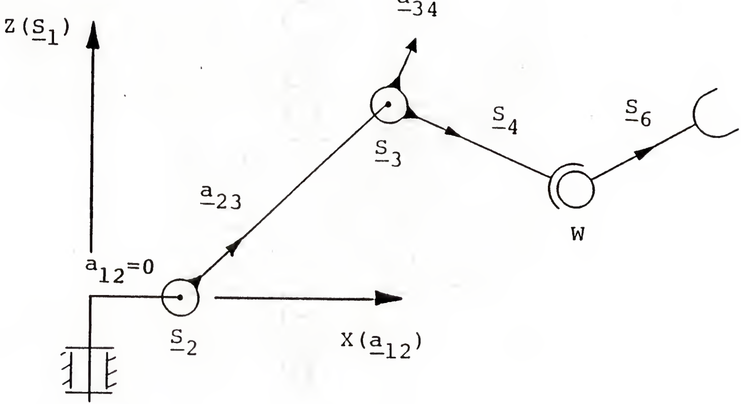

Fig. 3.6 The T3-776 Robot

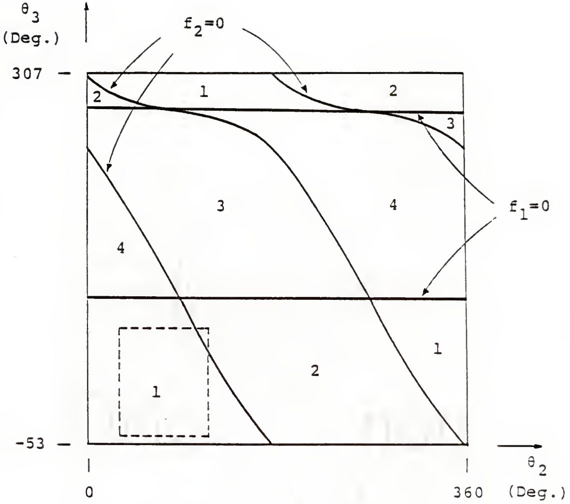

1:[1,1,1]   2:[1,-1,1]

3:[-1,-1,1]   4:[-1,1,1]

Fig. 3.7 The $\theta_2\theta_3$ Slice of the HSC of the T3-776 Robot at θ_5 = 30°

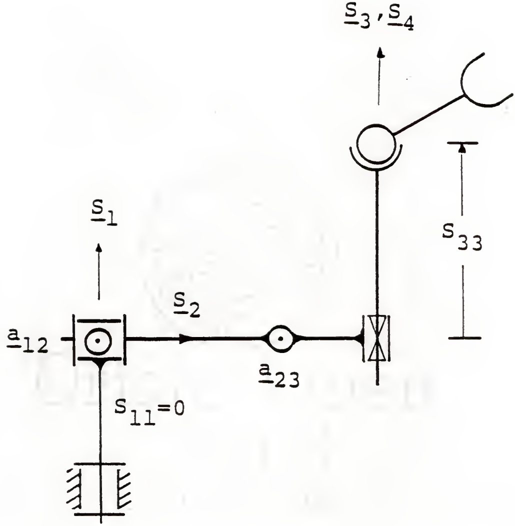

Fig. 3.8 Stanford Manipulator

$$|J| = [s_2]\ [S_{33}^2]\ [s_5] \qquad (3.24)$$

Hence the HSC is given by

$$[s_2]\ [S_{33}]\ [s_5] \equiv [F_1]\ [F_2]\ [F_3] = 0 \qquad (3.25)$$

and consists of 3 component manifolds resulting in 8 convex configurations which can be identified by row vectors of the form [sgn F_1, sgn F_2, sgn F_3]. Clearly the fourth joint and the dimensions S_{22}, θ_3 are passive.

The last example is a 6R manipulator with A = 4 and with the second, third and fourth joints parallel. The specified dimensions of the robot are

$$a_{12} = a_{56} = S_{22} = S_{33} = S_{44} = 0$$

$$\alpha_{12} = 90 \qquad \alpha_{23} = \alpha_{34} = 0 \qquad \alpha_{45} = 90 \qquad \alpha_{56} = 90$$

yielding the equation of the HSC as

$$a_{23}\ a_{34}\ [(s_3)\ (a_{23}\ c_2 + a_{34}\ c_{2+3} + a_{45}\ c_{2+3}\ c_4 + S_{55}\ c_{2+3}\ s_4$$
$$- a_{45}\ s_{2+3}\ s_4 + S_{55}\ s_{2+3}\ c_4)]\ [s_5] \equiv a_{23}\ a_{34}\ [(f_1)\ (f_2)]\ [f_3]$$
$$\equiv [F_1]\ [F_2] = 0 \qquad (3.26)$$

The first component manifold always yields 4 regions in the $\theta_2\theta_3\theta_4$ space regardless of any geometrical singularities that may exist due to special dimensions. Hence the manipulator has 8 configurations which can be identified by row vectors of the form [sgn f_1, sgn f_2, sgn f_3].

All of the manipulators investigated in this section have the property that each region CO_i is mapped onto some region in the position and orientation space in a one-to-one manner. Furthermore, the degrees of the manipulators are equal to their respective number of configurations, NC's, in each case.

3.6.2 Manipulators with 5 Degrees of Freedom

Consider the 5 DOF manipulator which consists of the first 5 links of the MBA robot. The minimal equation of the HSC is

$$[550s_{2+3}\ c_3\ c_4]^2 + [22s_3\ s_4\ (5 + 22c_2 + 25s_{2+3})]^2$$
$$+ [22c_3\ s_4\ (5 + 22c_2 + 25s_{2+3})]^2 + [550c_3\ c_4\ (5 + 22c_2)]^2 = 0 \qquad (3.27)$$

all solutions of which are given by the first three components of $\underline{t}_i$ (i = 1, 2, ..., 5) in equations (3.18) - (3.22). The HSC consists of 6 straight line segments, parallel to the θ_4-axis, due to the solutions $\underline{t}_1$, $\underline{t}_3$, $\underline{t}_4$; 2 closed curves, on the $\theta_4 = 90$ and $\theta_4 = 270$ planes, due to $\underline{t}_5$; and 4 line segments, parallel to the θ_2-axis, due to $\underline{t}_2$. It should be noted that the HSC consists of 3 disjoint curves in the $\theta_2\theta_3\theta_4$ space.

CHAPTER 4
MEASURES FOR THE POSITION AND ORIENTATION SPACE OF THE END EFFECTOR

In this chapter two alternative measures are introduced for the position and orientation space of the end effector. These measures are shown to be equivalent for the spherical wrist manipulators. Some applications are also presented.

4.1 Hand Freedom Numbers

Consider a 6-dimensional region D (in the joint space of a 6 DOF manipulator) such that the forward displacement mapping is one-to-one when restricted to D and $|J|$ does not change its sign on D. The Hand Freedom Number (HFN) corresponding to the region D will be defined as

$$\mathrm{HFN}(D) = \iiiint\!\!\iint_D \mathrm{Abs}\,(|J|)\, dV_q \qquad (4.1)$$

where dV_q is the differential hypervolume element of the joint space and Abs (...) denotes the absolute value function. This number, which has the dimension (length)^3, gives a quantitative measure of the total freedom of the end effector (considered as a rigid body in 3-space) when $\underline{q}$ is restricted to D. In other words, it induces a measure on the Position and Orientation of the Hand (POH) space.

The regions CO_i's, corresponding to the different configurations of the manipulator, and CO_{ij}'s satisfy the requirements of D for most industrial manipulators (see Section 6.1). Suppose now that $HFN(CO_{ij})$ is to be found using definition (4.1). It is necessary to determine the limits of the integrals which depend on the boundaries of CO_{ij}. Clearly, the hypersurfaces bounding any CO_{ij} have to be of the following two types:

(i) A hyperplane orthogonal to a joint variable axis.

(ii) A subset of the HSC.

Boundaries of the type (ii) can be difficult to handle if $A = 4$ and the HSC consists of only a single component manifold. In general it can be stated that the lower the dimension of the active joint space and/or the higher the number of component manifolds, the easier it is to determine the $HFN(CO_{ij})$'s.

The cumulative hand freedom numbers of a manipulator with unlimited and limited revolute joint motions are defined as

$$CHFN_u = \sum_{i=1}^{NC} HFN(CO_i) \tag{4.2}$$

and

$$CHFN_l = \sum_{i=1}^{NC_l} \sum_{j=1}^{m_i} HFN(CO_{ij}) \tag{4.3}$$

respectively, where NC and NC_l are the number of configurations and subconfigurations. These numbers are directly proportional to the motion ranges of the passive and naturally passive joints regardless of their upper and lower bounds. The motion range of a joint i is defined as $q_{ir} = q_{iu} - q_{il}$ with $q_{il} \leq q_i \leq q_{iu}$.

The naturally passive and passive dimensions of the manipulator can be changed arbitrarily without affecting HFN[1] (see Table 3.1 for the passive dimensions of different types of 6 DOF robots with arbitrary dimensions). However, any one of the HFN's is clearly dependent on the vector of active linear dimensions, $\underline{l}$. Consider now (i) group 0 manipulators, (ii) group 1 and group 2 manipulators with no active P joints and (iii) all group 3 manipulators. Further, let the joint motion ranges of the prismatic joints in cases (ii) and (iii) be catenated to $\underline{l}$. Now, if HFN' corresponds to $\underline{l}'$, and $\underline{l}'$ is changed to $\underline{l}'' = c\underline{l}'$ where c is a nonzero positive real number then

$$\mathrm{HFN}'' = c^{(3-g)}\mathrm{HFN}' \qquad (4.4)$$

Here g denotes the group number (0, 1, 2 or 3) of a 6 DOF manipulator, i.e., the number of P joints. Finally, it is useful to normalize HFN for the (i), (ii) and (iii) classes since it is dependent on the size of $\underline{l}$. Hence, $\|\mathrm{HFN}\|_k$, HFN normalized with respect to the k'th norm of $\underline{l}$, will be defined to be that value of HFN corresponding to $\|\underline{l}\|_k = 1$.

It should be noted that $\mathrm{HFN}(\mathrm{CO}_i)$ is infinite for manipulators with unlimited prismatic joints. Hence, for such manipulators $\mathrm{HFN}(\mathrm{CO}_i)$ will, by definition, refer to the HFN corresponding to the configuration i when all the sliding joints are limited.

---

[1] In this paragraph HFN is used to abbreviate any one of the four quantities, $\mathrm{HFN}(\mathrm{CO}_i)$, $\mathrm{HFN}(\mathrm{CO}_{ij})$, CHFN_u or CHFN_l.

4.2 A Second Measure

The definition of HFN(D) is a very general one and is applicable to any type of manipulator. However, it does not supply us with a physical feel for the freedom of the end effector, and it is convenient to define another measure, M(D), in terms of a point and an axis on the end effector. This measure is applicable to all manipulators that have revolute joints as their final joints.

$$M(D) = \theta_{6r} \iiint_{D'} R(x,y,z)\ dV \tag{4.5}$$

where D is a 6-dimensional region in the joint space (with $\theta_{61} \leq \theta_6 \leq \theta_{6u}$) such that the forward displacement mapping is one-to-one when restricted to D; (x,y,z) are the coordinates of the point H on the end effector (see Fig. 4.1) in some fixed cartesian coordinate system; dV is the differential volume element of the xyz space; D' is the collection of all points in the xyz space that can be reached by H when $\underline{q} \in D$; and R(x,y,z) is a scalar point function which will be called the Orientational Freedom Number at the point (x,y,z). It should be noted that M(D) includes a 3-dimensional measure for the orientation space whereas the solid angle proposed by Roth (1976) is a 2-dimensional measure. Furthermore, the multi-valued nature of the reverse displacement mapping is accounted for in M(D).

In equation (4.5) R(x,y,z) = 0 whenever $(x,y,z) \notin D'$. If the point (x,y,z) belongs to D', however, then R(x,y,z) is determined in the following manner. First, at the point (x,y,z) H is connected to the ground using a hypothetical spherical joint. The directed line HP (see Fig. 4.1) is considered to be rigidly connected to link 5. Then the resulting 2 DOF closed loop mechanism is given all the possible

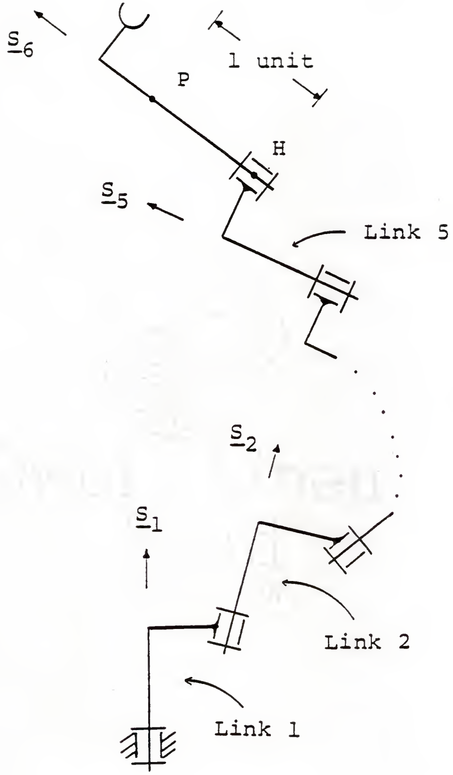

Fig. 4.1 The Point H and Axis HP on the End Effector

motions with the constraint that $\underline{q} \in D$ at all times. As a result of the totality of these motions, the point P describes a region, D", on the unit sphere centered at H. R(x,y,z) is defined to be the area of D", which is designated by A(D").

Clearly the measure M(D) is physically meaningful, whereas HFN(D) is not. Generally M(D) is difficult to compute in practice. However, the computation of HFN(D) is relatively simple. This raises the issue of the equivalence of the two measures which leads to the following theorem.

Theorem 4.1: Consider a 6 DOF spherical wrist (SW) manipulator. Let D_{123} and D_{45} denote regions in the $q_1q_2q_3$ space and $\theta_4\theta_5$ space, respectively, such that $|J| \neq 0$ for any point in D_{123} or D_{45}. Also, let $D = D_{123} \times D_{45} \times D_6$ where D_6 is the interval $\theta_{61} \leq \theta_6 \leq \theta_{6u}$ in the θ_6 space and × denotes the cartesian product. Then

$$HFN(D) = M(D) = \theta_{6r} \cdot V(D') \cdot R \qquad (4.6)$$

where V(D') is the volume of D' and

$$R = R(x,y,z) = \mathrm{Abs}\ \left(\iint_{D_{45}} (s_{45}\ s_{56}\ s_5)\ d\theta_4\ d\theta_5 \right)$$

Proof: The dimensions a_{45}, a_{56} and S_{55} are zero for an SW manipulator. Hence the Jacobian $[J_4]$ can be expressed in the form

$$[J_4] = \begin{bmatrix} M_1 & M_3 \\ M_2 & 0 \end{bmatrix} \qquad (4.7)$$

using Table 2.1. Here 0 is the 3 × 3 null matrix,

$$M_3 = \begin{bmatrix} 0 & 0 & X_5 \\ 0 & -s_{45} & Y_5 \\ 1 & c_{45} & Z_5 \end{bmatrix} \tag{4.8}$$

and M_1, M_2 are 3 × 3 matrices which can be explicitly determined using the same table when the types of the first 3 joints are specified. The matrices M_1 and M_2 are functions of q_2, q_3 and θ_4. Utilizing the screw transformation matrix (see Section 2.2)

$$[{}^f\$_4] = \begin{bmatrix} {}^fR_4 & 0 \\ 0 & {}^fR_4 \end{bmatrix} \tag{4.9}$$

the Jacobian $[J_f]$ can be defined as

$$[J_f] = [{}^f\$_4]\,[J_4] = \begin{bmatrix} {}^fR_4\,M_1 & {}^fR_4\,M_3 \\ {}^fR_4\,M_2 & 0 \end{bmatrix} \tag{4.10}$$

where ${}^fR_4$ is the 3 × 3 rotation matrix converting the coordinates of a vector in the fourth system to the coordinates in the f'th system, which is a fixed one. Components of ${}^fR_4$ are functions of θ_4, $\underline{q}_p = [q_1, q_2, q_3]^T$ and the first 3 link dimensions. It follows from equation (4.10) that $|J| = |{}^fR_4\ M_2| \cdot |{}^fR_4\ M_3| = |{}^fR_4\ M_2| \cdot |M_3|$. Thus

$$\mathrm{HFN}(D) = \iiint_{D_{123}} |{}^fR_4\ M_2|\ dq_1\ dq_2\ dq_3 \iint_{D_{45}} |M_3|\ d\theta_4\ d\theta_5 \int_{D_6} d\theta_6$$

which simplifies to

$$\mathrm{HFN}(D) = \theta_{6r} \iiint_{D_{123}} |{}^fR_4\ M_2|\ dq_1\ dq_2\ dq_3 \iint_{D_{45}} (s_{45}\ s_{56}\ s_5)\ d\theta_4\ d\theta_5 \tag{4.11}$$

It is necessary to find R(x,y,z) in order to determine M(D). Suppose the point H (which coincides with the center of the wrist for an SW manipulator) is connected to the ground by a spherical joint at the point (x,y,z). Then $\underline{q}_p$, and hence the reference frame B_3, is fixed. Let the coordinates of P (see Fig. 4.1) in B_3 be $[l,m,n]^T$. Clearly, $[l,m,n]^T = \underline{S}_{6,3}$. Thus,

$$l = X_{45} \qquad m = Y_{45} \qquad n = Z_{45} \tag{4.12}$$

which defines a mapping from the $\theta_4\theta_5$ space into the unit sphere centered at the point (x,y,z). Therefore,

$$R(x,y,z) = A\ (D") = \iint_{D_{45}} \sqrt{EG-F^2}\ d\theta_4\ d\theta_5 \tag{4.13}$$

where E, F and G are the coefficients of the first fundamental form of the surface (see for instance Taylor and Mann, 1983) given by (4.12). These coefficients are defined as

$$E = (\frac{\partial l}{\partial \theta_4})^2 + (\frac{\partial m}{\partial \theta_4})^2 + (\frac{\partial n}{\partial \theta_4})^2$$

$$F = \frac{\partial l}{\partial \theta_4}\frac{\partial l}{\partial \theta_5} + \frac{\partial m}{\partial \theta_4}\frac{\partial m}{\partial \theta_5} + \frac{\partial n}{\partial \theta_4}\frac{\partial n}{\partial \theta_5}$$

$$G = (\frac{\partial l}{\partial \theta_5})^2 + (\frac{\partial m}{\partial \theta_5})^2 + (\frac{\partial n}{\partial \theta_5})^2$$

Expanding the right-hand sides of the equation set (4.12) and utilizing the above definitions,

$$E = s_{45}^2 + s_{56}^2 - 2\, s_{45}^2\, s_{56}^2 + s_{45}^2\, s_{56}^2\, s_5^2 + 2\, s_{45}\, c_{45}\, s_{56}\, c_{56}\, c_5$$

$$F = s_{45}\, s_{56}\, c_{56}\, c_5 + c_{45}\, s_{56}^2 \qquad G = s_{56}^2$$

Substituting in (4.13) yields

$$R(x,y,z) = \text{Abs}\ (\iint_{D_{45}} (s_{45}\, s_{56}\, s_5)\, d\theta_4\, d\theta_5) \qquad (4.14)$$

Clearly, R(x,y,z) is the same for all $(x,y,z) \in D'$. Hence, definition (4.5) reduces to

$$M(D) = \theta_{6r} \cdot R(x,y,z) \cdot V(D') \qquad (4.15)$$

where V(D') is the volume of D'. V(D') can be determined by considering the mapping from the $q_1q_2q_3$ space into the xyz space which will be symbolically represented as

$$x = f_1(q_1,q_2,q_3) \qquad y = f_2(q_1,q_2,q_3)$$

$$z = f_3(q_1,q_2,q_3) \qquad (4.16)$$

On the other hand, from the last 3 rows of $[J_f]$ it can be deduced that

$\underline{V} = [\dot{x}\ \dot{y}\ \dot{z}]^T = [{}^fR_4\ M_2]\ \dot{\underline{q}}_p$ where $\underline{V}$ is the translational velocity of point H in the f'th reference frame. Here the product $[{}^fR_4\ M_2]$ does not depend on θ_4 although both ${}^fR_4$ and M_2 are functions of θ_4. Hence, $[{}^fR_4\ M_2]$ must be the Jacobian matrix of the mapping given by equation (4.16), and $\frac{\partial\ (f_1,f_2,f_3)}{\partial\ (q_1,q_2,q_3)} = |{}^fR_4\ M_2|$. Hence,

$$V(D') = \iiint_{D_{123}} |{}^fR_4\ M_2|\ dq_1\ dq_2\ dq_3 \tag{4.17}$$

Substituting the equations (4.17), (4.14) into (4.15) and comparing the result with (4.11), it follows that $HFN(D) = M(D) = \theta_{6r} \cdot V(D') \cdot R$.

■

4.3 Lowest Upper Bounds of the Hand Freedom Numbers

Suppose now that the 1 norm is being used in $\|HFN(CO_i)\|_k$ and the lowest upper bounds of $\|HFN(CO_i)\|_1$ are required for group 0, 1, 2 and 3 SW manipulators with no active P joints. If definition (4.1) is employed to formulate $HFN(CO_i)$, it is necessary to maximize a multiple integral (with a varying integrand and region of integration) with respect to the dimensions of the manipulator subject to the constraint $\|\underline{l}\|_1 = 1$. Clearly, this optimization problem is extremely difficult to solve even with numerical methods. However, from Theorem 4.1 $HFN(CO_i) = \theta_{6r} \cdot R \cdot V(CO_i')$. Then it follows that $\theta_{6r} = 2\pi$, $\alpha_{45} = \alpha_{56} = \pm\ \pi/2$, $\theta_{4r} = 2\pi$, $0 \leq \theta_5 \leq \pi$ (or $\pi \leq \theta_5 \leq 2\pi$) are necessary and sufficient conditions for the product $(\theta_{6r} \cdot R)$ to be a maximum. This yields $(\theta_{6r} \cdot R)_{max} = 8\pi^2$. The original problem is thus reduced to maximizing $V(CO_i')$ subject to $\|\underline{l}\|_1 = 1$. The solution of this problem for the manipulators belonging to groups 0, 1, 2 and 3 yields the following results.

Group 0: Dimensions of the ideal RRRRRR manipulator (see Fig. 4.2(a)) are

$S_{22} = 0 \qquad S_{33} = 0 \qquad S_{44} = 0 \qquad S_{55} = 0$

$a_{12} = 0 \qquad a_{23} = 0.5 \qquad a_{34} = 0.5 \qquad a_{45} = 0 \qquad a_{56} = 0$

$\alpha_{12} = \pi/2 \qquad \alpha_{23} = 0 \qquad \alpha_{34} = 0 \qquad \alpha_{45} = \pi/2 \qquad \alpha_{56} = \pi/2$

yielding

$$|J| = 0.125\ [(s_3)\ (c_2 + c_{2+3})]\ [s_5] \qquad (4.18)$$

$$\|\mathrm{HFN}(\mathrm{CO}_i)\|_{m0} = \|\mathrm{HFN}(\mathrm{CO}_j)\|_1 = 32\pi^3/3 \qquad j = 1, 2, \ldots, 8$$

$$\|\mathrm{CHFN}_u\|_{m0} = \|\mathrm{CHFN}_u\|_1 = 256\pi^3/3$$

Group 1: Dimensions of the ideal PRRRRR manipulator (see Fig. 4.2(b)) are

$S_{22} = 0 \qquad S_{33} = 0 \qquad S_{44} = 0 \qquad S_{55} = 0$

$a_{12} = 0 \qquad a_{23} = 1/3 \qquad a_{34} = 1/3 \qquad a_{45} = 0 \qquad a_{56} = 0$

$\alpha_{12} = 0 \qquad \alpha_{23} = 0 \qquad \alpha_{34} = 0 \qquad \alpha_{45} = \pi/2 \qquad \alpha_{56} = \pi/2$

and $S_{11r} = 1/3$, yielding

$$|J| = -0.\bar{1}\ [s_3]\ [s_5] \tag{4.19}$$

$\|HFN(CO_i)\|_{m1} = \|HFN(CO_j)\|_1 = 32\pi^3/27$ $j = 1, 2, 3, 4$

$\|CHFN_u\|_{m1} = \|CHFN_u\|_1 = 128\pi^3/27$

Group 2: Dimensions of the ideal PPRRRR manipulator (see Fig. 4.2(c)) are

$\theta_2 = 0$ $S_{33} = 0$ $S_{44} = 0$ $S_{55} = 0$

$a_{12} = 0$ $a_{23} = 0$ $a_{34} = 1/3$ $a_{45} = 0$ $a_{56} = 0$

$\alpha_{12} = \pi/2$ $\alpha_{23} = 0$ $\alpha_{34} = 0$ $\alpha_{45} = \pi/2$ $\alpha_{56} = \pi/2$

and $S_{11r} = S_{22r} = 1/3$, yielding

$$|J| = 0.\bar{3}\ [s_3]\ [s_5] \tag{4.20}$$

$\|HFN(CO_i)\|_{m2} = \|HFN(CO_j)\|_1 = 16\pi^2/27$ $j = 1, 2, 3, 4$

$\|CHFN_u\|_{m2} = \|CHFN_u\|_1 = 64\pi^2/27$

Group 3: Dimensions of the ideal PPPRRR manipulator (see Fig. 4.2(d)) are

$\theta_2 = \pi/2$ $\theta_3 = -\pi/2$ $S_{44} = 0$ $S_{55} = 0$

$a_{12} = 0$ $a_{23} = 0$ $a_{34} = 0$ $a_{45} = 0$ $a_{56} = 0$

$\alpha_{12} = -\pi/2$ $\alpha_{23} = \pi/2$ $\alpha_{34} = \pi/2$ $\alpha_{45} = \pi/2$ $\alpha_{56} = \pi/2$

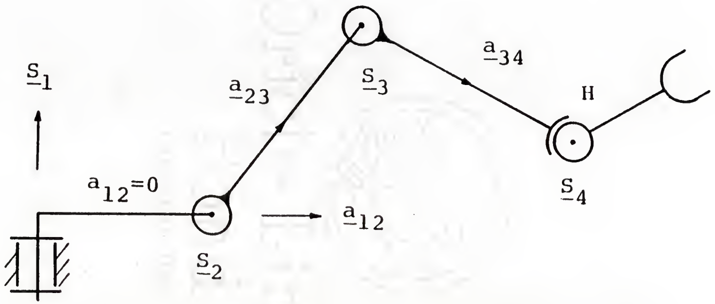

(a) Group 0

Fig. 4.2 Ideal Spherical Wrist Manipulators

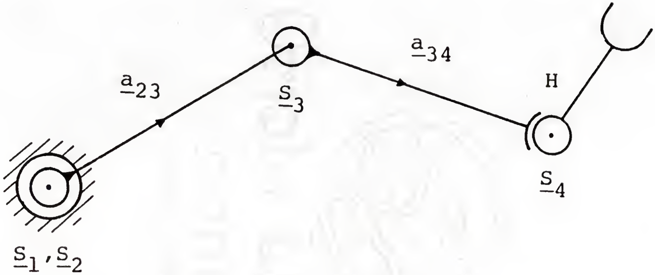

(b) Group 1

Fig. 4.2--continued.

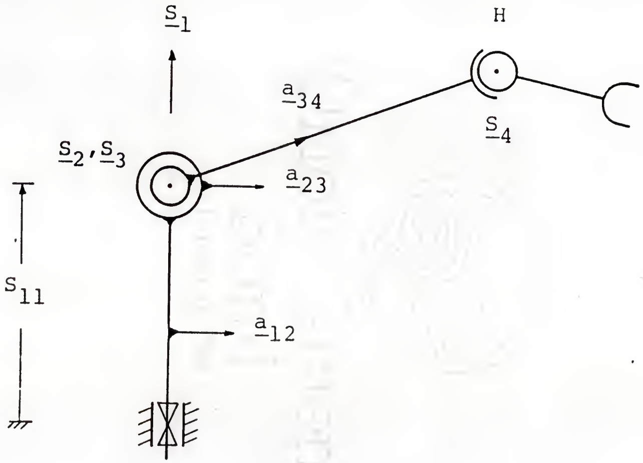

(c) Group 2

Fig. 4.2--continued.

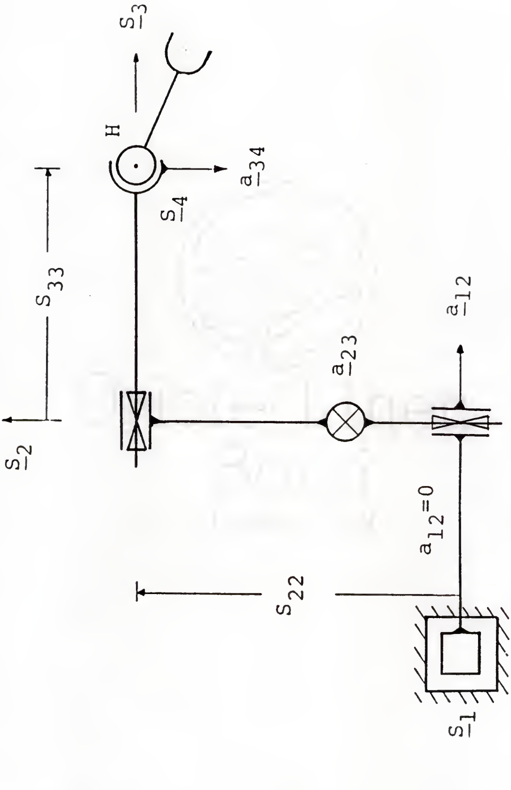

(d) Group 3

Fig. 4.2--continued.

and $S_{11r} = S_{22r} = S_{33r} = 1/3$, yielding

$$|J| = [s_5] \tag{4.21}$$

$$\|HFN(CO_i)\|_{m3} = \|HFN(CO_j)\|_1 = 8\pi^2/27 \qquad j = 1, 2$$

$$\|CHFN_u\|_{m3} = \|CHFN_u\|_1 = 16\pi^2/27$$

The results (summarized in Table 4.1) indicate that the lowest upper bounds of $\|HFN(CO_i)\|_1$ and $\|CHFN_u\|_1$'s for group 0, 1, 2 and 3 SW manipulators are in descending order.

The manipulators listed above yield the maximum possible value of $\|HFN(CO_i)\|_1$ for all configurations. Such configurations will be defined as ideal configurations, i.e., the j'th configuration of a group g SW manipulator with no active P joints is an ideal configuration if $\|HFN(CO_j)\|_1 = \|HFN(CO_i)\|_{mg}$. Further if all configurations of a manipulator are ideal, all passive linear dimensions are zero and $\|CHFN_u\|_1 = \|CHFN_u\|_{mg}$ the manipulator will be said to be an ideal manipulator. It should be noted that the group 0 ideal manipulator defined here is essentially the same as the optimal 6R manipulator derived by Paden (1985) using a differential geometry approach. Ideal manipulators have the following useful properties:

(i) The reachable and dextrous workspaces (see Kumar and Waldron, 1980) of the wrist are identical.

(ii) There are no holes or voids in the workspace except for the ideal group 2 manipulator (see Fig. 4.3).

Table 4.1 Lowest Upper Bounds of $\|HFN(CO_i)\|_1$ and $\|CHFN_u\|_1$ for the Spherical Wrist Manipulators.

g	$\|HFN(CO_i)\|_{mg}$	$\|CHFN_u\|_{mg}$
0	$32\pi^3/3$	$256\pi^3/3$
1	$32\pi^3/27$	$128\pi^3/27$
2	$16\pi^2/27$	$64\pi^2/27$
3	$8\pi^2/27$	$16\pi^2/27$

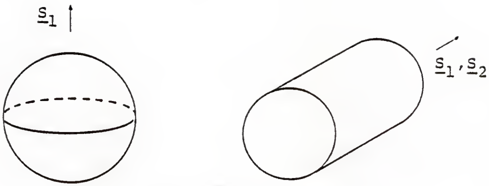

(a) Group 0

(b) Group 1

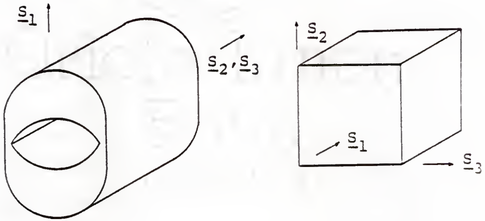

(c) Group 2

(d) Group 3

Fig. 4.3 Wrist Workspaces of the Ideal Spherical Wrist Manipulators

(iii) The end effector has maximum cumulative freedom per volume of the wrist workspace (V_W) for a given $\|\underline{l}\|_1$, i.e., the ratio $\|CHFN_u\|_1/V_W$ is a maximum. Hence an ideal manipulator supplies its end effector with maximum freedom while occupying a given physical space. The group 2 ideal manipulator does not have this property. In fact the ratio $\|CHFN_u\|_1/V_W$ does not have an upper bound for group 2 SW manipulators with no active P joints.

(iv) Special configurations are in general restricted to the outer wrist workspace boundary. The locus of such configurations for the ideal group 0, 1 and 2 manipulators are the surface of the unit sphere and the diameter which is coincident with the first joint axis, the central axis and surface of the cylinder, and the planar portions of the outer wrist workspace, respectively (see Fig. 4.3).

Ideal manipulators yielding a prespecified workspace volume can be designed simply by applying an appropriate scale factor, c, to the dimensions listed above. The hand freedom numbers of the resulting manipulator can be easily obtained using equation (4.4). It should be noted that ideal manipulators are in general unique except for the attachment of the spherical wrist to the first 3 links. For instance, if the fourth joint axis of the ideal group 0 manipulator intersects the third joint axis orthogonally (rather than being parallel to it) and the fifth and sixth joints intersect the fourth one orthogonally the resulting manipulator would still be an ideal group 0 manipulator.

The concepts introduced in this chapter are useful in the kinematic design, motion planning, control and performance evaluation of manipulators of all types. Some examples are given below:

(a) HFN(CO_i), a quantitative measure of the total freedom of the hand corresponding to the i'th configuration, is a function of the dimensions of the robot and the prismatic joint limits. HFN(CO_{ij}) depends in addition on the revolute joint limits. For good design the joint limits should be decided such that the HFN(CO_{ij})'s are in the same order of magnitude. Relatively inefficient CO_{ij}'s, having low HFN(CO_{ij})'s, should either be totally eliminated or made more efficient by changing the joint limits.

(b) Let $\underline{A}$ and $\underline{B}$ denote the end points of the specified path of the end effector in the POH space during a motion planning task. Further, let $\underline{q}_{A1}$, $\underline{q}_{A2}$ and $\underline{q}_{B1}$, $\underline{q}_{B2}$ be the pre-images of A and B under the forward displacement mapping, such that $\underline{q}_{A1}, \underline{q}_{B1} \in CO_{ij}$ and $\underline{q}_{A2}, \underline{q}_{B2} \in CO_{kl}$. Now, if HFN($CO_{ij}$) > HFN($CO_{kl}$), then the prespecified motion of the end effector is more likely to be feasible when the manipulator is in the (ij)'th subconfiguration.

(c) $CHFN_l$ is a quantitative measure of the cumulative freedom of the end effector considered as a rigid body. Different manipulators can be rated according to their $CHFN_l$'s.

(d) $CHFN_l/CHFN_u$ gives the fraction of the $CHFN_u$ utilized under the revolute joint limitations. A relatively small ratio indicates that the revolute joint limits are too tight and/or they have been designed inefficiently. In order to utilize a given size reachable hyperprism (in the joint space) in the most efficient manner, it should be located such that Abs($|J|$) is maximized inside.

(e) $\|HFN(CO_i)\|_1$ and $\|CHFN_u\|_1$ serve as quantitative measures of the efficiency of the design of the dimensions concerning the freedom of the hand corresponding to CO_i and the totality of the configurations, respectively. These measures are not dependent on the size of $\underline{l}$ and can be normalized using $\|HFN(CO_i)\|_{mg}$ and $\|CHFN\|_{mg}$.

4.4 Example

The new concepts introduced in Section 4.1 will now be illustrated using the MBA robot, which is the first example in Section 3.6.1. Firstly, let the regions CO_1, CO_2, ..., CO_8 correspond to the configurations [1, -1, 1], [1, -1, -1], [1, 1, 1], [1, 1 -1], [-1, 1, 1], [-1, 1, -1], [-1, -1, 1] and [-1, -1, -1], respectively. The joint limits of the active joints are given by $\theta_{2l} = (3/2)\pi$, $\theta_{2u} = (79/72)\pi$, $\theta_{3l} = -\pi/4$, $\theta_{3u} = (5/4)\pi$, $\theta_{5l} = -(2/3)\pi$ and $\theta_{5u} = (2/3)\pi$. Furthermore, $\theta_{1r} = (17/18)\pi$, $\theta_{4r} = (3/2)\pi$ and $\theta_{6r} = (10/9)\pi$. Then it follows that each configuration has a single subconfiguration under the joint limitations, i.e., $m_i = 1$ for $i = 1, 2, ..., 8$. Now, from equation (4.1)

$$\mathrm{HFN}(\mathrm{CO}_{11}) = \iiiint\!\!\iint_{\mathrm{CO}_{11}} \mathrm{Abs}\ (|J|)\ dV_q \tag{4.22}$$

Substituting $|J|$ from equation (3.13) and simplifying by taking advantage of the component manifolds, passive and naturally passive joints we obtain

$$\mathrm{HFN}(\mathrm{CO}_{11}) = 550\ [\theta_{1r}\ \theta_{6r}\ \theta_{4r}]\ [I_{23}]\ [I_5] \tag{4.23}$$

where

$$I_{23} = -\iint_{ABCA} (c_3)\ (5 + 22c_2 + 25s_{2+3})\ d\theta_2\ d\theta_3$$

$$I_5 = \int_0^{0.\bar{6}\pi} s_5\ d\theta_5$$

and ABCA is the region shown in Fig. 4.4. It should be recalled that the HSC of the MBA robot consists of 2 component manifolds involving 2 and 1 joint variables, respectively. Therefore, the sextuple integral in equation (4.22) reduces to the product of a double integral, I_{23}, and a single one, I_5. This conclusion is a general one applicable to all manipulators having reducible HSC's. The determination of I_{23} is tremendously simplified if the double integral is evaluated over the region ABCA'A rather than ABCA (see Fig. 4.4). AA'C is the straight line given by $\theta_3 = (-2.0469804)\ \theta_2 + 11.015553$, where θ_2 and θ_3 are in radians. The error introduced by this approximation is negligible for all practical purposes, because the area of the deleted region AA'CA is very small and the value of the integrand over AA'CA

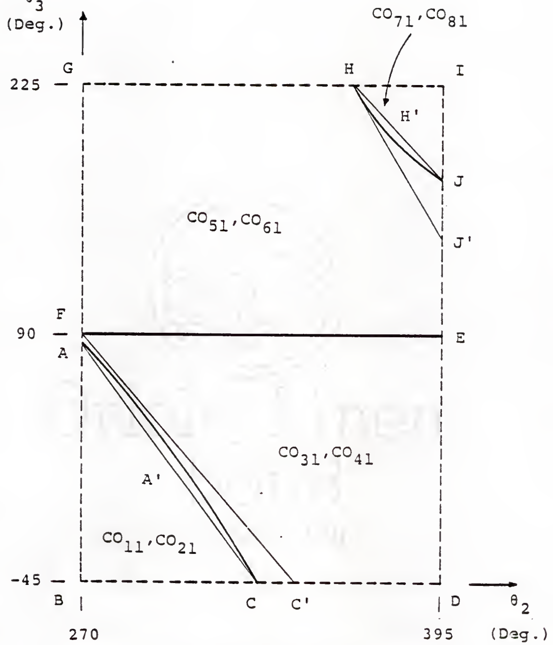

Fig. 4.4 Subconfigurations of the MBA Robot

is close to zero. Now, substituting θ_{1r}, θ_{4r} and θ_{6r} and carrying out the integrations, equation (4.23) yields $HFN(CO_{11}) = 388{,}395$ inch^3. Clearly, $HFN(CO_{21}) = HFN(CO_{11})$. Similarly, the hand freedom numbers of the remaining subconfigurations are determined as

$$HFN(CO_{31}) = HFN(CO_{41}) = 2{,}715{,}200 \text{ inch}^3$$

$$HFN(CO_{51}) = HFN(CO_{61}) = 4{,}778{,}715 \text{ inch}^3$$

$$HFN(CO_{71}) = HFN(CO_{81}) = 190 \text{ inch}^3$$

These results have been obtained using the regions FC'DEF, GFEJ'HG and HH'JIH instead of FACDEF, GFEJHG and HJIH, respectively (see Fig. 4.4). The equations of the lines FC', HJ' and HH'J are

$$\theta_3 = (-1.875)\theta_2 + 10.406526$$

$$\theta_3 = (-3.764328)\theta_2 + 29.529397$$

$$\theta_3 = (-2.437173)\theta_2 + 20.502986$$

respectively, where θ_2 and θ_3 are in radians. The HFN's of the subconfigurations CO_{71} and CO_{81} clearly indicate that they are very inefficient. Hence, in the design stage of the robot they should have been either totally eliminated or made more efficient by changing the joint limits of θ_2 and θ_3. The cumulative hand freedom number of the manipulator, on the other hand, is determined from equation (4.3), yielding $CHFN_1 = 15{,}765{,}000$ inch^3. Here it should be recalled that in general the same size reachable hyperprisms in the joint space do not yield the same $CHFN_1$'s. For instance if the reachable region in the $\theta_2\theta_3$ space is changed to GFEIG and FBDEF, respectively, the corresponding $CHFN_1$'s would be 9,557,810 and 6,207,190 $inch^3$.

It is easier to determine the $HFN(CO_i)$'s using Theorem 4.1:

$$HFN(CO_i) = \theta_{6r} \cdot V(CO_i') \cdot R \qquad (i = 1, 2, \ldots, 8)$$

where $\theta_{6r} = 2\pi$ and

$$R = \int_{\theta_5=0(\pi)}^{\pi(2\pi)} \int_{\theta_4=0}^{2\pi} (s_{45}\ s_{56}\ s_5)\, d\theta_4\, d\theta_5 = 4\pi \qquad (i = 1, 2, \ldots, 8)$$

Thus

$$HFN(CO_i) = 8\pi^2 \cdot V(CO_i') \qquad (i = 1, 2, \ldots, 8)$$

Further $V(CO_i') = V(abca)$ for i = 3, 4, 5, 6 and $V(CO_i') = V(acda)$ for i = 1, 2, 7, 8; where V(abca) and V(acda) are the volumes of revolutions obtained by rotating the hatched areas abca and acda around the z-axis, respectively (see Fig. 4.5). Hence,

$$HFN(CO_i) = 43{,}457{,}056 \text{ inch}^3 \qquad (i = 3, 4, 5, 6)$$

$$HFN(CO_i) = 26{,}313{,}058 \text{ inch}^3 \qquad (i = 1, 2, 7, 8)$$

and from equation (4.2) $CHFN_u = 279{,}080{,}456$ $inch^3$.

The active linear dimensions of the MBA robot are a_{12}, a_{23}, and S_{44}. Hence $\|\underline{l}\|_1 = |a_{12}| + |a_{23}| + |S_{44}| = 5 + 22 + 25 = 52$ inches. Now, let $\underline{l}' = [5\ 22\ 25]^T$, $g = 0$, $c = 1/\|\underline{l}'\|_1 = 1/52$ and

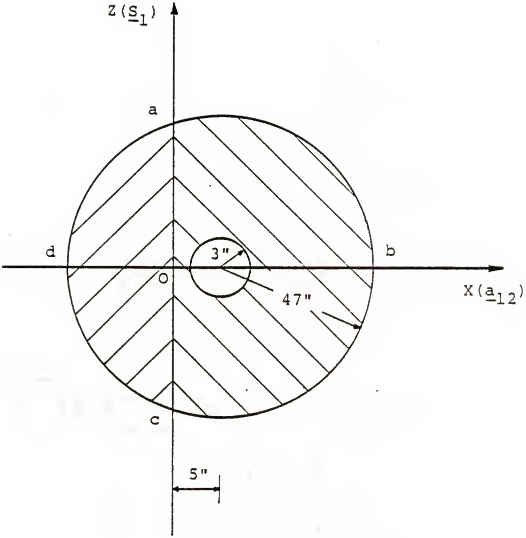

Fig. 4.5 XZ Slices of the CO_i''s for the MBA Robot

HFN' = $CHFN_u$ in equation (4.4). Thus $\|CHFN_u\|_1 = (1/52)^3$ and $(CHFN_u) = (1/52)^3$ (279,080,456) = 1985 inch^3.

The design efficiency of the MBA robot can be evaluated using the following quantities which are independent of the size of $\underline{1}$.

(i) The freedom corresponding to the j'th configuration is ($100t_j$) percent of the freedom corresponding to the ideal configuration where $t_j = \|HFN(CO_j)\|_1 / \|HFN(CO_i)\|_{m0}$. For the MBA robot $t_1 = t_2 = t_7 = t_8 = 0.566$ and $t_3 = t_4 = t_5 = t_6 = 0.934$.

(ii) $\|CHFN_u\|_1 / \|CHFN_u\|_{m0} = 0.75$ which indicates that the cumulative freedom of the end effector is 75% of the ideal group 0 manipulator.

(iii) The freedom corresponding to the (j1)'th subconfiguration is ($100r_j$) percent of the freedom corresponding to the j'th configuration where $r_j = HFN(CO_{j1})/HFN(CO_j)$. For the MBA robot, $r_1 = r_2 = 0.015$, $r_3 = r_4 = 0.062$, $r_5 = r_6 = 0.110$ and $r_7 = r_8 = 0.722 \times 10^{-5}$.

(iv) $CHFN_1/CHFN_u = 0.056$ which indicates that only 5.6% of the available cumulative freedom is used under the joint limitations.

CHAPTER 5
REVERSE VELOCITY ANALYSIS

In this chapter systematic and efficient methods are developed for the reverse velocity analysis. These methods take advantage of any special geometry that the manipulator may have. Furthermore, they can be easily extended to the complete reverse velocity analysis of 1 DOF single loop spatial mechanisms where all of the joint velocities are required.

5.1 Manipulators with 6 Degrees of Freedom

5.1.1 Manipulators Without Any Special Geometry

Let B denote the reference frame attached to the end effector of a 6 DOF manipulator such that the origin 0 is at the tip of the vector $S_{77}\,\underline{S}_7$ and the coordinate axes are parallel to the axes of $\hat{B}_1$. Here the x axes of the frames $\hat{B}_1$ and B are parallel to an imaginary $\underline{a}_{01}$ which can be any convenient unit vector in the place perpendicular to $\underline{S}_1$, and θ_1 is measured from $\underline{a}_{01}$ to $\underline{a}_{12}$ around $\underline{S}_1$ (see Fig. 5.1). Furthermore let $[J_B]$, the Jacobian formulated in the reference frame B, be the special Jacobian discussed in Chapter 2 viz. $[J_B]$ transforms $\dot{\underline{q}}$ into $\underline{V}_B = [\underline{\omega}_B\ \underline{v}_B]^T$ where $\underline{\omega}_B$ and $\underline{v}_B$ are the angular velocity of the end effector and the translational velocity of the point 0 on the end effector. Further, the components of both $\underline{\omega}_B$ and $\underline{v}_B$ are expressed in the frame B.

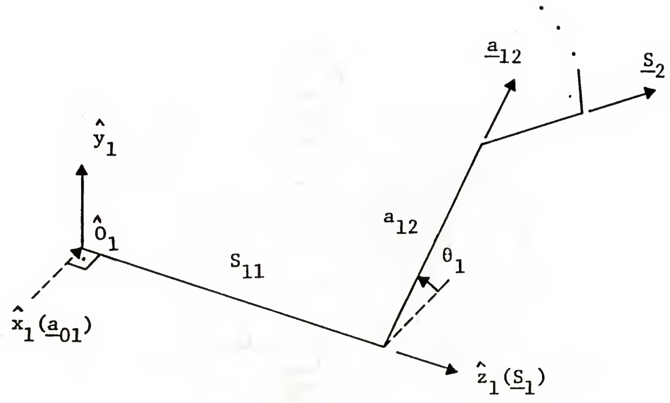

Fig. 5.1 Reference Frame $\hat{B}_1$

The Jacobian $[J_B]$ of a 6 DOF manipulator can be determined using any of the Jacobians $[J_g]$ or $[\hat{J}_g]$ (g=1,2,...,6) together with an appropriate screw transformation matrix, i.e.,

$$[J_B] = [{}^B\$_g][J_g] \tag{5.1}$$

$$[J_B] = [{}^B\$_{\hat{g}}][\hat{J}_g] \tag{5.2}$$

where

$$[{}^B\$_g] = \begin{bmatrix} [{}^BR_g] & [0] \\ [{}^BR_g][E_g] & [{}^BR_g] \end{bmatrix} \tag{5.3}$$

and

$$[E_g] = \begin{bmatrix} 0 & -m_g & l_g \\ m_g & 0 & -k_g \\ -l_g & k_g & 0 \end{bmatrix} \tag{5.4}$$

from equations (2.15) and (2.17), respectively. The matrices $[{}^B\$_{\hat{g}}]$ and $[E_{\hat{g}}]$ can be obtained from (5.3) and (5.4) by replacing the subscript g with $\hat{g}$. The rotation matrices $[{}^BR_g]$, $[{}^BR_{\hat{g}}]$ and the nonzero components of $[E_g]$, $[E_{\hat{g}}]$ (g=1,2,...,6) can be determined by using Table 3.3 in Lipkin and Duffy (1985) and elementary rotation matrices. The details are omitted here and the results are presented below.

$$[{}^{B}R_{g}] = \begin{bmatrix} P_{12..g} & U_{12..g} & X_{12..f} \\ -U_{gf..1} & U^{*}_{gf..1} & -W_{fe..1} \\ R_{23..g} & W_{23..g} & Z_{23..f} \end{bmatrix} \tag{5.5}$$

$$k_{g} = -(a_{gh} + a_{hi}P_{h} + a_{ij}P_{hi} + \dots + a_{67}P_{hi..6}$$

$$+ S_{ii}X_{h} + S_{jj}X_{hi} + \dots + S_{77}X_{hi..6}) \tag{5.6}$$

$$l_{g} = -(a_{hi}Q_{h} + a_{ij}Q_{hi} + \dots + a_{67}Q_{hi..6} - S_{hh}s_{gh}$$

$$+ S_{ii}Y_{h} + S_{jj}Y_{hi} + \dots + S_{77}Y_{hi..6}) \tag{5.7}$$

$$m_{g} = -(a_{hi}R_{h} + a_{ij}R_{hi} + \dots + a_{67}R_{hi..6} + S_{hh}c_{gh}$$

$$+ S_{ii}Z_{h} + S_{jj}Z_{hi} + \dots + S_{77}Z_{hi..6}) \tag{5.8}$$

$$[{}^{B}R_{\hat{g}}] = \begin{bmatrix} P_{fe..1} & -Q_{fe..1} & R_{fe..1} \\ -U_{fe..1} & V_{fe..1} & -W_{fe..1} \\ X_{fe..2} & -Y_{fe..2} & Z_{fe..2} \end{bmatrix} \tag{5.9}$$

$$k_{\hat{g}} = -(a_{gh}\bar{P}_{g} + a_{hi}P_{hg} + \dots + a_{67}P_{6..hg} + S_{hh}\bar{R}_{g}$$

$$+ S_{ii}R_{hg} + \dots + S_{77}R_{6..hg}) \tag{5.10}$$

$$l_{\hat{g}} = a_{gh}\bar{U}_{g} + a_{hi}U_{hg} + \dots + a_{67}U_{6..hg} + S_{hh}\bar{W}_{g}$$

$$+ S_{ii}W_{hg} + \dots + S_{77}W_{6..hg} \tag{5.11}$$

$$m_{\hat{g}} = -(a_{hi}\bar{X}_h + a_{ij}X_{ih} + \dots + a_{67}X_{6..ih} + S_{gg}$$

$$+ S_{hh}c_{gh} + S_{ii}\bar{Z}_h + S_{jj}Z_{ih} + \dots + S_{77}Z_{6..ih}) \quad (5.12)$$

where g=3,4 and defghij designate successive positive integers in ascending order. The definitions of the P,Q,R,U,V,W,X,Y,Z terms in equations (5.5) - (5.12) are given in Appendix A and a multiply subscripted U^* term, with ascending or descending subscripts, is defined as

$$U^*_{ih..ed} = s_i U_{h..ed} + c_i V_{h..ed} \quad (5.13)$$

Equations (5.3) - (5.12) yield the components of $[{}^B\$_3]$, $[{}^B\$_4]$, $[{}^B\$_{\hat{3}}]$ and $[{}^B\$_{\hat{4}}]$ in closed form. The remaining screw transformation matrices namely, $[{}^B\$_1]$, $[{}^B\$_2]$, $[{}^B\$_5]$, $[{}^B\$_6]$, $[{}^B\$_{\hat{1}}]$, $[{}^B\$_{\hat{2}}]$, $[{}^B\$_{\hat{5}}]$, $[{}^B\$_{\hat{6}}]$, are omitted since they do not yield $[J_B]$ efficiently via equation (5.1) or (5.2). This is because the matrices $[J_g]$ and $[\hat{J}_g]$ are complicated for g=1,2,5,6 (see Table 2.3(d) for the optimal coordinate systems of 6 DOF manipulators). Furthermore the corresponding screw transformation matrices will also be complicated.

It follows from equations (5.1) and (5.2) that

$$[J_B]^{-1} = [J_g]^{-1}\,[{}^g\$_B] \quad (5.14)$$

$$[J_B]^{-1} = [\hat{J}_g]^{-1}\,[{}^{\hat{g}}\$_B] \quad (5.15)$$

respectively, where from equation (2.19)

$$[{}^{g}\$_{B}] = \begin{bmatrix} [{}^{B}R_{g}]^{T} & [0] \\ [E_{g}]^{T}\,[{}^{B}R_{g}]^{T} & [{}^{B}R_{g}]^{T} \end{bmatrix} \tag{5.16}$$

$$[{}^{\hat{g}}\$_{B}] = \begin{bmatrix} [{}^{B}R_{g}]^{T} & [0] \\ [E_{\hat{g}}]^{T}\,[{}^{B}R_{\hat{g}}]^{T} & [{}^{B}R_{\hat{g}}]^{T} \end{bmatrix} \tag{5.17}$$

Equations (5.1), (5.2) and (5.14), (5.15) can be used to obtain $[J_B]$ and $[J_B]^{-1}$ for any type of 6 DOF manipulator in closed form. In order to obtain $[J_B]^{-1}$ it is necessary to invert a Jacobian $[J_g]$ or $[\hat{J}_g]$, the closed forms of which can be readily obtained from Table 2.1. This inversion process can be simplified by partitioning an appropriate Jacobian into submatrices.

5.1.2 Manipulators With Special Geometry

Consider an n×n nonsingular matrix T. Let T be partitioned such that

$$T = \begin{bmatrix} T_1 & T_2 \\ T_3 & T_4 \end{bmatrix} \tag{5.18}$$

where T_1, T_2, T_3 and T_4 are a×a, a×b, b×a and b×b submatrices, respectively (n=a+b). It can then be shown that

$$T^{-1} = \begin{bmatrix} t_1 & t_2 \\ t_3 & t_4 \end{bmatrix} \tag{5.19}$$

where

$$t_1 = (T_1 - T_2T_4^{-1}T_3)^{-1} \tag{5.20}$$

$$t_2 = -t_1T_2T_4^{-1} \tag{5.21}$$

$$t_3 = -T_4^{-1}T_3t_1 \tag{5.22}$$

$$t_4 = T_4^{-1} - T_4^{-1}T_3t_2 \tag{5.23}$$

Here t_1, t_2, t_3, t_4 are a×a, a×b, b×a, b×b submatrices, respectively, and the matrix T_4 is nonsingular. Equations (5.20) - (5.23) simplify considerably if any one of the submatrices T_1, T_2 or T_3 is the null matrix. It will next be shown that for certain classes of manipulators at least one of the Jacobians $[J_1],\ldots,[J_6],[\hat{J}_1],\ldots,[\hat{J}_6]$ can be transformed into an equivalent Jacobian matrix which can be partitioned such that T_2 in equation (5.18) is a 4×2 null submatrix.

The 6 DOF manipulators can be classified and labelled according to the geometry of the axes of a pair of successive joints α and β. The axes of these joints may be

(i) Intersecting ($a_{\alpha\beta}=0$),

(ii) Parallel or antiparallel ($s_{\alpha\beta}=0$),

(iii) Orthogonal ($c_{\alpha\beta}=0$),

(iv) Nonorthogonal and skew ($c_{\alpha\beta}\neq 0$, $a_{\alpha\beta}\neq 0$, $s_{\alpha\beta}\neq 0$)

or a combination of these where $\alpha\varepsilon\{1,2,\ldots,5\}$ and $\beta=\alpha+1$. The class of a manipulator will be described by the format xxx-xx where the symbol x will denote a capital letter or an integer. The first symbol in the format is one of the letters A, S, C or N which label the cases (i)-(iv), respectively. The second and third symbols are integers which designate α and β. Finally the last pair of symbols are either one of the letters R or P and denote the types of the α'th and β'th joints, respectively. For example, if the second and third joints of a manipulator are revolute and prismatic joints, respectively, and the axes of these joints are orthogonal, then the manipulator will belong to the class C23-RP.

Consider now the following special classes of manipulators and the corresponding transformed Jacobians.

1) $A\alpha\beta$-RR manipulators:

$$[J'_\alpha] = [K_{25}][K_{36}][J_\alpha][K_c] \tag{5.24}$$

$$[\hat{J}'_\beta] = [K_{25}][K_{36}][\hat{J}_\beta][K_c] \tag{5.25}$$

2) $S\alpha\beta$-RR manipulators:

$$[J'_\alpha] = [K_{36}][J_\alpha][K_c] \tag{5.26}$$

$$[\hat{J}'_\beta] = [K_{36}][\hat{J}_\beta][K_c] \tag{5.27}$$

3) $S\alpha\beta$-PR manipulators:

$$[\hat{J}'_\beta] = [K_{35}][\hat{J}_\beta][K_c] \tag{5.28}$$

4) $S\alpha\beta$-RP manipulators:

$$[J'_\alpha] = [K_{35}][J_\alpha][K_c] \tag{5.29}$$

5) Cαβ-PR manipulators:

$$[J'_\alpha] = [K_{25}][J_\alpha][K_c] \tag{5.30}$$

$$[\hat{J}'_\beta] = [K_{36}][\hat{J}_\beta][K_c] \tag{5.31}$$

6) Cαβ-RP manipulators:

$$[J'_\alpha] = [K_{36}][J_\alpha][K_c] \tag{5.32}$$

$$[\hat{J}'_\beta] = [K_{25}][\hat{J}_\beta][K_c] \tag{5.33}$$

7) Nαβ-PP manipulators:

$$[J'_\alpha] = [J_\alpha][K_c] \tag{5.34}$$

$$[\hat{J}'_\beta] = [\hat{J}_\beta][K_c] \tag{5.35}$$

where $\alpha=1,2,\ldots,5$; $\beta=\alpha+1$ and

$$[K_c] = [K_{\beta 6}][K_{\alpha 5}] \tag{5.36}$$

Here $[K_{ip}]$ denotes the 6×6 elementary transformation matrix which is obtained from the identity matrix $[I_6]$ by interchanging the i'th and p'th columns. If a 6×6 matrix [M] is premultiplied (postmultiplied) by $[K_{ip}]$, the i'th and p'th rows (columns) of [M] are interchanged. Clearly, $[K_{ip}]^{-1} = [K_{ip}]$.

It should be noted that both the natural (i.e., unprimed) and the transformed (i.e., primed) Jacobians describe the same linear transformation which is from the actuator velocity space into the hand velocity space. However, the domain and range spaces are coordinatized differently. The natural Jacobian $[J_\alpha]([\hat{J}_\alpha])$ transforms the actuator velocity vector $\underline{\dot{q}} = [\dot{q}_1 \ldots \dot{q}_6]^T$ into the hand velocity vector $\underline{V}_\alpha = [\underline{\omega}_\alpha \; \underline{v}_\alpha]^T = [\omega_{\alpha x} \; \omega_{\alpha y} \; \omega_{\alpha z} \; v_{\alpha x} \; v_{\alpha y} \; v_{\alpha z}]^T$ $(\hat{\underline{V}}_\alpha = [\hat{\underline{\omega}}_\alpha \; \hat{\underline{v}}_\alpha]^T = [\hat{\omega}_{\alpha x} \; \hat{\omega}_{\alpha y} \; \hat{\omega}_{\alpha z} \; \hat{v}_{\alpha x} \; \hat{v}_{\alpha y} \; \hat{v}_{\alpha z}]^T)$, where $\underline{\omega}_\alpha(\hat{\underline{\omega}}_\alpha)$ and $\underline{v}_\alpha(\hat{\underline{v}}_\alpha)$ designate the angular velocity of the end effector and the translational velocity of a point on the end effector which is instantaneously coincident with $0_\alpha(\hat{0}_\alpha)$. Here both vectors are expressed in $B_\alpha(\hat{B}_\alpha)$. The transformed Jacobians

$$[J'_\alpha] = [K_r][J_\alpha][K_c] \tag{5.37}$$

and

$$[\hat{J}'_\alpha] = [K_r][\hat{J}_\alpha][K_c] \tag{5.38}$$

on the other hand, transforms

$$\underline{\dot{q}}' = [K_c]^{-1} \; \underline{\dot{q}} \tag{5.39}$$

into

$$\underline{V}'_\alpha = [K_r] \; \underline{V}_\alpha \tag{5.40}$$

and

$$\hat{\underline{V}}'_\alpha = [K_r] \; \hat{\underline{V}}_\alpha \tag{5.41}$$

respectively. Clearly all of the transformation matrices $[K_r]$ and $[K_c]$ in equations (5.24) - (5.35) are simple, orthogonal matrices. They recoordinatize the actuator and hand velocity spaces via equations (5.39) - (5.41) merely by changing the order of the base vectors.

The transformed Jacobians given by equations (5.24) - (5.35) can be partitioned as in equation (5.18) where a=4 and b=2. This yields $T_2=0$ for each case and the inverses of the transformed Jacobians can be obtained from (5.20) - (5.23). Therefore,

$$t_1 = T_1^{-1} \tag{5.42}$$

$$t_2 = 0 \tag{5.43}$$

$$t_3 = -T_4^{-1}T_3T_1^{-1} \tag{5.44}$$

$$t_4 = T_4^{-1} \tag{5.45}$$

where the T_4^{-1} matrices for the transformed Jacobians given by equations (5.24) - (5.35) are

$$[T_4]^{-1} = \begin{bmatrix} c_{\alpha\beta}/s_{\alpha\beta} & 1 \\ -1/s_{\alpha\beta} & 0 \end{bmatrix} \tag{5.46}$$

$$[T_4]^{-1} = \begin{bmatrix} 1/s_{\alpha\beta} & 0 \\ -c_{\alpha\beta}/s_{\alpha\beta} & 1 \end{bmatrix} \tag{5.47}$$

$$[T_4]^{-1} = \begin{bmatrix} 1/a_{\alpha\beta} & 1 \\ -1/(a_{\alpha\beta}c_{\alpha\beta}) & 0 \end{bmatrix} \tag{5.48}$$

$$[T_4]^{-1} = \begin{bmatrix} 1/(a_{\alpha\beta}c_{\alpha\beta}) & 0 \\ -1/a_{\alpha\beta} & 1 \end{bmatrix} \tag{5.49}$$

$$[T_4]^{-1} = \begin{bmatrix} 0 & 1/c_{\alpha\beta} \\ 1 & 0 \end{bmatrix} \tag{5.50}$$

$$[T_4]^{-1} = \begin{bmatrix} 1 & 0 \\ 0 & 1/c_{\alpha\beta} \end{bmatrix} \tag{5.51}$$

$$[T_4]^{-1} = \begin{bmatrix} -a_{\alpha\beta} & 1 \\ -1/s_{\alpha\beta} & 0 \end{bmatrix} \tag{5.52}$$

$$[T_4]^{-1} = \begin{bmatrix} 1/s_{\alpha\beta} & 0 \\ 0 & 1 \end{bmatrix} \tag{5.53}$$

$$[T_4]^{-1} = \begin{bmatrix} 0 & 1 \\ -1/s_{\alpha\beta} & 0 \end{bmatrix} \tag{5.54}$$

$$[T_4]^{-1} = \begin{bmatrix} 1/s_{\alpha\beta} & 0 \\ a_{\alpha\beta} & 1 \end{bmatrix} \tag{5.55}$$

$$[T_4]^{-1} = \begin{bmatrix} c_{\alpha\beta}/s_{\alpha\beta} & 1 \\ -1/s_{\alpha\beta} & 0 \end{bmatrix} \tag{5.56}$$

$$[T_4]^{-1} = \begin{bmatrix} 1/s_{\alpha\beta} & 0 \\ -c_{\alpha\beta}/s_{\alpha\beta} & 1 \end{bmatrix} \tag{5.57}$$

respectively. Hence the inverses of the transformed Jacobians given by (5.24) - (5.35) can be determined by inverting a single 4×4 submatrix, T_1, only.

Suppose now that a 6 DOF manipulator belongs to one of the 7 special classes identified previously. The corresponding transformed Jacobian will be of the form (5.37) or (5.38), say (5.37) for instance. The inverse, $[J'_\alpha]^{-1}$, can be effectively determined as described in the previous paragraph. The inverse of the natural Jacobian $[J_\alpha]$ can then be expressed as

$$[J_\alpha]^{-1} = [K_c][J'_\alpha]^{-1}[K_r] \tag{5.58}$$

Substituting (5.58) into (5.14) together with g=α,

$$[J_B]^{-1} = [J''_\alpha]^{-1}\ [{}^{\alpha}\$'_B] \tag{5.59}$$

where $[J''_\alpha]^{-1} = [K_c]\ [J'_\alpha]^{-1}$ and $[{}^{\alpha}\$'_B] = [K_r]\ [{}^{\alpha}\$_B]$. These matrices can simply be obtained by interchanging the appropriate rows of $[J'_\alpha]^{-1}$ and $[{}^{\alpha}\$_B]$ as depicted by $[K_c]$ and $[K_r]$, respectively.

For most industrial manipulators the closed form of $[J_B]^{-1}$ will be simple. Hence it will be efficient to use $[J_B]^{-1}$ for the reverse velocity analysis. However, if $[J_B]^{-1}$ is too complicated, the matrices $[^{\alpha}\$'_B]$ and $[J''_{\alpha}]^{-1}$ in (5.59) should not be premultiplied. In this case $\dot{\underline{q}}$ can be more efficiently determined by multiplying the given $\underline{V}_B$ with $[^{\alpha}\$'_B]$ and $[J''_{\alpha}]^{-1}$, respectively.

Suppose now that a single dimension of a manipulator is specified such that the manipulator belongs to one of the 7 classes identified previously and the corresponding transformed Jacobian is $[J'_{\alpha}]$. The number of terms in T_1, i.e., the 4×4 submatrix in the upper left-hand corner of $[J'_{\alpha}]$, will be a minimum if α is the optimal coordinate system for the manipulator (see Section 2.2). The submatrix T_1 will simplify even further if some of the remaining dimensions are also special, i.e., a linear dimension(s) is zero and/or an angular dimension(s) is a multiple of $\pi/2$ or π. Therefore, it follows that, if possible, the transformed Jacobian corresponding to the optimal coordinate system is the best one to be used in equation (5.59). Here it is useful to note that a manipulator can belong to more than one class and for a given class there may be two alternatives for the transformed Jacobian.

Equations (5.24) - (5.35) can also be used in the kinematic design stage of the manipulator in order to design manipulators with efficient reverse velocity analyses. The first step in the design process is the determination of the type of the manipulator, after which the optimal coordinate system(s) can be obtained from

Table 2.3(d). Suppose for example that the α'th coordinate system is the optimal one. It is always possible to include the manipulator into one of the 7 classes such that $[J'_\alpha]$ is the corresponding transformed Jacobian. The design constraint necessary to achieve this involves only a single dimension (a_{ij} or α_{ij}) for which there may be several alternatives. Hence this constraint is not overly restrictive at all and allows other design criterion to be satisfied simultaneously.

5.2 Manipulators Containing a Planar Pair

Let the 6 DOF manipulators containing three successive joints which are kinematically equivalent to a planar (E) pair be classified according to the format E(xxx)-x. The symbols inside the parentheses are either an R or a P, designating the types of the joints (in ascending order) that are equivalent to the planar pair. The last symbol is an integer which stands for the joint number of the first of the joints simulating the E-pair. For example, if the third, fourth, and fifth joints of a manipulator are of the types R, P, and P, respectively, and if these kinematic pairs are equivalent to an E-pair, then the robot will be said to belong to the class E(RPP)-3. There are altogether 7 such classes which are listed in Table 5.1 together with the special dimensions of the kinematic chain equivalent to the E-pair. In this table d=1,2,3,4; e=d+1 and f=d+2.

The last column of Table 5.1 lists the transformed Jacobians which can be obtained from equations (5.37) and (5.38) where

Table 5.1 Dimensions and Transformed Jacobians of the 6 DOF Manipulators Containing Planar Pairs.

Class	α_{de} (Deg.)	α_{ef} (Deg.)	θ_e (Deg.)	Transformed Jacobians
E(RRR)-d	0	0	-	$[J'_d],[J'_e],[J'_f],[\hat{J}'_d],[\hat{J}'_e],[\hat{J}'_f]$
E(PRR)-d	90	0	-	$[J'_e],[J'_f],[\hat{J}'_e],[\hat{J}'_f]$
E(RPR)-d	90	90	180	$[J'_d],[J'_f],[\hat{J}'_d],[\hat{J}'_f]$
E(RRP)-d	0	90	-	$[J'_d],[J'_e],[\hat{J}'_d],[\hat{J}'_e]$
E(RPP)-d	90	-	90	$[J'_d],[\hat{J}'_d]$
E(PRP)-d	90	90	-	$[J'_e],[\hat{J}'_e]$
E(PPR)-d	-	90	90	$[J'_f],[\hat{J}'_f]$

α=d,e,f and

$$[K_r] = [K_{36}] \tag{5.60}$$

$$[K_c] = [K_{f6}][K_{e5}][K_{d4}] \tag{5.61}$$

Every transformed Jacobian shown in this table can be partitioned as in equation (5.18) where a=b=3. This yields T_2=0 for each case and the inverses of the transformed Jacobians can be conveniently determined from (5.42) - (5.45). Some of the T_4^{-1} matrices for the transformed Jacobians are listed below.

E(RRR)-d manipulators:

$$[T_4]_d^{-1} = \frac{1}{a_{de}a_{ef}} \begin{bmatrix} a_{ef}c_e/s_e & a_{ef} & a_{de}a_{ef} \\ -(a_{de}+a_{ef}c_e)/s_e & -a_{ef} & 0 \\ a_{de}/s_e & 0 & 0 \end{bmatrix} \tag{5.62}$$

$$[T_4]_e^{-1} = \frac{1}{a_{de}a_{ef}} \begin{bmatrix} a_{ef}/s_e & 0 & 0 \\ -(a_{de}c_e+a_{ef})/s_e & a_{de} & a_{de}a_{ef} \\ a_{de}c_e/s_e & -a_{de} & 0 \end{bmatrix} \tag{5.63}$$

E(PRR)-d manipulators:

$$[T_4]_e^{-1} = \frac{1}{a_{ef}} \begin{bmatrix} a_{ef}/s_e & 0 & 0 \\ -c_e/s_e & 1 & a_{ef} \\ c_e/s_e & -1 & 0 \end{bmatrix} \tag{5.64}$$

$$[\hat{T}_4]_f^{-1} = \frac{1}{a_{ef}} \begin{bmatrix} a_{ef}/s_e & 0 & 0 \\ -c_e/s_e & 1 & 0 \\ c_e/s_e & -1 & a_{ef} \end{bmatrix} \tag{5.65}$$

E(RPR)-d manipulators:

$$[T_4]_d^{-1} = \begin{bmatrix} 1/S_{ee} & 0 & 1 \\ (a_{de}-a_{ef})/S_{ee} & -1 & 0 \\ -1/S_{ee} & 0 & 0 \end{bmatrix} \tag{5.66}$$

E(RRP)-d manipulators:

$$[T_4]_d^{-1} = \frac{1}{a_{de}} \begin{bmatrix} c_e/s_e & 1 & a_{de} \\ -c_e/s_e & -1 & 0 \\ a_{de}/s_e & 0 & 0 \end{bmatrix} \tag{5.67}$$

$$[T_4]_e^{-1} = \frac{1}{a_{de}} \begin{bmatrix} 1/s_e & 0 & 0 \\ -1/s_e & 0 & a_{de} \\ a_{de}c_e/s_e & -a_{de} & 0 \end{bmatrix} \quad (5.68)$$

E(RPP)-d manipulators:

$$[T_4]_d^{-1} = \begin{bmatrix} 0 & 0 & 1 \\ -c_{ef}/s_{ef} & -1 & 0 \\ 1/s_{ef} & 0 & 0 \end{bmatrix} \quad (5.69)$$

E(PRP)-d manipulators:

$$[T_4]_e^{-1} = \begin{bmatrix} 1/s_e & 0 & 0 \\ 0 & 0 & 1 \\ c_e/s_e & -1 & 0 \end{bmatrix} \quad (5.70)$$

E(PPR)-d manipulators:

$$[\hat{T}_4]_f^{-1} = \begin{bmatrix} 1/s_{de} & 0 & 0 \\ -c_{de}/s_{de} & 1 & 0 \\ 0 & 0 & 1 \end{bmatrix} \quad (5.71)$$

where $[T_4]_\alpha$ and $[\hat{T}_4]_\alpha$ (α=d,e,f) denote the 3×3 submatrices in the lower right-hand corners of $[J'_\alpha]$ and $[\hat{J}'_\alpha]$, respectively. The remaining $[T_4]^{-1}$ matrices, to be used in equations (5.42) - (5.45) for the inversion of the transformed Jacobians listed in Table 5.1, can be obtained using (5.62) - (5.71) and the following relations:

$$[\hat{T}_4]_\alpha^{-1} = [T_4]_\alpha^{-1} \, [{}^{\alpha}R_{\hat{\alpha}}] \tag{5.72}$$

$$[\hat{T}_4]_f^{-1} = [K_{13}] \, [T_4']_d^{-1} \, [K_m] \tag{5.73}$$

where $\alpha = d,e,f$;

$$[{}^{\alpha}R_{\hat{\alpha}}] = \begin{bmatrix} c_\alpha & s_\alpha & 0 \\ -s_\alpha & c_\alpha & 0 \\ 0 & 0 & 1 \end{bmatrix} \tag{5.74}$$

$$[K_m] = \begin{bmatrix} 1 & 0 & 0 \\ 0 & -1 & 0 \\ 0 & 0 & 1 \end{bmatrix} \tag{5.75}$$

and $[T_4']_d^{-1}$ is the 3×3 matrix obtained by interchanging the subscripts de and ef by ef and de, respectively, in the components of $[T_4]_d^{-1}$. Hence the inverses of the transformed Jacobians listed in Table 5.1 can be determined by inverting a single 3×3 submatrix, T_1, only.

The inverse of the base Jacobian, $[J_B]^{-1}$, can be determined from (5.59) where $[K_r]$ and $[K_c]$ are given by (5.60) and (5.61). Any of the transformed Jacobians shown in Table 5.1 can be used in (5.59). However, it is best to use the Jacobian $[J'_{min}]$ which is the transformed Jacobian with the least number of terms in the first 3 columns. Its inverse can thus be computed with a minimum effort. The transformed Jacobian $[J'_{min}]$ can be easily determined using equations (5.37) and (5.38) and Tables 2.1 and 2.2 once the type of the manipulator is known.

5.3 Manipulators Containing a Spherical Pair

Three successive revolute joints, say the d'th, e'th and f'th ones, with the property that $a_{de} = a_{ef} = S_{ee} = 0$ are kinematically equivalent to a spherical pair. A manipulator containing such a special 3R chain will be said to be an S-d manipulator (d=1,2,3,4). For an S-d manipulator consider the transformed Jacobians $[J'_d]$,$[J'_e]$, $[\hat{J}'_e]$ and $[\hat{J}'_f]$ which are defined by (5.37) and (5.38) where

$$[K_r] = [K_{14}][K_{25}][K_{36}] \tag{5.76}$$

$$[K_c] = [K_{f6}][K_{e5}][K_{d4}] \tag{5.77}$$

These Jacobians can be partitioned as in equation (5.18) with a=b=3. This yields T_2=0 for each case and the inverses of the transformed Jacobians can be conveniently determined from (5.42) - (5.45). The Jacobian $[J'_f]$($[\hat{J}'_d]$) will have the same property if the joint offset S_{ff}(S_{dd}) is also zero in addition to a_{de},a_{ef} and S_{ee}. The T_4^{-1} matrices for $[J'_d]$ and $[J'_e]$ are

$$[T_4]_d^{-1} = \frac{1}{s_{de}s_{ef}} \begin{bmatrix} s_{ef}c_e/s_e & c_{de}s_{ef} & s_{de}s_{ef} \\ -(s_{de}c_{ef}+c_{de}s_{ef}c_e)/s_e & -s_{ef} & 0 \\ s_{de}/s_e & 0 & 0 \end{bmatrix} \qquad (5.78)$$

and

$$[T_4]_e^{-1} = \frac{1}{s_{de}s_{ef}} \begin{bmatrix} s_{ef}/s_e & 0 & 0 \\ -(s_{de}c_{ef}c_e+c_{de}s_{ef})/s_e & s_{de}c_{ef} & s_{de}s_{ef} \\ s_{de}c_e/s_e & -s_{de} & 0 \end{bmatrix} \qquad (5.79)$$

respectively. The remaining inverses, namely $[T_4]_f^{-1}$, $[\hat{T}_4]_d^{-1}$, $[\hat{T}_4]_e^{-1}$ and $[\hat{T}_4]_f^{-1}$, can be easily obtained from equations (5.72), (5.73), (5.78) and (5.79). Hence the inverses of the transformed Jacobians can be determined by inverting a single 3×3 matrix, T_1, only.

The inverse of the base Jacobian, $[J_B]^{-1}$, can be determined from (5.59) where $[K_r]$ and $[K_c]$ are given by (5.76) and (5.77). Analogous to the manipulators containing E-pairs, it is best to use the transformed Jacobian $[J'_{min}]$ in equation (5.59) (see the last paragraph of section 5.2 for the definition and the determination of $[J'_{min}]$).

5.4 Singularities

The reverse velocity analysis of a manipulator breaks down whenever the manipulator is in a special (or singular) configuration, i.e., whenever the joint displacement vector $\underline{q}$ is on the HSC. In this section the equations of the HSC's for two broad and important classes of manipulators will be listed in closed-form. The first class is the well known spherical wrist (SW) manipulators which includes many industrial robots. The second class is the planar wrist (PW) manipulators defined in the next section.

5.4.1 Planar Wrist Manipulators

Planar wrist manipulators are analogous to their spherical wrist counterparts in many ways. As the name implies, the last 3 links of a PW manipulator are kinematically equivalent to a planar pair. The first 3 joint freedoms are employed to locate the end effector on a specified plane P such that $\underline{a}_{67}$ lies in P and $\underline{S}_7$ is parallel to the unique normal assigned to P. The last 3 joint freedoms simply control the position and orientation of $\underline{a}_{67}$ in P. Therefore, the motion of the end effector on a specified plane is decoupled from the positioning of the end effector on that plane. Consider now the following properties of the PW manipulators:

(i) The reverse displacement analysis can be easily and efficiently tackled in real time (see section 6.2.2).

(ii) The reverse velocity analysis can be reduced to the inversion of a 3×3 submatrix (see section 5.2) and thus lends itself to fast computation.

(iii) The fourth joint of a PW manipulator is always passive; and the HSC, which reduces to at most a 2-manifold in the 3-dimensional active joint space, consists of two component manifolds (see Theorem 3.1). Therefore, the identification of the HSC and the configurations is enhanced extensively.

(iv) There are seven different classes of PW manipulators (excluding the arrangement of the first three joints). These classes are E(RRR)-4, E(PRR)-4, E(RPR)-4, E(RRP)-4, E(RPP)-4, E(PRP)-4 and E(PPR)-4 (see Table 5.1 for the corresponding dimensions and transformed Jacobians). This leads to flexibility in the kinematic design, allowing other design criteria to be satisfied simultaneously.

(v) Many industrial tasks require a manipulator(s) to perform operations on different prespecified planes. Planar wrist manipulators are especially suitable for such cases because most of the time it is only necessary to control the last three joints. Furthermore, for the PW manipulators the problems of obstacle avoidance and interference of two robots operating in parallel can be efficiently tackled using the algorithms developed for planar robots by Young (1986).

It, therefore, follows that the PW manipulators are suitable for the control and motion planning algorithms as much as their SW counterparts. However, as a direct consequence of their kinematic designs, the PW manipulators are more suitable for tasks requiring planar motion whereas the SW manipulators may serve better for handling and transportation purposes.

It follows from Theorem 3.1 that the HSC of a PW manipulator is at most a 2-manifold in the 3-dimensional active joint space.

Furthermore, the HSC consists of 2 component manifolds, namely HSC_{11} and HSC_{22}. The second manifold, HSC_{22}, is dependent on the class of the PW manipulator. The equation of this manifold for the 7 different classes are listed in the following table (Table 5.2). It should be noted that besides the joint variables, the equation of the HSC_{22}'s also contain the dimensions which have to be nonzero. Furthermore, the second component manifold consists of the pair of planes $\theta_5=0$, $\theta_5=\pi$ for the classes E(RRR)-4, E(PRR)-4, E(RRP)-4 and E(PRP)-4; the plane $S_{55}=0$ for the class E(RPR)-4; and the null set for the classes E(RPP)-4 and E(PPR)-4.

The first component manifold HSC_{11}, on the other hand, depends on both the class of the manipulator and the types of the first three joints. The equation of this manifold for the PW manipulators RRRE, RPRE, RRPE and PRRE are listed below.

RRRE Manipulators:

$$\begin{aligned} s_{34}[a_{12}(&s_{12}s_{23}^2s_{34}s_3c_3 - s_{12}s_{23}c_{23}c_{34}s_3 - c_{12}s_{23}^2c_{34}c_2s_3 \\ &- c_{12}s_{23}c_{23}s_{34}c_2s_3c_3 + c_{12}s_{23}s_{34}s_2s_3^2) + a_{23}(s_{12}s_{34}c_2s_3c_3 \\ &+ s_{12}s_{23}c_{34}s_2c_3 + s_{12}c_{23}s_{34}s_2c_3^2) + S_{22}(s_{12}s_{23}^2c_{34}s_2s_3 \\ &+ s_{12}s_{23}c_{23}s_{34}s_2s_3c_3 + s_{12}s_{23}s_{34}c_2s_3^2)] = 0 \end{aligned} \qquad (5.80)$$

RPRE Manipulators:

$$\begin{aligned} s_{34}(&s_{12}s_{23}c_{23}s_{34}c_2s_3c_3 + s_{12}s_{23}s_{34}s_2c_3^2 - s_{12}c_{23}c_{34}s_2c_3 \\ &- s_{12}c_{23}^2c_{34}c_2s_3 + c_{12}s_{23}^2s_{34}s_3c_3 - c_{12}s_{23}c_{23}c_{34}s_3) = 0 \end{aligned} \qquad (5.81)$$

Table 5.2 Equations of HSC_{22} for the PW Manipulators.

Class	Equation of HSC_{22}
E(RRR)-4	$a_{45}a_{56}s_5 = 0$
E(PRR)-4	$a_{56}s_5 = 0$
E(RPR)-4	$S_{55} = 0$
E(RRP)-4	$a_{45}s_5 = 0$
E(RPP)-4	$s_{56} = 0$
E(PRP)-4	$s_5 = 0$
E(PPR)-4	$s_{45} = 0$

RRPE Manipulators:

$$s_{12}c_{34}(s_{23}c_{34}s_2 + c_{23}s_{34}c_3s_2 + s_{34}s_3c_2) = 0 \qquad (5.82)$$

PRRE Manipulators:

$$\begin{aligned} s_{23}s_{34}(s_3)(s_{12}s_{34}s_2s_3 &- s_{12}s_{23}c_{34}c_2 - s_{12}c_{23}s_{34}c_2c_3 \\ &+ c_{12}c_{23}c_{34} - c_{12}s_{23}s_{34}c_3) = 0 \qquad (5.83) \end{aligned}$$

The remaining possible types of PW manipulators PPPE, RPPE, PRPE and PPRE are not considered here because they cannot supply the end effector with the full 6 degrees of freedom, i.e., $|J|$ for each of these manipulators vanishes identically.

The first component manifold, HSC_{11}, can be determined using equations (5.80) - (5.83) if the PW manipulator belongs to either one of the classes E(RRR)-4, E(RPR)-4, E(RRP)-4 or E(RPP)-4. Furthermore, the closed-form of Abs($|J|$) can be obtained by multiplying one of the expressions on the left-hand sides of these equations with one of the expressions on the left-hand sides of the equations given in the second column of Table 5.2. Here the expressions to be used depend on the types of the first 3 joints and the class of the PW manipulator.

For the PW manipulators that belong to the classes E(PRR)-4, E(PRP)-4 or E(PPR)-4 the equations that are analogous to (5.80) - (5.83) (i.e., the equations obtained from $|J|$) are excessively complicated and will not be listed here. Instead, equations (5.80) - (5.83) will be modified so that they yield the points on HSC_{11} for the aforementioned classes of manipulators. Firstly it is noted that the points on HSC_{11} given by equations (5.80) - (5.83) are the singular points of the transformation representing the positioning of the wrist plane (see Section 6.2.2), i.e., $\frac{\partial(p_1,p_2,p_3)}{\partial(q_1,q_2,q_3)} = 0$ is an equation of the HSC_{11} where p_1,p_2,p_3 are given by equations (6.32) - (6.34). Consider now the angles α_{35} and θ_3' for the E(PRR)-4, E(PRP)-4 manipulators; and α_{36} and θ_3'' for the E(PPR)-4 manipulators. Here α_{35} $[\alpha_{36}]$ is the angle measured from $\underline{S}_3$ to $\underline{S}_5$ $[\underline{S}_6]$ around $\underline{a}_{35} = \underline{S}_3 \times \underline{S}_5$ $[\underline{a}_{36} = \underline{S}_3 \times \underline{S}_6]$ and $\theta_3'[\theta_3'']$ is the angle measured from $\underline{a}_{23}$ to $\underline{a}_{35}$ $[\underline{a}_{36}]$. These angles are given by the equations

$$c_{35} = -s_{34}c_4 \quad , \quad s_{35} = \sqrt{1 - s_{34}^2c_4^2} \tag{5.84}$$

$$\theta_3' = \theta_3 + \gamma' \tag{5.85}$$

$$c_{36} = s_{34}s_4 \quad , \quad s_{36} = \sqrt{1 - s_{34}^2s_4^2} \tag{5.86}$$

$$\theta_3'' = \theta_3 + \gamma'' \tag{5.87}$$

where

$$\cos\gamma' = c_{34}c_4/s_{35} \quad , \quad \sin\gamma' = s_4/s_{35} \tag{5.88}$$

$$\cos\gamma'' = -c_{34}s_4/s_{36} \quad , \quad \sin\gamma'' = c_4/s_{36} \tag{5.89}$$

and $c_{35} = \cos\alpha_{35}$, $s_{35} = \sin\alpha_{35}$, etc. Suppose now that α_{34} and θ_3 in the right-hand sides of the equations (6.32) - (6.34) are replaced by α_{35} and θ_3'. The resulting expressions thus obtained from (6.32), (6.33) yield the p_1 and p_2 coordinates of the wrist plane of a

E(PRR)-4 or E(PRP)-4 manipulator. The expression obtained from (6.34), plus a term which does not involve any joint variables, yields the p_3 coordinate of the wrist plane. It, therefore, follows that the points on HSC_{11} (i.e., the singular points of the transformation representing the positioning of the wrist plane) for the PW manipulators belonging to the classes E(PRR)-4 and E(PRP)-4 can be obtained from equations (5.80) - (5.83) after replacing α_{34} and θ_3 by α_{35} and θ_3'. Similarly, α_{34} and θ_3 in equations (5.80) - (5.83) should be replaced by α_{36} and θ_3'' if the manipulator belongs to the class E(RRP)-4.

5.4.2 Spherical Wrist Manipulators

For an SW manipulator $|J| = |M_2|\ |M_3|$ (see equation (4.7)) and the equations of the 2 component manifolds of the HSC, HSC_{11} and HSC_{22}, are $|M_2|=0$ and $|M_3|=0$, respectively. The 3×3 matrix M_3 is defined by equation (4.8) and hence an equation of the HSC_{22} is given by (also see Paul and Stevenson (1983))

$$|M_3| = s_{45}s_{56}s_s = 0 \tag{5.90}$$

The matrix M_2 depends on the types of the first 3 joints of the manipulator. The equations of HSC_{11}, given by $|M_2|=0$, are listed below for all possible types of SW manipulators.

PPPS Manipulators:

$$s_{12}s_{23}s_2 = 0 \tag{5.91}$$

RPPS Manipulators:

$$s_{23}[a_{12}c_{12}s_2 + a_{34}(s_{12}s_{23}c_2s_3 - c_{12}c_{23}s_3) + S_{22}s_{12}c_2$$
$$+ S_{33}(s_{12}c_{23}c_2 + c_{12}s_{23})] = 0 \tag{5.92}$$

PRPS Manipulators:

$$a_{23}s_{12}c_{23}s_2 + a_{34}(s_{12}c_{23}s_2c_3 + s_{12}c_{23}^2c_2s_3 + c_{12}s_{23}c_{23}s_3)$$
$$- S_{33}(s_{12}s_{23}c_{23}c_2 + c_{12}s_{23}^2) = 0 \tag{5.93}$$

PPRS Manipulators:

$$a_{34}s_{12}(c_{23}s_2c_3 + c_2s_3) = 0 \tag{5.94}$$

PRRS Manipulators:

$$a_{34}[a_{23}(s_{12}s_{23}s_2c_3 + c_{12}s_3) + a_{34}(s_{12}s_{23}c_{23}c_2s_3c_3$$
$$+ s_{12}s_{23}s_2c_3^2 + c_{12}s_3c_3 - c_{12}c_{23}^2s_3c_3) + S_{33}(c_{12}s_{23}c_{23}c_3$$
$$- s_{12}s_{23}^2c_2c_3)] = 0 \tag{5.95}$$

RPRS Manipulators:

$$a_{34}[-a_{12}(c_{12}c_2s_3 + c_{12}c_{23}s_2c_3) - a_{23}c_{12}s_3$$
$$+ a_{34}(s_{12}s_{23}s_2s_3^2 - s_{12}s_{23}c_{23}c_2s_3c_3 + c_{12}c_{23}^2s_3c_3 - c_{12}s_3c_3)$$
$$+ S_{22}(s_{12}s_2s_3 - s_{12}c_{23}c_2c_3) + S_{33}(s_{12}c_{23}s_2s_3$$
$$- s_{12}c_{23}^2c_2c_3 - c_{12}s_{23}c_{23}c_3)] = 0 \tag{5.96}$$

RRPS Manipulators:

$$\begin{aligned}
&a_{12}[a_{23}c_{12}c_{23}s_2 + a_{34}(c_{12}c_{23}s_2c_3 + c_{12}c_{23}^2c_2s_3 \\
&\quad - s_{12}s_{23}c_{23}s_3) + S_{33}(s_{12}s_{23}^2 - c_{12}s_{23}c_{23}c_2)] \\
&\quad + a_{23}(S_{22}s_{12}c_{23}c_2 + S_{33}s_{12}c_2) + a_{34}[S_{22}(s_{12}c_{23}c_2c_3 \\
&\quad - s_{12}c_{23}^2s_2s_3) + S_{33}(s_{12}c_2c_3 - s_{12}c_{23}s_2s_3)] \\
&\quad + S_{33}(S_{22}s_{12}s_{23}c_{23}s_2 + S_{33}s_{12}s_{23}s_2) = 0 \qquad (5.97)
\end{aligned}$$

RRRS Manipulators:

$$\begin{aligned}
&a_{34}\{a_{12}[a_{23}(c_{12}s_{23}s_2c_3 - s_{12}s_3) + a_{34}(s_{12}c_{23}^2s_3c_3 - s_{12}s_3c_3 \\
&\quad + c_{12}s_{23}s_2c_3^2 + c_{12}s_{23}c_{23}c_2s_3c_3) - S_{33}(s_{12}s_{23}c_{23}c_3 + c_{23}s_{23}^2c_2c_3)] \\
&\quad + a_{23}[-a_{23}s_{12}c_2s_3 + a_{34}(s_{12}c_{23}s_2s_3^2 - s_{12}c_2s_3c_3) \\
&\quad + S_{22}s_{12}s_{23}c_2c_3 - S_{33}s_{12}s_{23}s_2s_3] + a_{34}S_{22}(s_{12}s_{23}c_2c_3^2 \\
&\quad - s_{12}s_{23}c_{23}s_2s_3c_3) + S_{22}S_{33}s_{12}s_{23}^2s_2c_3\} = 0 \qquad (5.98)
\end{aligned}$$

Equations (5.91) - (5.98) have been obtained by assuming that $S_{44}=0$ since such an assumption simplifies them extensively. These equations yield the singular points of the mapping representing the positioning of the wrist point H (see the proof of Theorem 4.1) and the coordinates of this point in the reference frame $\hat{B}_3$ is $(a_{34}c_3, a_{34}s_3, S_{33})$. If, however, $S_{44}\neq 0$ the coordinates of H expressed in $\hat{B}_3$ will be $(a'_{34}c'_3, a'_{34}s'_3, S'_{33})$. Here, $c'_3=\cos\theta'_3$, $s'_3=\sin\theta'_3$ and

$$a'_{34} = \sqrt{a_{34}^2 + S_{44}^2 s_{34}^2} \qquad (5.99)$$

$$S'_{33} = S_{33} + S_{44} c_{34} \qquad (5.100)$$

$$\theta'_3 = \theta_3 + \gamma \qquad (5.101)$$

where γ is determined from

$$\cos\gamma = a_{34}/a'_{34} \quad , \quad \sin\gamma = -(S_{44} s_{34})/a'_{34} \qquad (5.102)$$

It thus follows that the equations of the HSC_{11} for all types of SW manipulators with $S_{44} \neq 0$ can be obtained from (5.91) - (5.98) upon replacing a_{34}, S_{33} and θ_3 by a'_{34}, S'_{33} and θ'_3, respectively.

CHAPTER 6
CONFIGURATIONS OF 6 DEGREE-OF-FREEDOM MANIPULATORS

6.1 One-to-Oneness of the Configurations

The measure $HFN(CO_i)$ can be directly computed from equation (4.1) iff the Forward Displacement Mapping (FDM) is one-to-one when restricted to the region CO_i (see Section 3.4 for the definition of CO_i). If, on the other hand, $FDM|CO_i$ is not one-to-one, then it is necessary to partition the region CO_i into subregions D_{ij} such that $FDM|D_{ij}$ is one-to-one, $\bigcup_j D_{ij} = CO_i$ and $D_{ij} \cap D_{ik} = \phi$. The measure $HFN(CO_i)$ is then given by $\sum_j HFN(D_{ij})$ where each $HFN(D_{ij})$ is computed from equation (4.1). Clearly, the identification of the regions D_{ij}'s and the computation of the corresponding measures $HFN(D_{ij})$'s can be quite challenging. Hence it is useful to be able to identify the manipulators for which $FDM|CO_i$ is one-to-one. For these manipulators, the motion planning and quick decision making algorithms may be rendered more efficient by taking advantage of the one-to-oneness of the regions CO_i's. Furthermore $DEG \leq NC$ and $DEG_1 \leq NC_1$ (see Section 3.4 for the definitions). The second inequality, for instance, can be used at the design stage when the joint limitations are determined.

In this section a theorem on the one-to-oneness of $FDM|CO_i$ is proved. This theorem is applicable to a broad class of manipulators (to be defined in the next paragraph). Global univalence, i.e., one-to-oneness, theorems can be used for the manipulators which are not covered by the theorem proved here. Parthasarathy (1983) presents a comprehensive review of the currently existing theorems. These theorems consider differentiable maps of the form $F:D \subset R^n \rightarrow R^n$ and state the conditions on the map F and the region D such that $F|D$ is one-to-one. However, in most cases D is assumed to be rectangular and the conditions on F are difficult to check and satisfy.

A 6 DOF manipulator will be said to be an echelon manipulator if it has the following properties (this definition has been inspired by Litvin and Castelli, 1985):

(i) The FDM (from the joint space into the POH space) can be represented by a finite number of class $C^{(1)}$ transformations. Each such transformation $T^j:H \rightarrow R^6$ is given by

$$\underline{v}^j = \underline{f}^j(\underline{q}) \tag{6.1}$$

where $\underline{v}^j$ is a coordinatization of a portion of the POH space, $\underline{q}=(q_1,q_2,\ldots,q_6)$ is the joint variable vector and H is a hyperprism in the joint space (see Section 3.2). The domain of each coordinatization $\underline{v}^j$ is an open subset of the POH space, D^j, and $\bigcup_j D^j$ covers the POH space. If $\underline{v}^j$ and $\underline{v}^k$ are two such coordinatizations and $D^j \cap D^k \neq \phi$, then there exists $C^{(1)}$ functions $\underline{g}_{jk}$ and $\underline{g}_{jk}^{-1}$ such that

$$\underline{v}^j = \underline{g}_{jk}(\underline{v}^k) \quad , \quad \underline{v}^k = \underline{g}_{jk}^{-1}(\underline{v}^j) \tag{6.2}$$

for all points in $D^j \cap D^k$.

(ii) The equation set (6.1) can be transformed into the echelon form

$$
\begin{aligned}
&F_1^j(\underline{v}^j, q_1) = 0 \\
&F_2^j(\underline{v}^j, q_1, q_2) = 0 \\
&\vdots \\
&F_6^j(\underline{v}^j, q_1, q_2, \ldots, q_6) = 0
\end{aligned}
\tag{6.3}
$$

for each transformation T^j. Furthermore, for e=1,2,...,6

$$
\begin{aligned}
F_e^j(\underline{v}^j, q_1, q_2, \ldots, q_e) &= \prod_{b=1}^{m_e} F_{e;b}^j(\underline{v}^j, q_1, q_2, \ldots, q_e) \\
&= \prod_{b=1}^{m_e} (I_{e;1b}^j c_e + I_{e;2b}^j s_e + I_{e;3b}^j)
\end{aligned}
\tag{6.4}
$$

or

$$
F_e^j(\underline{v}^j, q_1, q_2, \ldots, q_e) = J_{e;1}^j t_e + J_{e;2}^j
\tag{6.5}
$$

if q_e is an angular joint variable; and

$$
\begin{aligned}
F_e^j(\underline{v}^j, q_1, q_2, \ldots, q_e) &= \prod_{b=1}^{m_e} F_{e;b}^j(\underline{v}^j, q_1, q_2, \ldots, q_e) \\
&= \prod_{b=1}^{m_e} (K_{e;1b}^j q_e^2 + K_{e;2b}^j q_e + K_{e;3b}^j)
\end{aligned}
\tag{6.6}
$$

or

$$
F_e^j(\underline{v}^j, q_1, q_2, \ldots, q_e) = L_{e;1}^j q_e + L_{e;2}^j
\tag{6.7}
$$

if q_e is a linear joint variable. Here $c_e=\cos(q_e)$, $s_e=\sin(q_e)$, $t_e=\tan(q_e/2)$ and $I^j_{e;1b}$, $I^j_{e;2b}$, $I^j_{e;3b}$, $J^j_{e;1}$, $J^j_{e;2}$, $K^j_{e;1b}(\neq 0)$, $K^j_{e;2b}$, $K^j_{e;3b}$, $L^j_{e;1}$, $L^j_{e;2}$ are continuous functions of $\underline{v}^j$, q_1, $q_2, \ldots, q_{e-1}$.

(iii) The pre-images of any given point in the POH space can be determined via an appropriate transformation T^j by successively solving $q_1, q_2, \ldots, q_6$ from the first, second, . . . , sixth equation of the set (6.3). This process should yield precisely the pre-images of the given point and nothing else.

(iv) If the first m equations (m=1,2,...,5) of the equation set (6.3) are satisfied by a real point $(\underline{v}^j, q_1, q_2, \ldots, q_m)$, there should exist at least one corresponding real point $(q_{m+1}, q_{m+2}, \ldots, q_6)$ which satisfies the remaining (6-m) equations.

Theorem 6.1: Every region CO_i corresponding to the i'th configuration of an echelon manipulator is mapped onto its image in a one-to-one manner under the forward displacement mapping.

Proof: The superscript j in equations (6.1) and (6.3) - (6.7) (designating the coordinatization used) will be dropped throughout the proof in order to simplify the notation; i.e., the (generic) forward displacement map will be represented by the equivalent equations

$$\underline{v} = \underline{f}(\underline{q}) \qquad (6.8)$$

and

$$F_e(\underline{v}, q_1, q_2, \ldots, q_e) = F_e(\underline{v}_e, q_e) = 0 \qquad (e=1,2,\ldots,6) \qquad (6.9)$$

where

$$\underline{v}_e = (\underline{v}, q_1, q_2, \ldots, q_{e-1}) \tag{6.10}$$

and the coordinate functions of equation (6.8) are given by $v_i = f_i(\underline{q})$ for $i=1,2,\ldots,6$. Here $\underline{v}=(v_1,v_2,\ldots,v_6)$ designates any one of the coordinatizations depending on the portion of the POH space under consideration. When it is necessary to change coordinates, equation (6.2) can be used without affecting the outcome of the proof.

For the sake of clarification, the proof is divided into 2 parts.

Part 1

The Jacobian of the equation system (6.9) is given by

$$\frac{\partial(F_1,F_2,\ldots,F_6)}{\partial(q_1,q_2,\ldots,q_6)} = \prod_{e=1}^{6} G_e(\underline{v},q_1,q_2,\ldots,q_e) \tag{6.11}$$

where

$$G_e(\underline{v},q_1,q_2,\ldots,q_e) = G_e(\underline{v}_e,q_e) \equiv \frac{\partial F_e(\underline{v},q_1,q_2,\ldots,q_e)}{\partial q_e} \tag{6.12}$$

for $e=1,2,\ldots,6$. The equations $|J|=0$, $\frac{\partial(f_1,f_2,\ldots,f_6)}{\partial(q_1,q_2,\ldots,q_6)} = 0$ and $\prod_{e=1}^{6} G_e(\underline{f}(\underline{q}),q_1,q_2,\ldots,q_e)=0$ are equivalent since the solution set of each equation yields the singular points of the forward displacement map. Singular points are points in the hyperprism H for which the rank of the induced linear map (between the tangent spaces of the joint and POH spaces) is strictly less than 6 (see Gibson, 1979, for a detailed coverage of the singularity theory and the associated concepts).

Part 2

Consider any point D in the POH space which is not on the bifurcation set, i.e., the image of the singularity set. The pre-images of D obtained by solving equation system (6.9) must all be distinct. Let the coordinates of the point D and its pre-images (which are assumed to be r in number) be designated by $\underline{v}_D$ and $\underline{q}_a=(q_{1;a},q_{2;a},\ldots,q_{6;a})$, respectively, where a=1,2,...,r (see Fig. 6.1). Consider now any one of the pre-images of D, say $\underline{q}_1$. Define

$$Q_e \equiv \{\underline{q}_a : \underline{v}_{e;a} = \underline{v}_{e;1} \text{ and } q_{e;a} \neq q_{e;1}\} \tag{6.13}$$

for all e such that $e \in \{1,2,\ldots,6\}$ and $F_e(\underline{v}_e,q_e)$ is given by either one of the equations (6.4) or (6.6), i.e.,

$$F_e(\underline{v}_e,q_e) = \prod_{b=1}^{m_e} F_{e;b}(\underline{v}_e,q_e) \tag{6.14}$$

where $\underline{v}_{e;a} = (\underline{v}_D,q_{1;a},q_{2;a},\ldots,q_{e-1;a})$.

Consider now the pre-image of the point D with the coordinate vector $\underline{q}_2$. This vector must belong to at least one set Q_e defined by equation (6.13). Suppose, for example, that it belongs to Q_3; i.e., $\underline{v}_{3;2}=\underline{v}_{3;1}$ and $q_{3;2} \neq q_{3;1}$. Let c denote any one of the infinitely many continuous paths in the joint space which join $\underline{q}_1$ and $\underline{q}_2$ (see Fig. 6.1). The path corresponding to c in the $\underline{v}_3 q_3$ space, $\bar{c}$, joins the points A and B with coordinates $(\underline{v}_{3;1},q_{3;1})$ and $(\underline{v}_{3;1},q_{3;2})$, respectively. A parametric representation of $\bar{c}$ can be obtained by

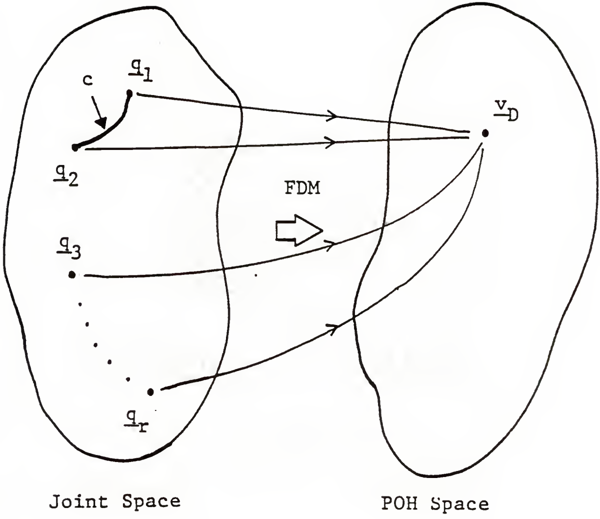

Fig. 6.1 The Point D and Its Pre-images

using a parametric representation of c and equation (6.8). Hence every point on the path $\bar{c}$ and the end points A,B satisfy the equation $F_3(\underline{v}_3,q_3)=0$. The function $F_3(\underline{v}_3,q_3)$ [obtained from equation (6.14) with e=3] can be expressed in the form

$$F_3(\underline{v}_3,q_3) = gh \tag{6.15}$$

where g denotes the function $F_{3;d}(\underline{v}_3,q_3)$ such that $F_{3;d}(\underline{v}_{3;1},q_{3;1})=0$ and

$$h = \prod_{\substack{b=1 \\ b\neq d}}^{m_3} F_{3;b}(\underline{v}_3,q_3) \tag{6.16}$$

The function $G_3(\underline{v}_3,q_3)$ can be obtained in terms of the functions g and h by differentiating equation (6.15) with respect to q_3. Hence,

$$G_3(\underline{v}_3,q_3) = \frac{\partial F(\underline{v}_3,q_3)}{\partial q_3} = g'h + h'g \tag{6.17}$$

where $g' = \frac{\partial g}{\partial q_3}$ and $h' = \frac{\partial h}{\partial q_3}$. The functions g, h, g' and h' are continuous since the functions $F_{3;b}(\underline{v}_3,q_3)$ and their partial derivatives with respect to q_3 are continuous (see the definition of these functions given by equation (6.4) or (6.6)). The equations g=0 and h=0 define, respectively, the hypersurfaces denoted by M_g and M_h in the $\underline{v}_3 q_3$ space. It follows from the definition of g that the point A is always on M_g. However, B can lie on either M_g or M_h.

$\underline{B \in M_g}$

The point D (in the POH space) is not on the bifurcation set by hypothesis. This means that the pre-images $\underline{q}_1$ and $\underline{q}_2$ are not on the

HSC given by $|J|=0$. Hence from the result of Part 1, the value of the function $G_3(\underline{v}_3,q_3)$ is not equal to zero at the points A and B. Since $g(A)=g(B)=0$ and $G_3(\underline{v}_3,q_3)$ is given by equation (6.17) it follows that $h(A)\neq 0$, $h(B)\neq 0$; i.e., $A \notin M_h$, $B \notin M_h$.

The equation $g|_{\underline{v}_3=\underline{v}_{3;1}}=0$, i.e., the function g restricted to the line $\underline{v}_3=\underline{v}_{3;1}$ equated to zero, represents a single equation in a single unknown, q_3. The q_3 coordinates of the points A and B, i.e., $q_{3;1}$ and $q_{3;2}$, are the two distinct roots of this equation which clearly cannot have more than 2 roots. Hence, $\text{sgn}(g'(A))=-\text{sgn}(g'(B))\neq 0$ where sgn denotes the sign function and $g'(A)$, $g'(B)$ denote the values of the function g' evaluated at the points A,B (recall that the roots of an equation $f(x)=0$ are separated from each other by the roots of $f'(x)=0$). Therefore, there must exist at least one point $\bar{\lambda} \in \bar{c}$ such that $g'(\bar{\lambda})=0$.

Consider now the path $\bar{c} \in M_g \cup M_h$ (see Fig. 6.2). If the entire path $\bar{c}$ lies on M_g then $g'(\bar{\lambda})=g(\bar{\lambda})=0$; and hence the function $G_3(\underline{v}_3,q_3)$ is zero at the point $\bar{\lambda}$ (see equation (6.17)). If, on the other hand, $\bar{c}$ does not entirely lie on M_g then there exists a point $\bar{\beta} \in \bar{c}$ such that $\bar{\beta}\in M_g \cap M_h$ (note that $\bar{c}$, M_g and M_h are continuous). Hence $g(\bar{\beta})=h(\bar{\beta})=0$; and the function $G_3(\underline{v}_3,q_3)$ is zero at the point $\bar{\beta}$ (see equation (6.17)).

$\underline{B \in M_h}$

It can be shown that $A \notin M_h$ and $B \notin M_g$ by analogy with the first paragraph of the case $B \in M_g$. Furthermore, by hypothesis $A \in M_g$ and

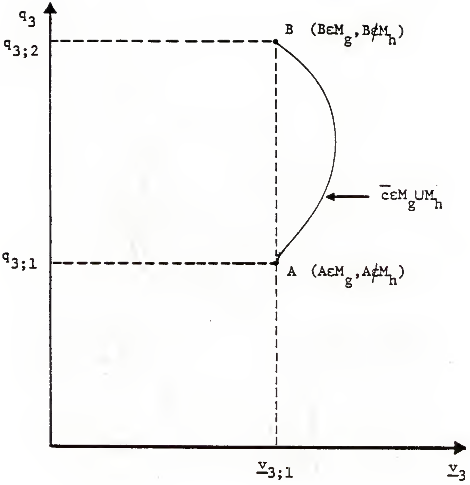
q_3
$q_{3;2}$
$q_{3;1}$
B $(B \in M_g, B \notin M_h)$
A $(A \in M_g, A \notin M_h)$
$\bar{c} \in M_g \cup M_h$
$\underline{v}_{3;1}$
$\underline{v}_3$

Fig. 6.2 The Case $B \in M_g$

$B \in M_h$. Since $\bar{c}$, M_g and M_h are continuous and $\bar{c} \in M_g \cup M_h$ there exists a point $\bar{\gamma} \in \bar{c}$ such that $\bar{\gamma} \in M_g \cap M_h$. Hence $g(\bar{\gamma})=h(\bar{\gamma})=0$; and the function $G_3(\underline{v}_3,q_3)$ is zero at the point $\bar{\gamma}$ (see equation (6.17)).

The above two cases indicate that there always exists at least one point, say $\bar{\alpha}$, on $\bar{c}$ such that the value of the function $G_3(\underline{v}_3,q_3)$ is zero at $\bar{\alpha}$. It then follows from the result of part 1 that there is a corresponding point, α, on c such that $|J|=0$. Hence the pre-images with the coordinate vectors $\underline{q}_1$ and $\underline{q}_2$ cannot be in the same region CO_i (recall that c denotes any one of the infinitely many continuous paths joining $\underline{q}_1$ and $\underline{q}_2$ in the joint space). Analogously, it can be shown that $\underline{q}_1$ and q_3, $\underline{q}_1$ and $\underline{q}_4$, ... , $\underline{q}_1$ and $\underline{q}_r$ cannot belong to the same region CO_i. The theorem then follows immediately since each pre-image of the point D belongs to a different region CO_i.

■

The reverse displacement analyses of all types of SW manipulators (involving the positioning of the wrist point) are presented in closed-form by Kohli and Spanos (1984a, 1984b). Using these analyses it can be shown that the SW manipulators RPPS, PRPS, PPRS, PPPS are echelon manipulators and hence Theorem 6.1 is applicable to them. For each of the remaining types of SW manipulators it is necessary to substitute the dimensions of the manipulator into the equation system representing the reverse displacement analysis which is of the form of equation (6.1). The SW manipulator under consideration will be an echelon manipulator if each equation of this system can be expressed in either one of the forms given by equations (6.4) - (6.7). It should be noted that Kohli and Spanos (1984a, 1984b) give three alternative reverse displacement analyes [as opposed to 1 in the original work of Pieper (1969)] for each type of SW manipulator. Here any one of these analyses can be utilized.

6.2 Planar Wrist Manipulators

In this section the PW manipulators are investigated in detail. Firstly the reverse displacement analysis is performed using the concept of signed-planes. The solutions thus obtained for the joint variables can be efficiently used for kinematic synthesis and on-line computation purposes. Furthermore the totality of the uncertainty and stationary configurations are identified using these solutions. The reverse displacement analysis also reveals that the PW manipulators PRRE, RPRE and RRPE are echelon manipulators and hence Theorem 6.1 is applicable to them.

6.2.1 Signed-Planes

Consider the set of all planes in R^3. Let 2 free vectors, $\underline{N}_1$ and $\underline{N}_2$, be attached to every plane in this set. These vectors are normal to the plane and furthermore $\underline{N}_1=-\underline{N}_2$, $\|\underline{N}_1\|_2=\|\underline{N}_2\|_2=1$. The set which consists of all the planes in R^3, together with their corresponding $\underline{N}_1$ and $\underline{N}_2$ vectors attached to them, will be called the signed-plane space (SP space). It should be noted that the plane P with $\underline{N}_1$ attached to it is considered to be distinct from the same plane with $\underline{N}_2$ attached to it. Now, let $\underline{N}=(N_x,N_y,N_z)$ designate either one of the normal vectors $\underline{N}_1$ or $\underline{N}_2$. The set of all signed-planes in the SP space, excluding the ones for which $N_z=1$, can be identified by finite vectors of the form $\underline{p}=(p_1,p_2,p_3)$ which will be called the p-coordinates. Here,

$$p_1 = N_x/(1 - N_z) \tag{6.18}$$

$$p_2 = N_y/(1 - N_z) \tag{6.19}$$

$$p_3 = \underline{N} \cdot \underline{r} \tag{6.20}$$

and $\underline{r}$ is the position vector of any point on the signed-plane. It should be noted that $|p_3|$ is the minimum distance between the signed-plane and the origin.

When the coordinate vector $\underline{p}$ is given, $\underline{N}$ can be obtained from the equations

$$N_x = 2p_1/D \tag{6.21}$$

$$N_y = 2p_2/D \tag{6.22}$$

$$N_z = (p_1^2 + p_2^2 - 1)/D \tag{6.23}$$

where $D=p_1^2+p_2^2+1$. Furthermore,

$$\underline{r}_m = p_3\underline{N} \tag{6.24}$$

where $\underline{r}_m$ is the position vector of the point on the signed-plane which is closest to the origin. Thus, the signed-plane corresponding to $\underline{p}$ can be determined uniquely from equations (6.21) - (6.24).

The SP space can also be coordinatized via finite vectors of the form $\underline{n}=(n_1,n_2,n_3)$ which will be called the n-coordinates. Here,

$$n_1 = N_x/(1 + N_z) \qquad (6.25)$$

$$n_2 = N_y/(1 + N_z) \qquad (6.26)$$

$$n_3 = p_3 = \underline{N} \cdot \underline{r} \qquad (6.27)$$

The equations of the inverse transformation are

$$N_x = 2n_1/E \qquad (6.28)$$

$$N_y = 2n_2/E \qquad (6.29)$$

$$N_z = (1 - n_1^2 - n_2^2)/E \qquad (6.30)$$

$$\underline{r}_m = n_3\underline{N} \qquad (6.31)$$

where $E=n_1^2+n_2^2+1$. In this coordinatization the signed-planes for which $N_z=-1$ are excluded.

It should be noted that equations (6.18) and (6.19) ((6.25) and (6.26)) represent the stereographic projection where the points on the unit sphere $N_x^2+N_y^2+N_z^2=1$ are projected onto the equatorial plane $N_z=0$ using the north pole $\underline{N}=(0,0,1)$ (south pole $\underline{N}=(0,0,-1)$) as the center of projection (see, for example, Klein, 1939). Therefore the equator, the northern (southern) hemisphere with the north (south) pole deleted, and the southern (northern) hemisphere are mapped onto the unit circle $p_1^2+p_2^2=1$ ($n_1^2+n_2^2=1$), the exterior of the unit circle, and the interior of the unit circle, respectively. The north (south) pole is the vanishing point of the transformation and is mapped onto the line at infinity in the p_1p_2 (n_1n_2) plane.

6.2.2 Reverse Displacement Analysis

The signed-plane which contains the point $\hat{O}_4$, i.e., the tip of the vector $a_{34}\underline{a}_{34}$, and has a normal parallel to the δ'th revolute joint axis $\underline{S}_\delta$ where $\delta\in\{4,5,6\}$ will be called the wrist plane of the PW manipulator. Here δ depends on the class of the PW manipulator. The p-coordinates of the wrist plane (in terms of the joint variables) can be determined in any coordinate system. Suppose, for example, that $\delta=4$ and the reference frame to be used is $\hat{B}_1$. Hence, $\underline{N}=(N_x,N_y,N_z)$ in equations (6.18) and (6.19) must be replaced by $\underline{S}_{4,\hat{1}}=(X_{123},X^*_{123},Z_{23})$ (see Table 2.1) yielding

$$p_1 = X_{123}/(1 - Z_{23}) \tag{6.32}$$

$$p_2 = X^*_{123}/(1 - Z_{23}) \tag{6.33}$$

The p_3 coordinate is obtained from equation (6.20) yielding

$$\begin{aligned} p_3 &= \underline{S}_4 \cdot (S_{11}\underline{S}_1 + a_{12}\underline{a}_{12} + S_{22}\underline{S}_2 + a_{23}\underline{a}_{23} + S_{33}\underline{S}_3 + a_{34}\underline{a}_{34}) \\ &= S_{11}Z_{23} + a_{12}X_{23} + S_{22}Z_3 + a_{23}X_3 + S_{33}c_{34} \end{aligned} \tag{6.34}$$

where the inner products have been evaluated by noting that $\underline{a}_{hi} \cdot \underline{S}_m = X_{ij\ldots m}$ and $\underline{S}_h \cdot \underline{S}_m = Z_{ij\ldots m}$ (see Table 3.1.a in Lipkin and Duffy, 1984).

The coordinates of the wrist plane can also be determined in terms of the location of the end effector which is usually specified by the vectors $\underline{R}$, $\underline{S}_6$ and $\underline{a}_{67}$. Here all 3 vectors are expressed in a convenient fixed coordinate system and $\underline{R}$ denotes the position vector of O_6. For example if the PW manipulator belongs to the class E(RRR)-4, then p_1 and p_2 can be obtained from equations (6.18) and (6.19) where N_x, N_y and N_z are replaced by the components of $\underline{S}_6$. The p_3 coordinate is given by

$$p_3 = \underline{R} \cdot \underline{S}_6 - (S_{44} + S_{55} + S_{66}) \tag{6.35}$$

Similarly, the p-coordinates of the wrist plane can be easily determined (using $\underline{R}$ and $\underline{S}_6$) for the remaining classes of PW manipulators (see Table 5.2). In the remainder of this section it will be assumed that p_1, p_2 and p_3 have been computed and are available as numbers.

The joint variables q_1, q_2 and q_3 will now be determined in terms of p_1, p_2 and p_3. This process is dependent on the types of the first 3 joints and the class of the manipulator. Hence the PW manipulators RRRE, RPRE, RRPE and PRRE will be analyzed individually assuming that $\delta=4$, i.e., the manipulator belongs to either one of the classes E(RRR)-4, E(RPR)-4, E(RRP)-4 or E(RPP)-4. The PW manipulators belonging to the classes E(PRR)-4 or E(PRP)-4, i.e., $\delta=5$, or to the class E(PPR)-4, i.e., $\delta=6$, can be analyzed in exactly the same way.

In the following analyses the coordinates of the wrist plane are formulated in the reference frame $(O_1\hat{x}_1\hat{y}_1\hat{z}_1)$ except for the PRRRE type. Here $(O_1\hat{x}_1\hat{y}_1\hat{z}_1)$ designates the coordinate system whose origin is at O_1 and whose axes are parallel to those of $\hat{B}_1$. In the PRRE manipulator the frame $(\hat{O}_1\hat{x}_2\hat{y}_2\hat{z}_2)$ is employed.

RRRE Manipulators: The p_1 and p_2 coordinates of the wrist plane (expressed in the $(0_1\hat{x}_1\hat{y}_1\hat{z}_1)$ system) are given by equations (6.32) and (6.33), respectively, whereas

$$p_3 = S_{22}Z_3 + S_{33}c_{34} + a_{12}X_{23} + a_{23}X_3 \tag{6.36}$$

Equations (6.32) and (6.33) can be solved for $s_1 \equiv \sin \theta_1$ and $c_1 \equiv \cos \theta_1$, yielding

$$s_1 = (p_2X_{23} - p_1Y_{23})/(1 + Z_{23}) \tag{6.37}$$

$$c_1 = (p_1X_{23} + p_2Y_{23})/(1 + Z_{23}) \tag{6.38}$$

These equations will yield a real, unique θ_1 iff

$$Z_{23} = p_o \tag{6.39}$$

which is essentially equation (6.23) expressed in the $(0_1\hat{x}_1\hat{y}_1\hat{z}_1)$ system. Here

$$p_o \equiv (p_1^2 + p_2^2 - 1)/(p_1^2 + p_2^2 + 1) \tag{6.40}$$

Equations (6.36) and (6.39) can be solved for s_2 and c_2, yielding

$$\begin{aligned} s_2 = (&a_{12}c_{12}X_3Z_3 - a_{23}s_{12}X_3Y_3 - S_{22}s_{12}Y_3Z_3 - S_{33}s_{12}c_{34}Y_3 \\ &- p_oa_{12}X_3 + p_3s_{12}Y_3)/\Delta \end{aligned} \tag{6.41}$$

$$\begin{aligned} c_2 = (&a_{23}s_{12}X_3^2 + S_{22}s_{12}X_3Z_3 + a_{12}c_{12}Y_3Z_3 + S_{33}s_{12}c_{34}X_3 \\ &- p_oa_{12}Y_3 - p_3s_{12}X_3)/\Delta \end{aligned} \tag{6.42}$$

provided that $\Delta \neq 0$, where

$$\Delta = a_{12}s_{12}(Z_3^2 - 1) \tag{6.43}$$

These equations will yield a real θ_2 iff

$$\begin{aligned}
&(a_{23}^2 s_{12}^2 s_{34}^2)s_3^2 + (Ds_{23}^2 s_{34}^2)c_3^2 + (-2a_{23}S_{22}s_{12}^2 s_{23}s_{34}^2)s_3c_3 \\
&+ (2a_{23}S_{22}s_{12}^2 c_{23}s_{34}c_{34} + 2a_{23}S_{33}s_{12}^2 s_{34}c_{34} - 2p_3a_{23}s_{12}^2 s_{34})s_3 \\
&+ (-2Ds_{23}c_{23}s_{34}c_{34} - 2S_{22}S_{33}s_{12}^2 s_{23}s_{34}c_{34} + 2p_oa_{12}^2 c_{12}s_{23}s_{34} \\
&+ 2p_3S_{22}s_{12}^2 s_{23}s_{34})c_3 + (Dc_{23}^2 c_{34}^2 - a_{12}^2 s_{12}^2 + 2S_{22}S_{33}s_{12}^2 c_{23}c_{34}^2 \\
&+ S_{33}^2 s_{12}^2 c_{34}^2 + p_o^2 a_{12}^2 - 2p_oa_{12}^2 c_{12}c_{23}c_{34} + p_3^2 s_{12}^2 - 2p_3S_{22}s_{12}^2 c_{23}c_{34} \\
&- 2p_3S_{33}s_{12}^2 c_{34}) = 0
\end{aligned} \tag{6.44}$$

where $D = a_{12}^2 + S_{22}^2 s_{12}^2$. The joint variable θ_3 can be determined by transforming equation (6.44) into a quartic in $t_3 = \tan(\theta_3/2)$. The corresponding values of θ_2 and θ_1 can be obtained from equations (6.41), (6.42) and (6.37), (6.39), respectively.

The above reverse displacement analysis is modified if Δ, which consists of 3 factors, is equal to zero. When $a_{12} = 0$, θ_3 is solved using equation (6.36) which simplifies to

$$(S_{22}s_{23}s_{34})c_3 + (-a_{23}s_{34})s_3 + (p_3 - S_{22}c_{23}c_{34} - S_{33}c_{34}) = 0 \tag{6.45}$$

This equation yields at most 2 values of θ_3 and the corresponding θ_2 values are solved from (6.39) which can be expressed in the form

$$(s_{12}Y_3)c_2 + (s_{12}X_3)s_2 + (c_{12}Z_3 - p_o) = 0 \qquad (6.46)$$

Equation (6.46) yields at most 2 values of θ_2 for a given θ_3. The corresponding θ_1 values can be obtained from equations (6.37) and (6.38).

When the second factor of Δ, s_{12}, is zero, equation (6.39) can be expressed in the form

$$c_3 = (c_{12}c_{23}c_{34} - p_o)/(c_{12}s_{23}s_{34}) \qquad (6.47)$$

which yields at most 2 solutions for θ_3. The corresponding θ_2 values (at most 2 for each θ_2) are obtained from equation (6.36) which can be arranged in the form

$$(a_{12}X_3)c_2 + (-a_{12}Y_3)s_2 + (a_{23}X_3 + S_{22}Z_3 + S_{33}c_{34} - p_3) = 0 \qquad (6.48)$$

The joint variable θ_1 can then be obtained using equations (6.37) and (6.38). Finally when the last factor of Δ, $(Z_3^2 - 1)$, is equal to zero, the manipulator is in an uncertainty configuration (see Section 6.2.3).

RPRE Manipulators: The joint variable θ_3 is solved using equation (6.39) which can be expressed in the form

$$(s_{34}\bar{Y}_2)c_3 + (s_{34}\bar{X}_2)s_3 + (c_{34}\bar{Z}_2 - p_o) = 0 \qquad (6.49)$$

This equation yields at most 2 solutions for θ_3. The corresponding values of θ_1 and S_{22} are determined from equations (6.37), (6.38) and (6.36), respectively.

RRPE Manipulators: The joint variable θ_2 is solved using equation (6.39) which can be expressed in the form

$$(s_{12}Y_3)c_2 + (s_{12}X_3)s_2 + (c_{12}Z_3 - p_0) = 0 \qquad (6.50)$$

This equation yields at most 2 solutions for θ_2. The corresponding values of θ_1 and S_{33} are determined from equations (6.37), (6.38) and (6.36), respectively.

PRRE Manipulators: The p_1 and p_2 coordinates of the wrist plane (expressed in the $(O_1\hat{x}_2\hat{y}_2\hat{z}_2)$ system) are

$$p_1 = X_{23}/(1 - Z_3) \qquad (6.51)$$

$$p_2 = X^*_{23}/(1 - Z_3) \qquad (6.52)$$

and the p_3 coordinate is given by equation (6.34). Equations (6.51) and (6.52) can be solved for s_2 and c_2, yielding

$$s_2 = (p_2X_3 - p_1Y_3)/(1 + Z_3) \qquad (6.53)$$

$$c_2 = (p_1X_3 + p_2Y_3)/(1 + Z_3) \qquad (6.54)$$

These equations will yield a real θ_2 iff

$$Z_3 = p_o \qquad (6.55)$$

which is essentially equation (6.23) expressed in the $(\hat{O}_1\hat{x}_2\hat{y}_2\hat{z}_2)$ system. The joint variable θ_3 can be solved by expanding equation (6.55),

$$c_3 = (c_{23}c_{34} - p_o)/(s_{23}s_{34}) \tag{6.56}$$

which yields at most 2 real solutions for θ_3. The corresponding values of θ_2 and S_{11} can be determined from equations (6.53), (6.54) and (6.34), respectively.

The joint variables q_1, q_2 and q_3 can thus be determined using the above analyses. The remaining variables q_4, q_5 and q_6 can be simply obtained from the reverse displacement analysis of an appropriate 3 DOF planar manipulator which depends on the class of the PW manipulator.

Suppose, for example, that the manipulator is of the class E(RRR)-4. Let $\underline{R} = (R_x, R_y, R_z)$ and $\underline{a}_{67} = (a_x, a_y, a_z)$ denote the position vector of O_6 and the unit vector $\underline{a}_{67}$, respectively. These vectors have already been specified in the $(O_1\hat{x}_1\hat{y}_1\hat{z}_1)$ system. Further, let $\underline{r} = (r_x, r_y, r_z)$ designate the vector $(a_{45}\underline{a}_{45} + a_{56}\underline{a}_{56})$ expressed in the coordinate system $\hat{B}_4$. Clearly,

$$\underline{r} = [{}^{\hat{1}}R_{\hat{4}}]^T\underline{R} - (a_{12}\underline{a}_{12} + a_{23}\underline{a}_{23} + a_{34}\underline{a}_{34} + S_{22}\underline{S}_2$$

$$+ \dots + S_{66}\underline{S}_6) \tag{6.57}$$

Here the vectors in the parentheses should be expressed in $\hat{B}_4$ and $[{}^{\hat{1}}R_{\hat{4}}]$ is the rotation matrix given by equation (5.9) together with $g=4$. The x and y components of $\underline{r}$ can be obtained by using equation (6.57) together with Table 3.3 in Lipkin and Duffy (1985), yielding

$$r_x = R_x P_{321} - R_y U_{321} + R_z X_{32} - a_{12} P_{32} - a_{23} \bar{P}_3 - a_{34} - S_{22} \bar{X}_3 \qquad (6.58)$$

$$r_y = -R_x Q_{321} + R_y V_{321} - R_z Y_{32} + a_{12} Q_{32} + a_{23} Q_3$$

$$+ S_{22} \bar{Y}_3 - S_{33} s_{34} \qquad (6.59)$$

The angle γ between $\underline{a}_{34}$ (i.e., $\hat{x}_4$) and $\underline{a}_{67}$ is determined from

$$\sin \gamma = -a_x Q_{321} + a_y V_{321} - a_z Y_{32} \qquad (6.60)$$

$$\cos \gamma = a_x P_{321} - a_y U_{321} + a_z X_{32} \qquad (6.61)$$

which are the y and x components of $\underline{a}_{67}$ (expressed in $\hat{B}_4$), respectively. The joint variables θ_4, θ_5 and θ_6 can now be easily determined by analyzing the 3R planar manipulator shown in Fig. 6.3. The fourth joint variable can be obtained by solving

$$(2r_x a_{45}) c_4 + (2r_y a_{45}) s_4 + (a_{56}^2 - a_{45}^2 - r_x^2 - r_y^2) = 0 \qquad (6.62)$$

whereas θ_5 and θ_6 are determined from

$$s_5 = (r_y c_4 - r_x s_4)/a_{56},$$

$$c_5 = (r_x c_4 + r_y s_4 - a_{45})/a_{56} \qquad (6.63)$$

and

$$\theta_6 = \gamma - \theta_4 - \theta_5 \qquad (6.64)$$

respectively.

It follows from the reverse displacement analyses performed in this section that the RPRE, RRPE, PRRE manipulators are echelon

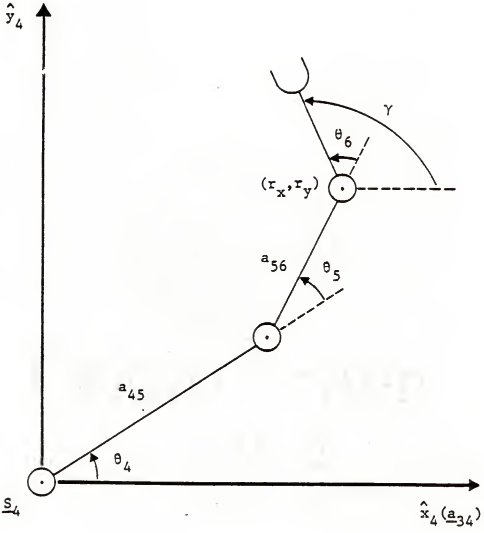

Fig. 6.3 Planar 3R Manipulator

manipulators and hence Theorem 6.1 is applicable to them. Here it should be noted that two equations of the form $s_i = K/L$ and $c_i = M/N$ (for instance equations (6.37) and (6.38)) is equivalent to a single equation of the form $Qt_i + R = 0$ where $t_i = \tan(\theta_i/2)$, $s_i = \sin\theta_i$, $c_i = \cos\theta_i$, $Q = f(K,L,M,N)$, $R = g(K,L,M,N)$ and $Q = R = 0$ iff $K = L = M = N = 0$. Any RRRE manipulator for which either one of the following conditions holds is also an echelon manipulator:

(i) $a_{12} = 0$ or $s_{12} = 0$.

(ii) Equation (6.44) can be expressed in the form of equation (6.4), i.e.,

$$(I_{11}c_3 + I_{21}s_3 + I_{31})(I_{12}c_3 + I_{22}s_3 + I_{32}) = 0 \qquad (6.65)$$

where $I_{11},\ldots,I_{32}$ are continuous functions of p_o and p_3.

6.2.3 Uncertainty and Stationary Configurations

Two distinct types of special configurations have been identified and named as uncertainty and stationary configurations by Lipkin and Duffy (1985). When the manipulator is in an uncertainty configuration "indeterminacies occur in the calculation of the joint variables." This means that the pre-image of a point in the POH space is at least a one dimensional set (rather than a finite number of points) in the joint space. If the manipulator is in a stationary configuration, however, "it is possible to compute the joint variables."

The uncertainty and stationary configurations of the PW manipulators can be identified using the reverse displacement analyses developed in the previous section. Here only the special configurations which involve the positioning of the wrist plane will be considered. The remaining special configurations are the ones associated with a planar 3 DOF robot which depends on the class of the PW manipulator. The types of these special configurations can be easily determined using the reverse displacement analyses for the planar manipulators which are well established.

Consider, for instance, the RRRE manipulators. Equations (6.37) and (6.38) will both degenerate when $Z_{23} = -1$ and the value of θ_1 is indeterminate. A similar situation will occur if the reverse displacement analysis is formulated in terms of the n-coordinates of the wrist plane (note that the reverse displacement analysis formulated in terms of the p-coordinates excludes the cases for which the p-coordinates of the wrist plane is of the form (∞,∞,p_3)). However in this case the expressions for s_1 and c_1 will degenerate when $Z_{23} = 1$. Similarly the expressions for s_2 and c_2, given by equations (6.41) and (6.42), will degenerate when $Z_3 = \mp 1$. The uncertainty configurations of the RPRE, RRPE and PRRE manipulators can be analogously determined using equations (6.36), (6.37), (6.38), (6.34), (6.53) and (6.54). The results are summarized in the second column of Table 6.1. Here the joint variables which become indeterminate are also indicated in parentheses.

Consider now the equations (6.44), (6.49), (6.50) and (6.56) for the RRRE, RPRE, RRPE and PRRE manipulators, respectively. Each of these equations is of the form

$$F(\underline{p},q) = 0 \qquad (6.66)$$

Table 6.1 Uncertainty and Stationary Configurations of the PW Manipulators

	Equations* which determine the		
Manipulator	Uncertainty Configurations		Stationary Configurations
RRRE	$Z_{23} = \mp 1$	(θ_1)	
	$Z_3 = \mp 1$	(θ_2)	
RPRE	$Z_{23} = \mp 1$	(θ_1)	$X_{32} = 0$
	$Z_3 = 0$	(S_{22})	
RRPE	$Z_{23} = \mp 1$	(θ_1)	$X_{23} = 0$
PRRE	$Z_3 = \mp 1$	(θ_2)	$s_3 = 0$
	$Z_{23} = 0$	(S_{11})	

* In these equations the variables α_{34} and θ_3 should be replaced by α_{35} and θ_3' [α_{36} and θ_3''] if the PW manipulator belongs to the classes E(PRR)-4 or E(PRP)-4 [E(PPR)-4]. The angles α_{35}, θ_3', α_{36} and θ_3'' can be obtained from equations (5.84) - (5.87).

where q denotes a joint variable. Suppose that a point $(\underline{p}_o, \underline{q}_o)$ in the $\underline{p}q$ space satisfies equation (6.66) and

$$\frac{\partial F(\underline{p},q)}{\partial q} \equiv G(\underline{p},q) = 0 \qquad (6.67)$$

This means that q_o is a real, multiple root of equation (6.66) for the given $\underline{p}_o$ and the point $(\underline{p}_o, q_o)$ corresponds to a special configuration (see the proof of Theorem 6.1). Furthermore since it is possible to compute the joint variable q, the point $(\underline{p}_o, q_o)$ corresponds to a stationary configuration. The set of all such points $(\underline{p}_o, q_o)$ make up the totality of the stationary configurations. The equation yielding these configurations in the $\underline{q}_{123}$ space $[\underline{q}_{123} \equiv (q_1, q_2, q_3)]$ is obtained by substituting $\underline{f}(\underline{q}_{123})$ for $\underline{p}$ in equation (6.67). Here the substitution is made after the differentiation and ensures that equation (6.66) is also satisfied. Furthermore, $\underline{p} = \underline{f}(\underline{q}_{123})$ denotes the equation sets (6.32), (6.33), (6.36) and (6.51), (6.52), (6.34) for the RRRE, RPRE, RRPE and PRRE manipulators, respectively.

The stationary configurations of the PW manipulators can be determined using the method desribed in the preceding paragraph. The results, with the exception of the RRRE manipulator, are listed in the third column of Table 6.1. It is easier to determine the stationary configurations of this manipulator by using the first component manifold HSC_{11} given by equation (5.80). The stationary configurations consist of all the points on HSC_{11} excluding the ones corresponding to the uncertainty configurations shown in the second column of Table 6.1. Note that the equations of HSC_{11} for the RPRE, RRPE and PRRE manipulators, i.e., equations (5.81) - (5.83), can be expressed in the forms

$$s_{34}(Z_3)(-X_{32}) = 0 \tag{6.68}$$

$$s_{12}s_{34}(X_{23}) = 0 \tag{6.69}$$

$$s_{23}s_{34}(s_3)(Z_{23}) = 0 \tag{6.70}$$

respectively. Each of these component manifolds consists solely of the uncertainty and stationary configurations listed already in Table 6.1, thus verifying the reverse displacement analyses.

6.2.4 Workspace of the Wrist Plane

The signed-planes that can be "reached" by the wrist plane of a PW manipulator can be determined by mapping the first component manifold of the HSC, HSC_{11}, onto the p_rp_3 and/or n_rn_3 planes. Here p_r and n_r are defined as

$$p_r = p_1^2 + p_2^2 \tag{6.71}$$

$$n_r = n_1^2 + n_2^2 \tag{6.72}$$

which, using equations (6.18), (6.19) and (6.25), (6.26), yield

$$p_r = (1 + N_z)/(1 - N_z) \qquad (N_z \neq 1) \tag{6.73}$$

$$n_r = (1 - N_z)/(1 + N_z) \qquad (N_z \neq -1) \tag{6.74}$$

respectively. This mapping can be achieved by utilizing an algorithm, the details of which will be presented using the RRRE manipulator.

For this manipulator, the coordinates of the wrist plane are expressed in the $(0_1\hat{x}_1\hat{y}_1\hat{z}_1)$ system. Hence equations (6.73) and (6.74) yield

$$p_r = (1 + Z_{23})/(1 - Z_{23}) \tag{6.75}$$

$$n_r = (1 - Z_{23})/(1 + Z_{23}) \tag{6.76}$$

and the p_3 coordinate (which is equal to the n_3 coordinate) is given by equation (6.36). The algorithm is as follows:

(i) The equation of HSC_{11}, given by equation (5.80), is expressed in the form

$$ac_2 + bs_2 + d = 0 \tag{6.77}$$

where a,b,d are functions of θ_3 and the dimensions of the manipulator.

(ii) The joint variable θ_3 is initialized. For instance θ_3 is assigned the value zero.

(iii) Equation (6.77) is solved and the real solutions are designated by $\theta_{2;1}$ and $\theta_{2;2}$.

(iv) The quantities $p_3(\theta_{2;1},\theta_3)$ and $p_r(\theta_{2;1},\theta_3)$ $[n_3(\theta_{2;1},\theta_3)$ and $n_r(\theta_{2;1},\theta_3)]$ are computed if $Z_{23}(\theta_{2;1},\theta_3) \leq 0$ $[Z_{23}(\theta_{2;1},\theta_3) \geq 0]$. Here $p_3(\theta_{2;1},\theta_3)$, $p_r(\theta_{2;1},\theta_3)$, $n_3(\theta_{2;1},\theta_3)$, $n_r(\theta_{2;1},\theta_3)$ and $Z_{23}(\theta_{2;1},\theta_3)$ denote the numerical values of p_3, p_r, n_3, n_r and Z_{23} evaluated at the point $(\theta_{2;1},\theta_3)$. The same computations are performed for the point $(\theta_{2;2},\theta_3)$.

(v) The points obtained in step (iv) are plotted on the p_rp_3 and/or n_rn_3 planes.

(vi) The joint variable θ_3 is incremented by $\Delta\theta_3$ and steps (iii) - (iv) are repeated if $\theta_3 < 360°$.

This algorithm yields a set of points (curves in general) which lie inside the rectangular strips $0 \leq p_r \leq 1$, $0 \leq n_r \leq 1$ in the p_rp_3 and n_rn_3 planes, respectively. If the second and third joints of the manipulator have joint limits, the boundaries of the feasible rectangular region (in the $\theta_2\theta_3$ space) should also be mapped into the insides of these strips. The totality of the images thus obtained and the lines $p_r = 0$, $p_r = 1$, $n_r = 0$, $n_r = 1$ define a number of regions each of which has an associated reachability number, r_i. If the (p_r,p_3) coordinates of a given signed-plane [the (n_r,n_3) coordinates if $p_r > 1$] belongs to a region with a reachability number r_i, then the wrist plane can reach that signed-plane in r_i distinct ways. The reachability number of a region R_i in the p_rp_3 plane is equal to the number of feasible, real $\underline{q}_{123} = (\theta_1,\theta_2,\theta_3)$ vectors which position the wrist plane such that its p-coordinates are $(\sqrt{e},0,f)$. Here (e,f) can be any point in R_i. The reachability numbers of the regions in the n_rn_3 plane can be similarly determined by performing the reverse displacement analysis (associated with the positioning of the wrist plane) for a single point in each region (see Section 6.2.2). It should be noted that the workspace of the wrist plane can be represented as the union of a finite number of finite regions in the p_rp_3 and n_rn_3 planes. Such a representation may not always be possible if only one of these planes is utilized.

The regions in the $p_r p_3$ and/or $n_r n_3$ planes and their respective reachabilities can be similarly determined for the PRRE manipulators. In this case the wrist plane coordinates are expressed in the $(\hat{0}_1 \hat{x}_2 \hat{y}_2 \hat{z}_2)$ system. Therefore equations (6.73), (6.74) yield $p_r = (1 + Z_3)/(1 - Z_3)$, $n_r = (1 - Z_3)/(1 + Z_3)$ and the p_3 coordinate is given by equation (6.34).

The image of HSC_{11} [under the transformation given by the coordinate functions (6.75) and (6.36)] for the RPRE and RRPE manipulators can be obtained without using the algorithm described via the RRRE manipulator. The stationary configurations of the RPRE robot, given by $X_{32} = 0$ (see Table 6.1), maps onto two vertical lines in the $p_r p_3$ plane. The uncertainty configurations given by $Z_{23} = -1$ maps onto the line $p_r = 0$ and the remaining uncertainty configurations given by $Z_3 = 0$ maps onto two points. For the RRPE manipulator the images of the stationary configurations given by $X_{23} = 0$ are two vertical lines.

The workspace (of the wrist point) of an SW manipulator can be analyzed similar to the workspace (of the wrist plane) of a PW manipulator. In this case, however, the points on the first component manifold, HSC_{11} (see equations (5.91) - (5.98)) and the boundaries of the feasible region in the $q_2 q_3$ space are mapped into the ρz space (xy space if the first joint is prismatic). Here $\rho = \sqrt{x^2 + y^2}$ and (x,y,z) denote the coordinates of 0_4 (i.e., the wrist point) expressed in the $(\hat{0}_1 \hat{x}_1 \hat{y}_1 \hat{z}_1)$ system. The reachability of each region (in the ρz plane) thus obtained is equal to the number of feasible, real

$\underline{q}_{123} = (q_1, q_2, q_3)$ vectors which position the wrist point such that its coordinates are (e,0,f). Here (e,f) can be any point in the region. It should be noted that the method described here for the workspace analysis of the SW manipulators is much more efficient than the one described by Kohli and Spanos (1984a, 1984b) which exploits the discriminants of polynomials and requires extensive amounts of algebraic manipulation.

6.3 Upper Bound of the Number of Configurations

The number of configurations (NC) of a manipulator was defined in Section 3.2. If this number is high for a manipulator, then:

(i) The workspace (in the POH space) will be complicated in general. In other words, it will consist of many disjoint regions (with different reachabilities) separated from each other by the image of the HSC under the foward displacement map.

(ii) The control, motion planning and rapid decision making algorithms will slow down since they will get complicated.

In this regard it is useful to be able to predict the upper bound of the NC for different types of manipulators.

In this section equations that yield (without any lengthy calculations) the upper bound of the number of configurations will be developed. These equations are applicable for manipulators the HSC's of which consist of component manifolds containing 2 or less joint variables. For example, all types of PW and SW manipulators satisfy this requirement.

A component manifold (of an HSC) that involves 2 joint variables will be said to be

(i) a linear manifold if its equation contains 2 linear joint variables,

(ii) an angular manifold if its equation contains 2 angular joint variables,

(iii) a hybrid manifold if its equation contains a linear and an angular joint variable.

The set of points (curves in general) satisfying the equations of linear, angular and hybrid manifolds in their respective hyperprisms (see Section 3.2) will be designated by C_l, C_a and C_h, respectively. The number of regions due to C_l, C_a and C_h (in their respective hyperprisms) will be denoted by $NR(C_l)$, $NR(C_a)$ and $NR(C_h)$.

The equation of a linear manifold is algebraic in the joint variables that it contains. However, this is not true for the angular and hybrid manifolds. The equations of these 2 manifolds can be transformed into algebraic ones using the identities

$$\sin \theta_i = 2t_i/(1 + t_i^2) \tag{6.78}$$

$$\cos \theta_i = (1 - t_i^2)/(1 + t_i^2) \tag{6.79}$$

where $t_i = \tan(\theta_i/2)$ and θ_i denotes an angular joint variable. The degrees, or orders, of the algebraic equations thus obtained will be

$$D_a = 2(\deg\theta_i + \deg\theta_j) \tag{6.80}$$

for an angular manifold containing the joint variables θ_i and θ_j; and

$$D_h = 2(\deg\theta_i) + \deg S_{jj} \tag{6.81}$$

for a hybrid manifold containing the joint variables θ_i and S_{ij}. Here $\deg\theta_i$ and $\deg S_{jj}$ denote the degree of the component manifold in respectively θ_i and S_{jj} which are defined in the same way as the degree of the HSC in a joint variable (see Section 3.1).

Let C_l', C_a' and C_h' denote the set of all points (curves in general) which satisfy the algebraic equations of the linear, angular and hybrid manifolds in the $S_{ii}S_{jj}$, t_it_j and t_iS_{jj} planes, respectively. Furthermore, let N_l, N_a and N_h designate the upper bounds of $NR(C_l)$, $NR(C_a)$ and $NR(C_h)$. These upper bounds can be determined using Theorem B.1 and Corollaries B.2, B.3 which are proved in Appendix B.

Determination of N_l: The equation of a linear manifold is algebraic in the joint variables that it contains. Hence, from Corollary B.2

$$N_l = I(n,b) = (n^2 - n + 2b + 2)/2 \tag{6.82}$$

where n and b are the degree and the number of irreducible factors of the equation of the manifold.

Determination of N_a: Consider the hyperprism H given by the cartesian product $H = \bar{\theta}_i \times \bar{\theta}_j$, where $\bar{\theta}_i = \{\theta_i: -\pi \le \theta_i \le \pi\}$ and $\bar{\theta}_j = \{\theta_j: -\pi \le \theta_j \le \pi\}$. The transformation T with the coordinate functions $t_i = \tan(\theta_i/2)$, $t_j = \tan(\theta_j/2)$ maps the inside of H in a 1-1 manner onto the affine $t_i t_j$ plane. The boundary of H corresponds to the line at infinity, l_∞, of this plane. Under the transformation T and with the substitutions (6.78) and (6.79) the curve C_a is transformed into an algebraic curve, C'_a, of order D_a. The curve C'_a will be finite if C_a does not cross the boundary of H. Furthermore, the topological property $NR(C_a)$ will be equal to $NR(C'_a)$ since both T and T^{-1} are continuous. Hence, from Corollary B.3

$$N_a = F(D_a,b) = (D_a^2 - 3D_a + 2b + 4)/2 \tag{6.83}$$

where D_a is given by equation (6.80) and b is the number of irreducible factors in the equation of C'_a. The hyperprism H is topologically equivalent to a torus and does not have any boundary curves. Therefore the boundary of the $t_i t_j$ plane, i.e., l_∞, cannot serve as the boundary of a region in H. Hence equation (6.83) is still valid even if C'_a is a nonfinite curve, i.e., C_a crosses the boundary of H.

The upper bound given by equation (6.83) cannot be achieved for a special type of angular manifold the trace of which (in H) will be designated by C_{as}. This special manifold consists of two subcomponent manifolds the traces of which (in H) are C_{1a} and C_{2a}. The equation of C_{1a} is of the form $As_i + Bc_i + D = 0$ where A,B,D are real numbers and $s_i = \sin \theta_i$, $c_i = \cos \theta_i$. Clearly C_{1a} consists of at most 2 distinct lines parallel to the θ_j axis. Each of these lines meets C_{2a} at most $2\deg\theta_j$ times where $\deg\theta_j$ denotes the degree of the angular manifold in θ_j. Therefore the total number of intersections of C_{1a} and C_{2a}

cannot exceed $4\deg\theta_j$. The number of regions due to C_{as} will be maximized if the following conditions are satisfied.

(i) The number of regions due to C_{2a} is equal to the upper bound given by equation (6.83).

(ii) The subcomponent manifold C_{2a} has a petal (see Appendix B) which meets C_{1a} in $4\deg\theta_j$ distinct points.

When these conditions are fulfilled the maximum of $NR(C_{as})$, denoted by N_{as}, will be given by

$$N_{as} = (2 + N_{2a}) - (1) + (4\deg\theta_j - 2) \tag{6.84}$$

where N_{2a} is the upper bound of $NR(C_{2a})$ determined from (6.83). Here the first 2 terms yield $NR(C_{as})$ provided that C_{1a} and C_{2a} are nonintersecting. The last term yields the number of regions which must be added due to the intersections according to condition (ii) (see Fig. 6.4). Equation (6.84) simplies to yield

$$N_{as} = N_{2a} + 4\deg\theta_j - 1 \tag{6.85}$$

Determination of N_h: Consider the hyperprism H given by the cartesian product $H = \bar{\theta}_i \times \bar{S}_{jj}$ where $\bar{\theta}_i = \{\theta_i: -\pi \leq \theta_i \leq \pi\}$ and $\bar{S}_{jj} = \{S_{jj}: -\infty < S_{jj} < \infty\}$. The transformation T with the coordinate functions $t_i = \tan(\theta_i/2)$, $S_{jj} = S_{jj}$ maps the inside of H in a 1-1 manner onto the affine t_iS_{jj} plane. The boundary of H corresponds to the l_∞ of this plane. Under the transformation T and the substitutions (6.78) and (6.79) the curve C_h is transformed into an

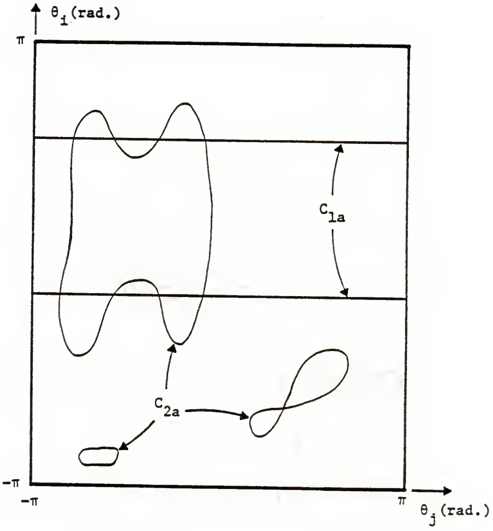

Fig. 6.4 An Angular Manifold with $N_{2a} = 5$ and $\deg\theta_j = 2$

algebraic curve, C_h', of order D_h. The curve C_h' has a horizontal asymptote (given by S_{jj} = cst.) for each simple intersection of C_h and the line $\theta_i = -\pi$. Such intersections of C_h' and l_∞ do not contribute to $NR(C_h)$ since the lines $\theta_i = -\pi$ and $\theta_i = \pi$ are considered to be the same, i.e., H is topologically a cylinder. The remaining intersections of C_h' and l_∞ are due to the vertical asymptotes of C_h' which are in 1-1 correspondence with the vertical asymptotes of C_h. Intersections of this sort do contribute to $NR(C_h)$ in the following manner. Consider an irreducible hybrid manifold C_h' of degree n, the equation of which is $A_m S_{jj}^{(m)} + A_{m-1} S_{jj}^{(m-1)} + \ldots + A_o = 0$. The number of vertical asymptotes of C_h', u, is given by the number of real zeros of A_m which is a polynomial in t_i. Equation (B.8) in the proof of Theorem B.1 then becomes $(P_i)_{max} = u + k = n + k - (n - u)$. This modification reduces N_{max} (given by equation (B.4)) and hence $I(n,1)$ by $(n - u)$, yielding $I'(n,1) = (n^2 - n + 4)/2 - (n - u)$. Finally using $I'(n,1)$, instead of $I(n,1)$, for every component curve of a hybrid manifold and following the proof of Corollary B.2 it can be shown that

$$N_h = I(D_h,b) - (D_h - \sum_{i=1}^{b} u_i) \tag{6.86}$$

which yields

$$N_h = (D_h^2 - 3D_h + 2b + 2)/2 + \sum_{i=1}^{b} u_i \tag{6.87}$$

Here D_h is given by equation (6.81), b is the number of irreducible factors of C'_h and u_i is the number of vertical asymptotes of the i'th component curve. Note that $\sum_{i=1}^{b} u_i$ cannot exceed $2\deg\theta_i$.

A component manifold may only contain a single joint variable. If this variable is an angular one, say θ_i, the associated hyperprism is simply an interval of the form $\theta_{io} \leq \theta_i \leq \theta_{io} + 2\pi$ where the end points are considered to be the same. The maximum number of regions (intervals in this case) due to this manifold is given by

$$N_\theta = 2\deg\theta_i \tag{6.88}$$

where $\deg\theta_i$ is the degree of the equation of the manifold in θ_i. If, however, the manifold contains a linear joint variable, say S_{ii}, then the hyperprism is the interval $-\infty < S_{ii} < \infty$. The maximum number of regions due to this manifold is

$$N_S = 1 + \deg S_{ii} \tag{6.89}$$

where $\deg S_{ii}$ is the degree of the equation of the manifold in S_{ii}.

The upper bounds of the number of configurations of the PW and SW manipulators can be obtained using equations (6.82), (6.83), (6.84), (6.87), (6.88) together with (5.80) - (5.83) and (5.91) - (5.98). The results are listed in Table 6.2. The third column, N_1, gives the upper bound of the number of regions due to the first component manifold (HSC_{11}) which involves the second and third joint variables. Here it is assumed that HSC_{11} is irreducible. The number of regions due to the second component manifold (HSC_{22}) of every manipulator shown in this table is 2. Hence the upper bound of NC is

Table 6.2 Upper Bounds of the Number of Configurations for the PW and SW Manipulators

Class of the Manipulator	Types of the First 3 Joints	N_1	NC	DEG_u
E(RRR)-4	RRR	12	24	8
	PRR	8	16	4
	RPR	4	8	4
	RRP	2	4	4
S-4	RRR	12	24	8
	PRR	12	24	8
	RPR	9	18	8
	RRP	6	12	8
	PRP	4	8	4
	RPP	2	4	4
	PPR	2	4	4
	PPP	1	2	2

$2N_1$ and is listed in the fourth column. The upper bounds of NC for the last 2 PW manipulators and the last 3 SW manipulators are achieved. This is because the HSC's of these manipulators consist of component manifolds containing a single joint variable. It appears that the upper bounds of NC for the remaining manipulators should also be attained. The last column of Table 6.2 contains the degrees of the manipulators (see Section 3.4). The degrees of the PW manipulators were established in Section 6.2.2 whereas the degrees of the SW manipulators are due to Pieper (1969). These degrees could also be determined by obtaining equivalent 1 DOF spatial mechanisms (see Duffy, 1980) and analyzing these single loop mechanisms using the methods developed in the same reference.

The manipulators in Table 6.2 are listed such that the upper bounds of their NC's are in descending order. The manipulators at the top of each list can potentially yield a high NC/DEG_u ratio and should be designed especially carefully. A high NC/DEG_u ratio is undesirable because it complicates, and hence slows down, the control and motion planning algorithms. Ideally this ratio should be 1 and each configuration of the manipulator should be mapped into the POH space in a one-to-one manner. The closed-form reverse displacement analyses of the PW manipulators performed in Section 6.2.2, the closed-form equations of the HSC obtained for the PW and SW manipulators in Section 5.4 and equations (6.82) - (6.84), (6.87) - (6.89) are useful in the kinematic design stage in this respect. Using these equations it is possible to predict (without any lengthy calculations) the affects of the variations in the dimensions of the manipulator on the ratio NC/DEG_u.

CHAPTER 7
SYMBOLIC MANIPULATION

Theorem 2.1 simplifies the determination of the HSC-K's (K=6,5,...) extensively. However, the identification of these hypersurfaces still involves a considerable amount of algebraic manipulation which includes, for instance, the formulation of the Plücker coordinates of the screws (representing the instantaneous joint motions) in different coordinate systems and finding expressions for the determinants of matrices. These manipulations are extremely time-consuming and error-prone when carried out manually. In order to remedy these problems a symbolic manipulation package (in APL) was developed in the summer of 1984. This package has been utilized throughout this work for the lengthy manipulations and it can be used for the following purposes:

(i) Determination of the fully expanded forms of the P, Q, R, U, V, W, X, Y and Z terms defined in Appendix A.

(ii) Determination of any Jacobian matrix $[J_i]$ or $[\hat{J}_i]$ (for any type of manipulator) in closed-form.

(iii) Determination of an equation of the HSC-K (for any type of manipulator) in closed-form where K=6,5,....

(iv) Determination of the adjoint Jacobian matrix.

(v) Implementation of the synthesis procedure for passive joints (see Section 3.5).

The developed package can also be used for general symbolic manipulation purposes. A similar but more detailed package has been later developed by Reischer (1986) which can be referred to for the fundamentals of symbolic manipulation.

CHAPTER 8
CONCLUSIONS

The singularity structure of the forward displacement mapping has been investigated in detail. This investigation has led to various novel concepts which have been demonstrated to be beneficial in the kinematic design and analysis, control, motion planning and performance evaluation of serial manipulators.

Important contributions include

- An efficient methodology for the identification of the hypersurfaces HSC-K's based on Theorem 2.1 and the minimal coordinate systems. Existence of component and/or subcomponent manifolds simplifies this methodology even further (see the first example in Section 3.6.1).
- Theorem 3.1 which predicts the existence of passive joints and component manifolds.
- Quantification of the freedom of the end effector via the hand freedom numbers which include considerations of joint limitations and scale.
- Theorem 6.1 which states that every region CO_i corresponding to the i'th configuration of an echelon manipulator is mapped onto its image in a one-to-one manner under the forward displacement mapping.

- Determination of the upper bounds for the number of regions formed by a linear, angular and hybrid manifold via the novel theorem and corollaries proved in Appendix B.

Tables 2.1 and 2.2 have proved to be useful. It appears that the same tables could also be beneficial in (i) the investigation (via screw theory) of the stationary and uncertainty configurations of single loop spatial mechanisms and (ii) the theory developed by Mohamed (1983) for the analysis of the special configurations and instantaneous kinematics of the fully-parallel robotic devices.

APPENDIX A
DEFINITIONS OF THE P, Q, R, U, V, W, X, Y AND Z ELEMENTS

In the following definitions e, f, g, h, i, j, k and l represent any set of successive integers in ascending order. Also $\sin \theta_\gamma$, $\cos \theta_\gamma$, $\sin \alpha_{\beta\gamma}$ and $\cos \alpha_{\beta\gamma}$ are abbreviated by s_γ, c_γ, $s_{\beta\gamma}$ and $c_{\beta\gamma}$, respectively, where β and γ are dummy variables standing for the subscripts.

1. Definitions of Single Subscripted Elements:

a) Ascending Subscripts:

$$P_i = c_i \qquad Q_i = c_{hi}s_i \qquad R_i = s_{hi}s_i \tag{A.1}$$

$$U_i = -s_i \qquad V_i = c_{hi}c_i \qquad W_i = s_{hi}c_i \tag{A.2}$$

$$X_i = s_{ij}s_i$$
$$Y_i = -(s_{hi}c_{ij} + c_{hi}s_{ij}c_i) \tag{A.3}$$
$$Z_i = (c_{hi}c_{ij} - s_{hi}s_{ij}c_i)$$

b) Descending Subscripts:

$$\bar{P}_i = c_i \qquad \bar{Q}_i = c_{ij}s_i \qquad \bar{R}_i = s_{ij}s_i \tag{A.4}$$

$$\bar{U}_i = -s_i \qquad \bar{V}_i = c_{ij}c_i \qquad \bar{W}_i = s_{ij}c_i \tag{A.5}$$

$$\begin{aligned}\bar{X}_i &= s_{hi}s_i \\ \bar{Y}_i &= -(s_{ij}c_{hi} + c_{ij}s_{hi}c_i) \\ \bar{Z}_i &= (c_{ij}c_{hi} - s_{ij}s_{hi}c_i)\end{aligned} \tag{A.6}$$

2. Definitions of Multiple Subscripted Elements:

a) Ascending Subscripts:

$$\begin{aligned}E_{fg\ldots jk} &= c_f E_{g\ldots jk} - s_f F_{g\ldots jk} \\ F_{fg\ldots jk} &= c_{ef}(s_f E_{g\ldots jk} + c_f F_{g\ldots jk}) - s_{ef} G_{g\ldots jk} \\ G_{fg\ldots jk} &= s_{ef}(s_f E_{g\ldots jk} + c_f F_{g\ldots jk}) + c_{ef} G_{g\ldots jk}\end{aligned} \tag{A.7}$$

b) Descending Subscripts:*

$$\begin{aligned}E_{kj\ldots gf} &= c_k E_{j\ldots gf} - s_k F_{j\ldots gf} \\ F_{kj\ldots gf} &= c_{kl}(s_k E_{j\ldots gf} + c_k F_{j\ldots gf}) - s_{kl} G_{j\ldots gf} \\ G_{kj\ldots gf} &= s_{kl}(s_k E_{j\ldots gf} + c_k F_{j\ldots gf}) + c_{kl} G_{j\ldots gf}\end{aligned} \tag{A.8}$$

where (E F G) = (P Q R), (U V W) or (X Y Z).

---

* If the E, F, and G terms on the right hand side of equation set (A.8) have a single subscript, they will be replaced by $\bar{E}$, $\bar{F}$, and $\bar{G}$ terms with the same subscript.

APPENDIX B
A THEOREM AND TWO COROLLARIES ON THE NUMBER OF REGIONS FORMED BY AN ALGEBRAIC CURVE

In this appendix a theorem and 2 corollaries, regarding the number of regions formed by an algebraic planar curve, will be proved. Equations (6.82), (6.83), (6.85) and (6.87) (which lead to the determination of the upper bound of the number of configurations, NC) are based on these theorems. Before proceeding it is useful to define[1] the following terms.

Circuit: A circuit is that part of a real plane curve which can be traced by a continuously moving real point which eventually comes back to every point already traced. Here by definition the points of the curve at infinity which are neighbouring points on any projection of the curve cannot introduce any discontinuities.

Multiple point: A point P is called a multiple point of order r, or an r-fold point, if every line through P (excluding the tangents) meets the curve r times at P.

Number of regions: The number of regions due to a plane curve C,[2] denoted by NR(C), is the minimum number of open connected sets which together with C cover the xy plane. The boundaries of these sets consist of the curve C and/or the line at infinity, l_∞, of the xy plane.

---

[1] The underlined terms are introduced by the author whereas the remaining definitions are standard (for instance, see Primrose, 1955; Coolidge, 1959).

[2] The definition of NR(C) will still be valid even if C consists solely of isolated points.

Connecting and free edges: Let σ be a node of a planar graph. This node will be said to have e edges associated with it if the graph, in the immediate vicinity of σ, is topologically equivalent to a point (the node) with e half rays emanating from it. The two edges that connect a node to the two neighbouring nodes on the same connected graph will be called the connecting edges. The remaining edges associated with σ are the free edges.

Leaf: Two free edges associated with the same node σ must meet at a fictitious node $\bar{\sigma}$. The topological circle consisting of σ, $\bar{\sigma}$ and the two free edges is called a leaf.

Petal: The topological circle consisting of only the nodes and connecting edges of a connected graph is called a petal.

Nesting: The inside (outside) of a petal is the region on the left (right) of the edges when a counter clockwise direction is assigned to the petal. The same definition also applies to the leaves. A set of petals and/or leaves will be said to nest if they are arranged such that each is inside the preceding one.

A theorem and 2 corollaries involving NR(C) will now be proved. In the proofs of these theorems it will be assumed that the xy plane, on which the curve C lies, is transformed into an ab plane using the transformation f given by the coordinate functions

$$a = x/(1 + \sqrt{x^2 + y^2}) \qquad (B.1)$$

$$b = y/(1 + \sqrt{x^2 + y^2}) \qquad (B.2)$$

This transformation maps the affine xy plane onto the open unit disk $a^2 + b^2 < 1$ in a 1-1 manner. The line at infinity is represented by the boundary of the disk, the opposite (or antipodal) points of which are identified to be the same point for topological purposes. The affine xy plane and the open unit disk are homeomorphic since f is bijective with a continuous inverse. Therefore NR(C), a topological property, remains invariant under the transformation f.

Theorem B.1: Let C be an irreducible algebraic plane curve of order n. Then, $NR(C) \leq N_{max}$ where,

(i) $$N_{max} = \{n^2 - 3n + 6 - [\sum_{r=3}^{n-1} U_r(r-1)(r-2) + \sum_{r=2}^{n-1} V_r(r)(r-1)]\}/2 \qquad (B.3)$$

if n is an even number and the curve is finite,

(ii) $$N_{max} = \{n^2 - n + 4 - [\sum_{r=3}^{n-1} U_r(r-1)(r-2) + \sum_{r=2}^{n-1} (V_r + W_r)(r)(r-1)]\}/2 \qquad (B.4)$$

if the curve is nonfinite.

Here U_r, W_r and V_r denote the number of real (finite), real (nonfinite) and imaginary r-fold points of the curve, respectively.

Proof: Assume that C has k real circuits. On each circuit identify

(i) any two ordinary, i.e., 1-fold, points,

(ii) the totality of the real, finite r-fold points ($r \geq 2$),

(iii) the totality of the real, nonfinite r-fold points ($r \geq 1$)

as the nodes. Hence, a planar graph consisting of k connected graphs will be formed where the edges are subsets of the curve C. Each node, i.e., an r-fold point, has at most 2r edges associated with it. Because if the contrary is assumed a general line intersects the curve with multiplicity m ($m > r$) at an r-fold point, which is a contradiction. Figure B.1 illustrates a curve with 2 circuits, AEBB'FDD'A'A and GHJ$\bar{\text{J}}$JG, 8 nodes and a fictitious node $\bar{J}$.

Let k_f and k_i designate the number of finite and nonfinite circuits of the curve, respectively. When $k_i = 0$ the curve is finite and the petals separate the closed unit disk into P_f disjoint regions where

$$P_f = 1 + k \tag{B.5}$$

If $k_i \geq 1$ however, the curve is nonfinite and

$$P_i \leq 1 + w + k - k_i \tag{B.6}$$

where

$$w = \sum_{r=1}^{n} r\, W_r \tag{B.7}$$

and P_i is the number of disjoint regions due to the petals. Now suppose $w > n$. Then, it follows that the number of intersections of

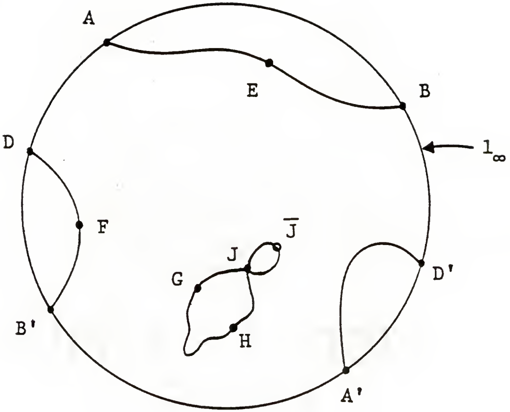

Fig. B.1   A Planar Curve with 2 Circuits

an n'th order curve and l_∞ is strictly more than n, which contradicts Bezout's Theorem (see for example Primrose, 1955). Hence $w \leq n$ and equation (B.6) yields

$$(P_i)_{max} = n + k \tag{B.8}$$

for $w = n$ and $k_i = 1$.

Since the number of leaves at a node corresponding to a finite r-fold point cannot exceed $(r - 1)$, the maximum number of regions corresponding to the insides of the leaves will be

$$L_{max} = \sum_{r=2}^{n-1} U_r(r - 1) \tag{B.9}$$

Thus for a finite and nonfinite n'th order curve with k circuits

$$N_{max} = P_f + L_{max} \tag{B.10}$$

and

$$N_{max} = (P_i)_{max} + L_{max} \tag{B.11}$$

respectively, which are invariant with respect to any nesting between the petals and/or leaves.

According to Harnack's first theorem (see Coolidge, 1959) an irreducible curve of order n with r-fold points of orders $s_1, s_2, \ldots$ cannot have more than k_{max} circuits, where

$$k_{max} = 1 + [(n - 1)(n - 2) - \Sigma s_i(s_i - 1)]/2 \qquad (B.12)$$

Substituting $k = k_{max}$ into equations (B.5) and (B.8) and substituting the results, along with equation (B.9), into (B.10) and (B.11), the equations (B.3) and (B.4) are obtained.

■

Let F(n,b) designate an upper bound of NR(C) where C is a finite algebraic curve of order n consisting of b irreducible component curves, i.e., the equation of C consists of b irreducible factors. Similarly, I(n,b) denotes an upper bound of NR(C) for a nonfinite C. It then follows from Theorem B.1 that

$$F(n,1) = (n^2 - 3n + 6)/2 \qquad (B.13)$$

$$I(n,1) = (n^2 - n + 4)/2 \qquad (B.14)$$

which are essentially lowest upper bounds since for any n there exists many nonsingular and singular curves that satisfy Harnack's First Theorem (see Theorem 13 in Chapter 4 and Harnack's Second Theorem in Coolidge, 1959). Existence of such curves is sufficient for the upper bounds given by (B.13) and (B.14) to be attained (see the proof of Theorem B.1).

Corollary B.2: $I(n,b) = (n^2 - n + 2b + 2)/2$ (B.15)

Proof: Let the nonfinite reducible curve and its component curves be designated by $C, C_1, C_2, \ldots, C_b$. These curves are of orders $n, n_1, n_2, \ldots n_b$, respectively ($n = n_1 + n_2 + \ldots + n_b$). The number of regions due to C, i.e., NR(C), will be maximized if the following conditions are satisfied.

(i) Each component curve C_i $(i=1,2,\ldots,b)$ is nonfinite and $NR(C_i) = I(n_i,1)$ which, using equation (B.14), yields

$$NR(C_i) = (n_i^2 - n_i + 4)/2 \tag{B.16}$$

(ii) Each pair of component curves, say C_i and C_j, meet at $n_i n_j$ real, distinct and finite points none of which lies on a finite petal of either C_i or C_j.

Firstly it will be assumed that none of the component curves meet at a finite point. Under this assumption, the number of regions due to C will be given by

$$\overline{NR}(C) = [\sum_{i=1}^{b} NR(C_i)] - (b - 1) \tag{B.17}$$

Here the summation $\Sigma\ NR(C_i)$ yields $\overline{NR}(C)$ when each component curve is assumed to be on a distinct plane. The number $(b - 1)$ is subtracted from this summation since all of the component curves are actually on the same plane.

Consider now two component curves C_i and C_j that meet as stated in condition (ii). Let $p_i(p_j)$ denote a nonfinite petal of $C_i(C_j)$. Each finite, distinct intersection of p_i and p_j introduces 1 region which is not counted in $\overline{NR}(C)$ (see Fig. B.2). Furthermore, the number of such intersections cannot exceed $n_i n_j$ according to Bezout's Theorem. Therefore the maximum number of unaccounted for regions due to the intersections between C_i and C_j is $n_i n_j$. It then follows that

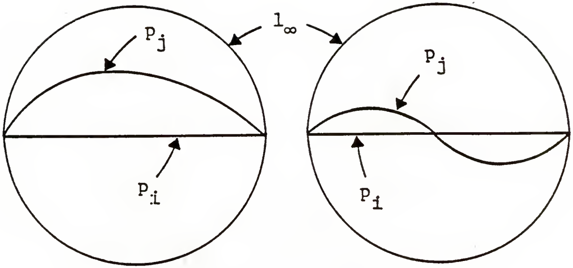

(a) Zero Intersections

(b) One Intersection

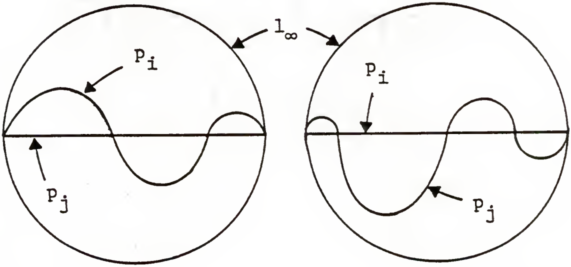

(c) Two Intersections

(d) Three Intersections

Fig. B.2 Intersections Between Petals* p_i and p_j

---

* In order to simplify the figure, the petals p_i and p_j are chosen such that they define 3 regions when there are zero intersections.

$$I(n,b) = \overline{NR}(C) + E \tag{B.18}$$

where

$$E = (n_1n_2 + n_1n_3 + \ldots + n_1n_b) + (n_2n_3 + n_2n_4 + \ldots n_2n_b) + \ldots + (n_{b-1}n_b) \tag{B.19}$$

is the total number of regions that must be added to $\overline{NR}(C)$ due to the intersections between every pair of component curves. Equation (B.15) is obtained using equations (B.16) - (B.19) and the identity

$$n_1^2 + n_2^2 + \ldots + n_b^2 = (n_1 + n_2 + \ldots + n_b)^2 - 2E \tag{B.20}$$

■

Corollary B.3: $F(n,b) = (n^2 - 3n + 2b + 4)/2$ (B.21)

Proof: Let the finite reducible curve and its component curves be designed by $C, C_1, C_2, \ldots, C_b$. These curves are of orders $n, n_1, n_2, \ldots, n_b$, respectively. Here $n, n_1, n_2, \ldots, n_b$ are even numbers and $n = n_1 + n_2 + \ldots + n_b$. The number of regions due to C, i.e., NR(C), will be maximized if the following conditions are satisfied.

(i) Each component curve C_i ($i=1,2,\ldots,b$) is finite and $NR(C_i) = F(n_i,1)$ which, using equation (B.13), yields

$$NR(C_i) = (n_i^2 - 3n_i + 6)/2 \tag{B.22}$$

(ii) Every component curve C_k has a unique circuit which will be designated by c_k ($k=1,2,\ldots,b$). Any pair of such circuits c_i and c_j meet at n_in_j real, distinct points.

When these conditions are fulfilled

$$F(n,b) = [\sum_{i=1}^{b} NR(C_i)] - [b - 1] + [E + 1] - [b] \qquad (B.23)$$

where E is given by equation (B.19). The first 2 terms of equation (B.23) yield the maximum value of NR(C) when no pairs of component curves intersect. The third term yields the number of regions due to the intersections between the component curves according to condition (ii). When this condition is fulfilled the circuits $c_1, c_2, \ldots, c_b$ form a single circuit with E leaves and one petal. This yields (E + 1) regions corresponding to each leaf and the inside of the petal. The fourth term, b, must be subtracted from the first three because the b regions corresponding to the insides of the petals of the circuits $c_1, c_2, \ldots, c_b$ have already been counted in the first term of equation (B.23). Equation (B.21) is obtained using equations (B.19), (B.20), (B.22) and (B.23).

■

The upper bounds I(n,n) and F(n,n/2) given by the Corollaries B.2 and B.3 are achieved. This is because there exists curves of order n satisfying conditions (i) and (ii) in the proofs of these corollaries. It appears that the remaining upper bounds I(n,b) and F(n,b) [$b=2,3,\ldots,(n - 1)$ and $b=2,3,\ldots,(n - 2)/2$] should also be achieved. Here it is useful to note that equations (B.15) and (B.21) can be expressed in the forms

$$I(n,b) = I(n,1) + (b - 1) \qquad (B.24)$$

$$F(n,b) = F(n,1) + (b - 1) \qquad (B.25)$$

REFERENCES

Coolidge, J.L., 1959, A Treatise on Algebraic Plane Curves, Dover Publications, New York.

Duffy, J., 1980, Analysis of Mechanisms and Robot Manipulators, John Wiley, New York.

Gibson, C.G., 1979, Singular Points of Smooth Mappings, Pitman, London.

Hadley, G., 1977, Linear Algebra, Addison-Wesley, Reading, Massachusetts.

Hunt, K.H., 1978, Kinematic Geometry of Mechanisms, Oxford University Press, Oxford.

Hunt, K.H., 1986, "Special Configurations of Robot-Arms via Screw Theory, Part 1, the Jacobian Matrix and Its Matrix of Cofactors," Robotica, Vol. 4, pp. 171-179.

Klein, F., 1939, Elementary Mathematics from an Advanced Standpoint Geometry, Dover Publications, New York.

Kohli, D., and Spanos, J., 1984a, "Workspace Analysis of Mechanical Manipulators Using Polynomial Discriminants," ASME Paper No. 84-DET-121.

Kohli, D., and Spanos, J., 1984b, "Workspace Analysis of Regional Structures of Manipulators," ASME Paper No. 84-DET-120.

Kumar, A., and Waldron, K.J., 1980, "The Dextrous Workspace," ASME Paper No. 80-DET-108.

Kumar, A., and Waldron, K.J., 1981, "The Workspaces of a Mechanical Manipulator," Journal of Mechanical Design, Vol. 103, No. 3, pp. 665-672.

Lipkin, H., and Duffy, J., 1985, "A Vector Analysis of Robot Manipulators," Chapter 5, Recent Advances in Robotics, Eds. G. Beni and S. Hackwood, John Wiley, New York.

Litvin, F.L., and Castelli, V.P., 1985, "Configurations of Robot's Manipulators and Their Identification, and the Execution of Prescribed Trajectories, Part 1, Basic Concepts," Journal of Mechanisms, Transmissions and Automation in Design, Vol. 107, No. 2, pp. 170-8.

Litvin, F.L., Castelli, V.P., and Shaheen, M., 1987, "Singularities in Motion and Displacement Functions for a 7 Degree-of-Freedom Manipulator," Journal of Robotic Systems, Vol. 4, No. 3, pp. 397-421.

Litvin, F.L., Costopoulos, T., Castelli, V.P., Shaheen, M., and Yukishige, Y., 1985, "Configurations of Robot's Manipulators and Their Identification, and the Execution of Prescribed Trajectories, Part 2, Investigations of Manipulators Having Five, Seven and Eight Degrees of Freedom," Journal of Mechanisms, Transmissions and Automation in Design, Vol. 107, No. 2, pp. 179-188.

Mohamed, M.G., 1983, "Instantaneous Kinematics and Joint Displacement Analysis of Fully-Parallel Robotic Devices," Ph.D. Dissertation, University of Florida, Gainesville.

Orin, D.E., and Schrader, W.W., 1984, "Efficient Computation of the Jacobian for Robot Manipulators," International Journal of Robotics Research, Vol. 3, No. 4, pp. 66-75.

Paden, B.E., 1985, "Kinematics and Control of Robot Manipulators," Ph.D. Dissertation, University of California, Berkeley.

Parthasarathy, T., 1983, On Global Univalence Theorems, Springer-Verlag, Berlin.

Paul, R.P., and Stevenson, C.H., 1983, "Kinematics of Robot Wrists," International Journal of Robotics Research, Vol. 2, No. 1, pp. 31-38.

Pieper, D.L., 1969, "The Kinematics of Manipulators under Computer Control," Ph.D. Dissertation, Stanford University, Palo Alto.

Primrose, E.J.F., 1955, Plane Algebraic Curves, Macmillan, London.

Reischer, M.B., 1986, "Symbolic Algebraic Computation of Kinematic and Dynamic Mechanism Parameters," M.S. Thesis, University of Florida, Gainesville.

Roth, B., 1976, "Performance Evaluation of Manipulators from a Kinematic Viewpoint," Performance Evaluation of Programmable Robots and Manipulators, NBS Special Publication 459, pp. 39-62.

Sugimoto, K., and Duffy, J., 1982, "Applications of Linear Algebra to Screw Systems," Mechanism and Machine Theory, Vol. 17, No. 1, pp. 73-83.

Sugimoto, K., Duffy, J., and Hunt, K.H., 1982, "Special Configurations of Spatial Mechanisms and Robot Arms," Mechanism and Machine Theory, Vol. 17, No. 1, pp. 119-132.

Sugimoto, K., and Matsumoto, Y., 1984, "Kinematic Analysis of Manipulators by Means of the Projective Transformation of Screw Coordinates," Robotics Research, Ed. M. Brady and R. Paul, MIT Press, Cambridge, pp. 695-705.

Taylor, R.H., 1979, "Planning and Execution of Straight Line Manipulator Trajectories," IBM Journal of Research and Development, Vol. 23, pp. 424-436.

Taylor, A.E., and Mann, W.R., 1983, Advanced Calculus, John Wiley, New York.

Vijaykumar, R., Waldron, K.J., and Tsai, M.J., 1986, "Geometric Optimization of Serial Chain Manipulator Structures for Working Volume and Dexterity," International Journal of Robotics Research, Vol. 5, No. 2, pp. 91-103.

Waldron, K.J., Wang, S.L., and Bolin, S.J., 1985, "A Study of the Jacobian Matrix of Serial Manipulators," Journal of Mechanisms, Transmissions and Automation in Design, Vol. 107, pp. 230-8.

Young, L., 1986, "A Theory for the Articulation of Robot Manipulators," Ph.D. Dissertation, University of Florida, Gainesville.

Yuan, M.S.C., and Freudenstein, F., 1971, "Kinematic Analysis of Spatial Mechanisms by Means of Screw Coordinates. Part 1--Screw Coordinates," Journal of Engineering for Industry, Vol. 93, pp. 61-66.

BIOGRAPHICAL SKETCH

Resit Soylu was born on July 17, 1956, in Ankara, Turkey. He received his B.S. and M.S. degrees in mechanical engineering from the Middle East Technical University, Ankara. In 1982, he began his graduate studies at the University of Florida on a fellowship awarded by the Scientific and Technical Research Council of Turkey.

I certify that I have read this study and that in my opinion it conforms to acceptable standards of scholarly presentation and is fully adequate, in scope and quality, as a dissertation for the degree of Doctor of Philosophy.

Joseph Duffy
J. Duffy, Chair
Professor of Mechanical Engineering

I certify that I have read this study and that in my opinion it conforms to acceptable standards of scholarly presentation and is fully adequate, in scope and quality, as a dissertation for the degree of Doctor of Philosophy.

GK Matthew
G.K. Matthew, Cochair
Associate Professor of Mechanical Engineering

I certify that I have read this study and that in my opinion it conforms to acceptable standards of scholarly presentation and is fully adequate, in scope and quality, as a dissertation for the degree of Doctor of Philosophy.

George N. Sandor
G.N. Sandor
Professor of Mechanical Engineering

I certify that I have read this study and that in my opinion it conforms to acceptable standards of scholarly presentation and is fully adequate, in scope and quality, as a dissertation for the degree of Doctor of Philosophy.

RG Selfridge
R.G. Selfridge
Professor of Computer and Information Sciences

I certify that I have read this study and that in my opinion it conforms to acceptable standards of scholarly presentation and is fully adequate, in scope and quality, as a dissertation for the degree of Doctor of Philosophy.

John Staudhammer

J. Staudhammer
Professor of Electrical Engineering

This dissertation was submitted to the Graduate Faculty of the College of Engineering and to the Graduate School and was accepted as partial fulfillment of the requirements for the degree of Doctor of Philosophy.

April, 1988

Dean, College of Engineering

Dean, Graduate School